Testing a Closed Loop Forming Algorithm on a Part Created by Discrete Die Stretch Forming

by

Mark S. Grodzinsky

B.S. in Electrical Engineering
M.I.T.
1994

Submitted to the Department of Electrical Engineering and Computer Science

in Partial Fulfillment of the Requirements for the Degree of

Master of Engineering in Electrical Engineering

at the Massachusetts Institute of Technology

February 5, 1996

Author___
Department of Electrical Engineering and Computer Science
February 5, 1996

Certified by_
David E. Hardt, Professor of Mechanical Engineering
Thesis Supervisor

Accepted by_____
R. Morgenthaler
Chairman, Department Committee on Graduate Theses

Testing a Closed Loop Forming Algorithm on a Part Created by Discrete Die Stretch Forming

by
Mark S. Grodzinsky

Submitted to the
Department of Electrical Engineering and Computer Science

February 5, 1996

In Partial Fulfillment for the Degree of
Master of Engineering in Electrical Engineering and Computer Science

ABSTRACT

Sheet metal forming is a very old process and there is a significant amount of empirical data concerning the material properties, cost and quality. However, the process is still run very inefficiently and does not take advantage of the present technology. Currently, tooling is a trial and error science which takes months to build and thousands of dollars to finance. Forming over a reconfigurable, discrete die cuts down lead times to hours and reduces cost tremendously. Parts can now be formed, measured, and input to a controller which will change the shape accordingly to create the proper part.

The closed loop shape control algorithm developed at MIT has been in use for many years in matched die forming. The discrete matched die press has been retrofitted to accomplish stretch forming. During the course of this thesis the stretch forming machine was built and a new control system was introduced. The new stretch forming machine had to be characterized to find out the repeatability of the process, as well as the machine capabilities when forming.

Once characterized the closed loop shape control algorithm had to be tested on the stretch forming operation. A measurement technique which employs the use of a coordinate measurement machine (CMM) had to be developed. The raw data from the CMM was manipulated so the minimum number of data points necessary were taken to recreate the part shape. The actual algorithm was then tested and the part shape converged on the defined reference shape in two cycles of the controller.

Thesis Supervisor: David E. Hardt
Title: Professor of Mechanical Engineering

ACKNOWLEDGMENTS

I would like to thank Professor David Hardt for the research opportunity and continual guidance throughout the course of this thesis and for never failing to mention how much he liked my hats. I would also like to thank Fred Cote for always being around when something needed to be designed or built, and letting me cut the long lines of people who were in need of his machining expertise. Thanks also to Gerry Wentworth for his patience teaching me the mysteries of the CMM. I'd like to give a very special thanks to Simona Socrate; for being my dinner buddy, relationship advisor, and ofcourse a brilliant engineer. Without her continuous support I doubt I would have made it to graduation.

Within the lab, I'd like to thank Boyd Bucher for teaching me the industrial work ethic. I'd like to thank Torben Thurow for allowing me to pass off my work to him while he was a UROP, and Ryan Boas for having nice shoes. I'd like to give a special thanks to Andrew Parris for helping to enlighten me to the mysteries of the mechanics of materials and philosophies of religion. Thanks to Marko Valjavec for broadening my mind to see past the Mac, to the wonders of the PC and for bringing the splendor of the European culture into the lab. Thanks to Upi Ummethala for being as addicted to caffeine as I am, and being a model partner in our management class. Thanks to Benny Budiman for continually making sure that our computers always had the latest versions of software which make the computers crash on a regular basis. Computing just wouldn't be as fun without the sense of urgency associated with it. I'd also like to thank Ken Amoruso for sharing the agony of thesis writing and job hunting with me. Finally, I'd like to thank Dave Sha for teaching me about time expansion, and how minutes could actually last hours.

I'd like to thank my parents, Fran and Steve, for their continual support throughout the years, in all of my endeavors. Thanks for all of the love and guidance you've given me and the pep talks that kept me going when the road to graduation got a little rocky.

Table of Contents

List of Figures

CHAPTER 1: INTRODUCTION

1.1 Problems With Sheet Metal Forming

Sheet metal forming is an old process and there is considerable empirical data concerning the material properties, cost and quality. However, the process is still run very inefficiently and does not take advantage of the present technology. In today's aerospace industry there are many types of sheet metal forming processes used, including matched die forming, roll bending, hydroforming, stretch forming, and deep drawing. The process that dominates the airplane panel production is stretch forming.

The main drawback with any of these processes that employ the use of a die, whether it be matched die forming, where two dies are used, or stretch forming, where only one die is used, is the extraordinary costs and lead times inherent in solid die manufacturing. Although there has been extensive research on the material properties of metal and bending theory, it is still very difficult to predict the shape of a die, given the desired part shape. As a result, the dies often have to be modified after forming tests have been done in order to make the part more accurate. This process can be both costly and time consuming, thus many sheet metal forming operations only prove to be financially feasible in the mass production of parts. For a particular aerospace company in the United States, a Kirksite die (zinc alloy based) used for stretch forming aircraft body panels takes on the average of 200 to 600 hours to fabricate, depending on the size of the part, at a rate of $90 per hour [Hamm, 1996]. Thus, the cost of producing a die can vary from $18,000 to $54,000. Combine this with the fact that approximately 300 of these dies must be made for an aircraft, and tooling costs now exceed $5,000,000.

On top of the major costs incurred in making the dies, there is also a great cost in inventory and upkeep of these dies. Because spare parts must be continued to be made for over 10 years after production stops on an airplane, all of the dies must be kept, stored

and maintained for this length of time. In some cases, the dies are left out doors which leads to high maintenance costs if that die needs to be employed again.

1.2 Flexible Sheet Metal Forming System

As technology continues to improve, the forming industry continues to improve with it. There are many finite element analysis (FEA) packages that can accurately model the mechanics of the forming process, which is crucial in predicting the die shape. Even though the die shapes are now made more accurately, and post fabrication machining on the dies has been reduced, the problem of housing and maintaining the dies has not been addressed. A single, "flexible" die could be the answer to this problem. At MIT there is presently research being done on a Flexible Sheet Metal Forming System which will facilitate rapid tool fabrication and will drastically reduce lead times and costs [Hardt, et. al. 1992]. A Discrete Die tool comprising 552 1/2 inch pins which create a die with approximately one foot square dimensions has been constructed. The pins are positioned through a computer controlled setting mechanism which can accurately set the pins to within one thousandths of an inch. Although the discrete tool completely eliminates the need for creating and storing many dies and changes the lead times from weeks to minutes, there are some draw backs that the discrete tool has as well. Since the die is made up of discrete pins, an interpolator pad must be used to smooth the die in order to prevent dimpling on the part. Extensive research on interpolator materials and methods for attaching it to the die has been done [Eigen, 1992; Walczyk, 1996]. The interpolator accomplishes the job of preventing dimples but it also cuts down on the resolution of the die, thus, there are some parts that the discrete tool can not be used to form. This problem virtually disappears in the production of airplane panels. The panels are usually a very simple curved geometry, with no small angles or discontinuities. Parts such as this are ideal for the discrete tool.

1.3 Closed Loop Shape Control System

Using the discrete tool, research has been done to develop a closed-loop shape control system for the sheet metal forming process [Webb, 1987; Ousterhout, 1991]. Initially a controller in which a point-by-point displacement algorithm was used for each individual pin and corresponding point on the sheet metal was tested [Webb, 1981]. Each of these points had their own independent control systems. Thus, for an NxN matrix of pins, there would be N^2 control systems. This control scheme had two major drawbacks; first, the rate at which the part converged to the desired shape was extremely slow, and second, each controller only affected a very localized area of the die. Thus, localized changes would be made in the die with no regard for the overall die shape. In response to this controller's failures, a new control scheme was devised in which a spatial frequency based control algorithm described both the part shapes and the die shapes in the frequency domain using Discrete Fourier Transforms (DFT) [Webb, 1987], [Webb & Hardt, 1991]. The next die shape was created using a shape control algorithm that took into account the previous two part and die shapes in the frequency domain to calculate the new pin positions for the next die. Using the old control scheme, there were very localized changes being made without regard for the overall die shape. By using the DFT to describe both the part and die shapes, the overall shape of the die was now being controlled during every localized change in the die shape.

All of the early research concentrated on the development of closed loop control algorithms to compensate for springback in both two dimensional axisymmetric [Webb, 1991] and three dimensional parts made by matched die forming [Ousterhout, 1993; Eigen, 1992]. This thesis concentrates on applying this same control algorithm to stretch forming.

1.4 Plan of Experimentation

A new discrete die stretch forming machine was built during the course of this thesis, but no previous characterization experiments have been done on it. Therefore, the first goal of this thesis is to develop a complete set of data encompassing the machine parameters. It will include the forming limitations of the machine, as well as the noise

margins inherent in the system. These noise margins will then be used as a stopping point for the convergence tests. When the error between a formed part shape and the reference shape falls within this noise margin, any part made thereafter may not be controlled by the machine.

Once the machine has been characterized, and the forming process has been optimized, the shape control algorithm can be applied to the stretch forming process. The goal of these experiments will be to create die shapes, based on frequency analysis of the previous two part and die shapes, that yield parts that lie within the noise margins of the reference shape. This will be accomplished by selecting two initial, "open loop" trials to produce the first "closed loop" die shape. The two "open loop" trials will be a die which is the exact shape of the reference shape, and a part formed over it, and a die which has a curvature which is 110% that of the reference shape, and its part formed over it. Once the first closed loop part has been made, it will be compared to the reference shape. If it lies within the noise margin, the process may be deemed a success and the part has successfully converged. If not, the 110% curvature die and corresponding part and the first closed loop die and corresponding part will be used to create a second closed loop die shape. This process will continue to iterate until the convergence criteria is met. Figure 1.1 shows two iterations through the closed loop shape control algorithm. $\hat{H}_1$ is the deformation transfer function that is used in the closed loop shape control algorithm to create the next die shape.

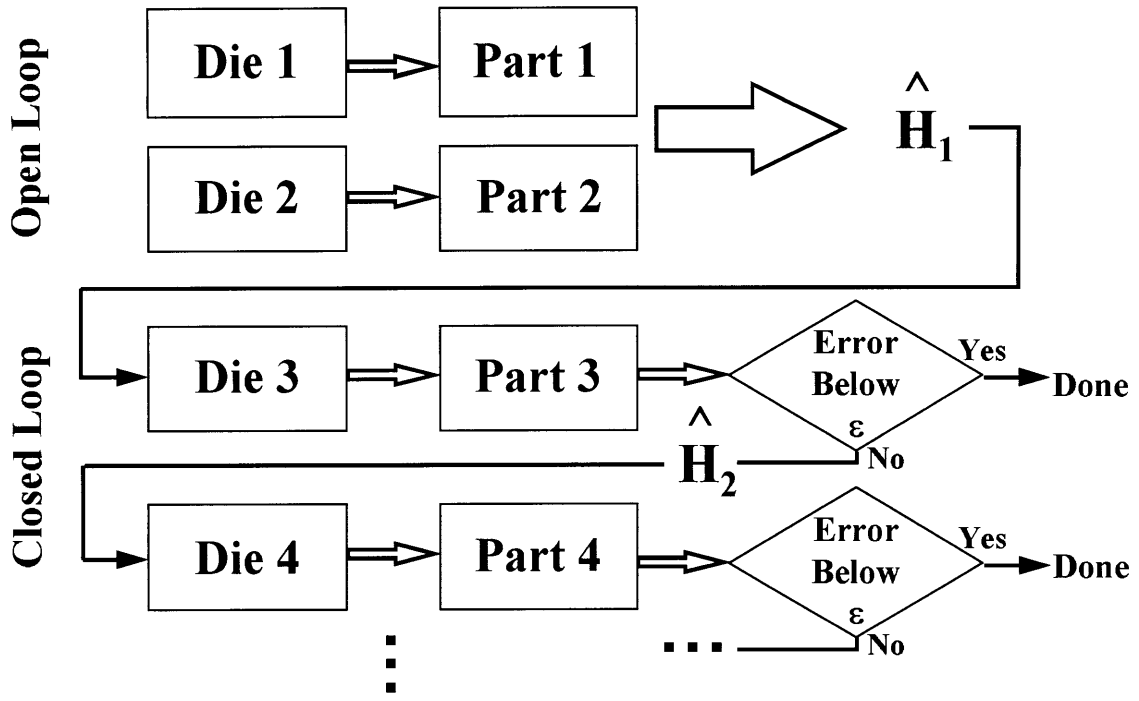

Figure 1.1: Two iterations Through the Closed Loop Shape Control Algorithm

1.5 What Lies Ahead

This thesis continues on the path defined by Ousterhout and Webb by testing the closed loop shape control algorithm for stretch forming. Although stretch forming is a very different process from matched die forming, the same springback analysis can be used and thus the same closed loop algorithm can be implemented. Figure 1.2 shows the block diagram of the overall closed loop shape control system and the chapters in which the individual blocks will be discussed.

The first section of Chapter 2 is mainly concerned with the physics behind the stretch forming process and the differences between it and pure bending. The second section goes through a thorough derivation of the closed loop shape control algorithm in the frequency domain. Chapter 3 deals with the retrofit of the matched die press to give it stretch forming capability. It will also go into the new motion control scheme of the press. In Chapter 4 there will be an in depth analysis on how a part is made using the machine, from setting up the die to forming and trimming the finished part. Chapter 5 will discuss

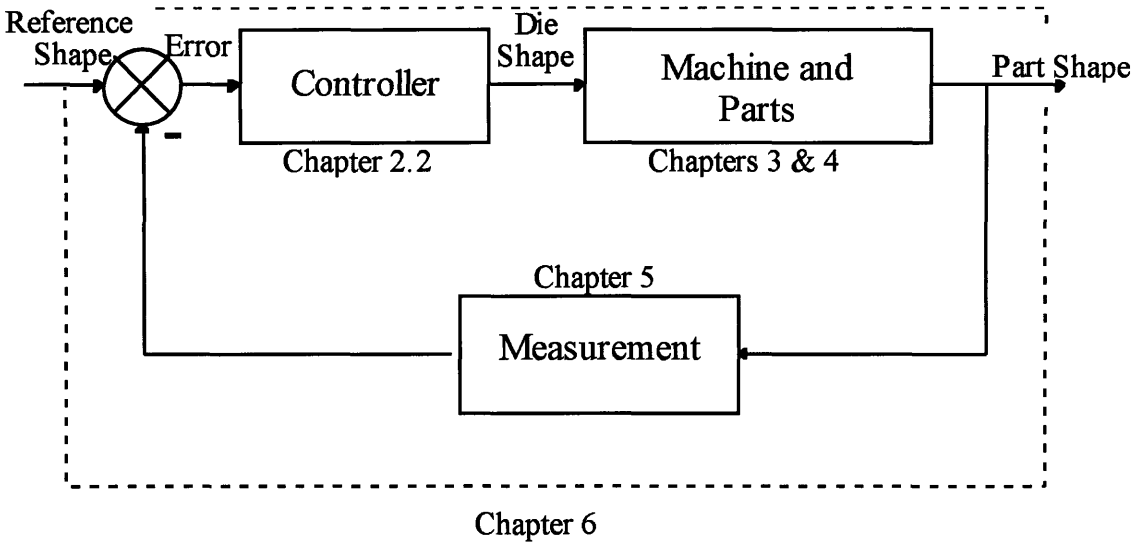

Figure 1.2: Block Diagram of Closed Loop Shape Control System

measurement techniques being used presently and some suggestions for future measurement systems. Chapter 6 deals with the evaluation of the closed loop control algorithm and how well the algorithm made the parts converge on the correct shape and simulation comparisons using FEA. Finally, Chapter 7 will give a summary of the results in this thesis and give recommendations for future work.

CHAPTER 2: BACKGROUND

2.1 Stretch Forming

[The material in this section has been adapted from Parris, 1996]

2.1.1 Material Model

Geometry for Bending and Stretching

The geometry for the material model which will be used to determine the stresses and strains within the material during forming is shown in Figure 2.1.

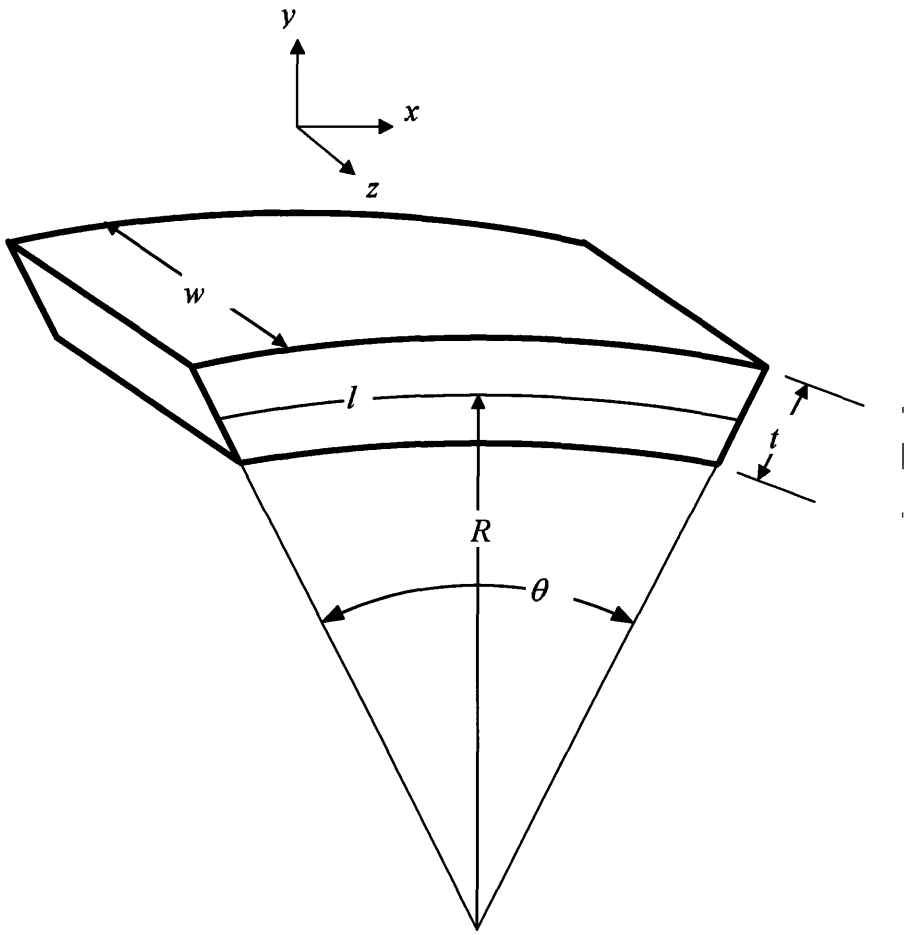

Figure 2.1: Geometry for Bending and Stretch Forming

In the figure, t represents the thickness and w represents the width. Although not shown in the figure, L represents the length of the material. These parameters describe the initial, unloaded workpiece. The bent, or loaded workpiece is described by R, the radius of curvature of the bend, and l, the length of the workpiece along the bend.

When a part is bent, strains are introduced which cause the material to stretch above the neutral axis, and compress below the neutral axis. The neutral axis is defined to be an imaginary line along which there is no strain during bending. For a sheet, this line runs along the length of the workpiece at the middle of the thickness, $t/2$, from the surface. This line is used as a zero reference for the y dimension which extends normally outward from it. The neutral axis is denoted by the dashed line in Figure 2.2. The arc length, $l(y)$, can be found by simple geometry to be dependent on the radius of curvature of the workpiece and the angle θ, which encloses the arc, in the following fashion, $l(y) = (R + y)\theta$, as seen in Figure 2.2.

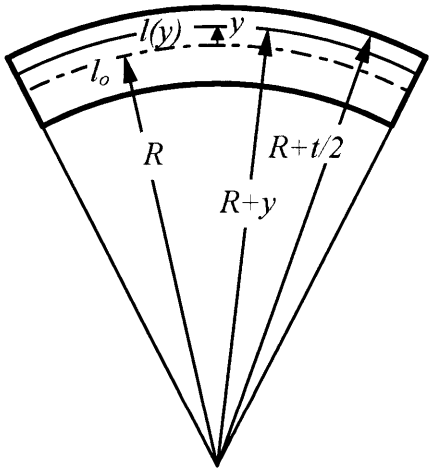

Figure 2.2: Changes in Arc Length Due to Changes in y

The stretch and compression, above and below the neutral axis, can be shown by looking at the arc length at the top and bottom of the sheet. At the top of the sheet the arc length is, $l(t/2) = (R + t/2)\theta$, while at the bottom of the sheet, the arc length is, $l(-t/2) = (R - t/2)\theta$. Since t is a positive, real number, it can be seen that the arc length at the top of the sheet is larger than that at the bottom of the sheet by the amount $t\theta$.

Engineering strain is defined to be the change in length over the original length, $\Delta l / l_o$. Within the material, this is:

$$e = \frac{l - l_o}{l_o} = \frac{(l_o + y\theta) - l_o}{l_o} = \frac{y\theta}{R\theta} = \frac{y}{R} \tag{2.1}$$

True strain is defined to be $\varepsilon = \ln(1+e)$. Engineering strain can be used to approximate the true strain as long as the engineering strains are kept low; less than 10%. Since the stretch forming process uses strains on the order of 1% to 3%, far below 10%, the engineering strain approximation will be used for ε.

Stress-Strain Model

The "power law" model is a very common approximation for the material stress-strain behavior in aluminum. Initially, for very small strains, the deformation is purely elastic, that is, there is a nearly linear relationship between the stress and strain. As the strain gets larger than the yield strain, the deformation is both elastic and plastic. In this region, the stress is proportional to the strain raised to the power n. Equations describing this behavior are:

$$\begin{aligned} \sigma &= E\varepsilon \quad \text{for } \sigma < \sigma_Y \quad (\varepsilon < \varepsilon_Y) \\ \sigma &= K\varepsilon^n \quad \text{for } \sigma > \sigma_Y \quad (\varepsilon > \varepsilon_Y) \end{aligned} \tag{2.2}$$

The accuracy of the "power law" model can be seen in Figure 2.3, where the approximation is plotted with the true stress-strain curve for Al 2024-O, with parameters σ_Y = 77 MPa, E = 68947 MPa, n = 0.210 up to a maximum strain of 5%.

2.1.2 Pure Bending

In order to bend a workpiece, a moment must be imposed throughout the material. That moment is defined to be $M = \int_{-t/2}^{t/2} y\sigma w dy$. Upon bending the material, the stresses

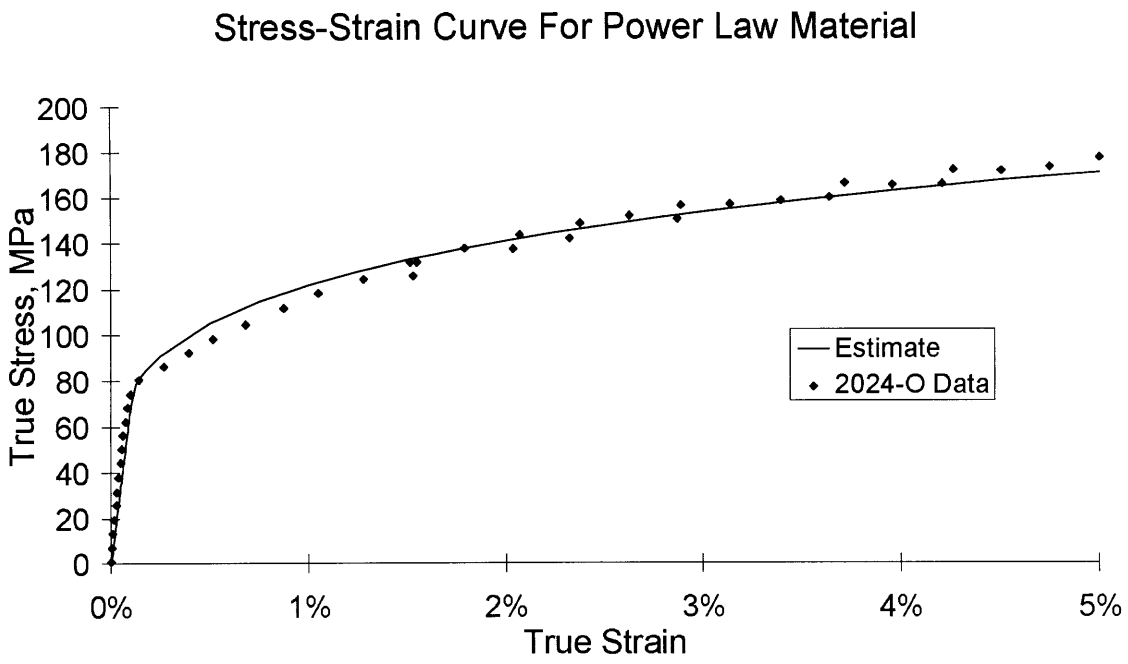

Figure 2.3: Actual and Estimated Stress-Strain Curves for Al 2024-O

(Data acquisition and estimation conducted by Andrew Parris)

within the workpiece change as a function of position with respect to the midplane.

$$\sigma = E\varepsilon = E\frac{y}{R_i} \qquad \text{for } \sigma < \sigma_Y \quad (\varepsilon < \varepsilon_Y)$$
$$\sigma = K\varepsilon^n = K\left(\frac{y}{R_i}\right)^n \qquad \text{for } \sigma > \sigma_Y \quad (\varepsilon > \varepsilon_Y) \tag{2.3}$$

When the part is released, that is, the moment is removed, the part will spring back in such a way to allow the moment to be exactly zero. When the part begins to spring back, the radius of curvature begins to increase which imposes a strain on the material. However, this imposed strain will never cause plastic deformation, thus the strain is purely elastic. The strain caused by the springback is:

$$\varepsilon_{SB} = -y\left(\frac{1}{R_f} - \frac{1}{R_i}\right) \tag{2.4}$$

The strain due to springback enters the equation for the final moment by changing the stress seen by the material from σ to $\sigma - E\varepsilon_{SB}$ in the final moment equation.

$$M = \int_{-t/2}^{t/2} y(\sigma - E\varepsilon_{SB})wdy = 0 \tag{2.5}$$

Solving this equation for the springback ratio, R_i / R_f gives the following result:

$$\frac{R_i}{R_f} = 1 - \frac{3R_i}{(t/2)^3}\left[\frac{1}{3R_i}\left(\frac{\sigma_Y R_i}{E}\right)^3 + \frac{K}{E(n+2)R_i^n}\left(\left(\frac{t}{2}\right)^{n+2} - \left(\frac{\sigma_Y R_i}{E}\right)^{n+2}\right)\right] \tag{2.6}$$

Figure 2.4 shows both the stresses due to pure bending and the unloaded or residual stresses left in the material once it has been released. The bending stress, the solid line, is simply σ, while the residual stress, the dotted line, is $\sigma - E\varepsilon_{SB}$.

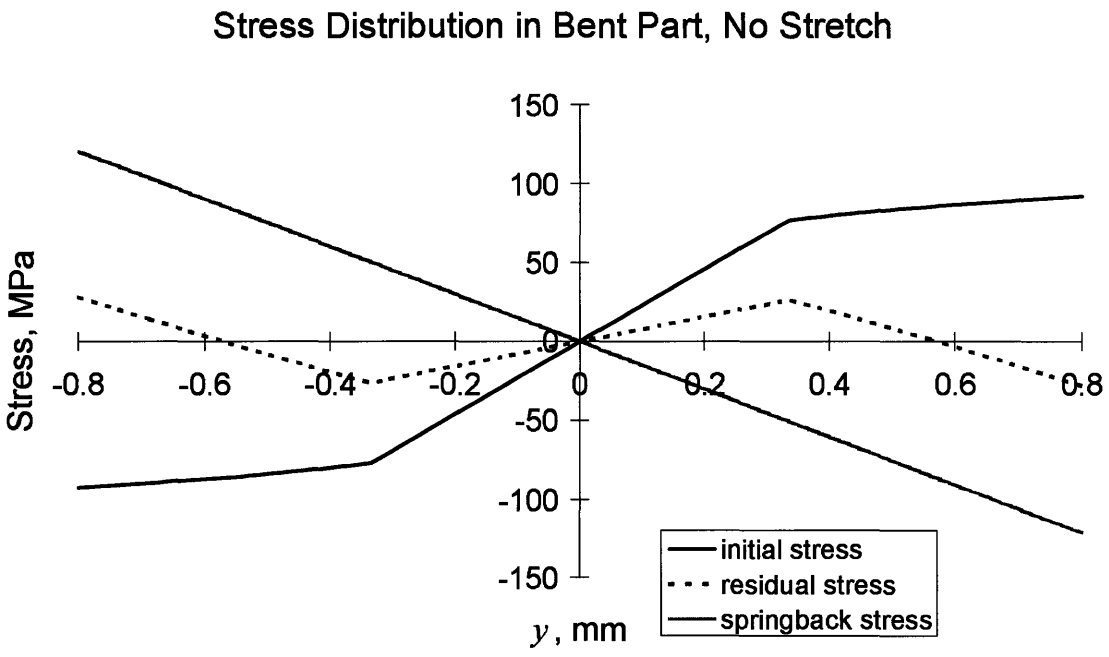

t = 1.6 mm, Ri = 300 mm

Figure 2.4: Bending and Residual Stresses for a Workpiece Deformed By Pure Bending a Power Law Material

2.1.3 Stretch Forming

In the stretch forming process, there are three possible stretch profiles:

1. pre-stretching the material, forming the part, no post-stretching
2. no pre-stretching, forming the part, post-stretching the material
3. pre-stretching the material, forming the part, post-stretching the material

Pre-Stretch With No Post-Stretch Forming

When a piece of sheet metal is stretched prior to forming, the entire stress-strain state of the material rises along the linear elastic region and into the plastic region, assuming the preload force induces greater strains than yield (see Figure 2.5). The pre-stretch stress is shown to be,

$$\sigma_o = K\varepsilon_o^{\,n} \tag{2.7}$$

where the *o* indicates the pre-stretch state of the material. Since stretch has been added to the process, the neutral axis shifts downward from the middle of the part. The line where the neutral axis used to be, is now called the midplane. When the material is then bent in this pre-stretched state, the midplane actually lengthens due to the fact that the increase in stresses at the top of the workpiece is less than the decrease in stresses at the bottom of the workpiece.

There are three strains that can be used to describe the state of the material. ε_o is the initial strain induced by the stretch, ε_{ST} is the elongation strain which reflects the midplane getting longer, and ε_B is the strain induced by bending.

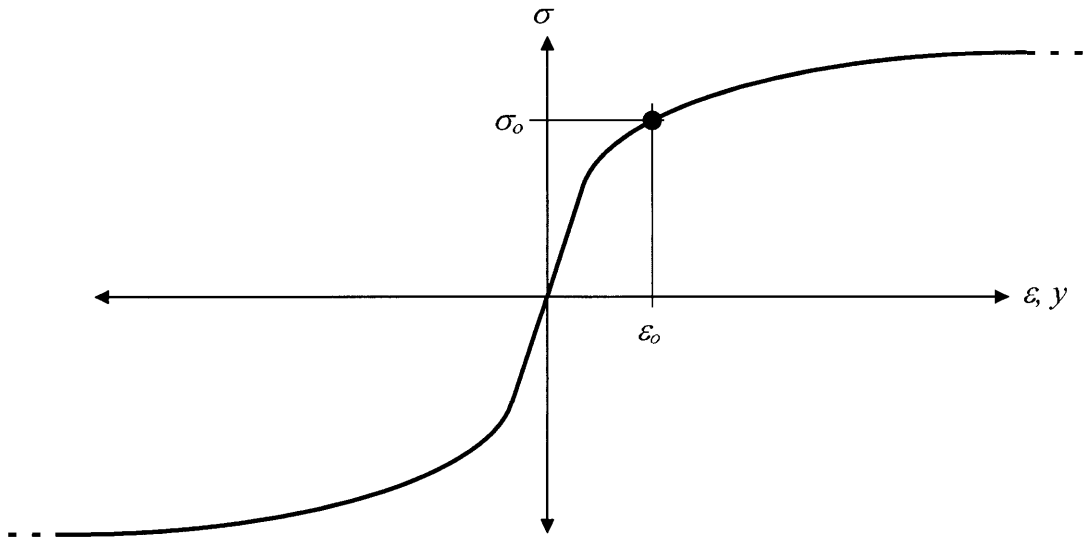

Figure 2.5: Stress-Strain Curve for Pre-stretch Bringing Material into Plastic Region

The stress distribution after wrap taking into account these three additive strains, is:

$$\sigma_i = \begin{Bmatrix} \text{A:} & -K\left|\varepsilon_o - 2\sigma_o/E - \left(\varepsilon_B + \varepsilon_{ST}\right)\right|^n & \text{for } \varepsilon_B + \varepsilon_{ST} < -2\sigma_o/E \\ \text{B:} & \sigma_o + E\left(\varepsilon_B + \varepsilon_{ST}\right) & \text{for } -2\sigma_o/E < \varepsilon_B + \varepsilon_{ST} < 0 \\ \text{C:} & K\left(\varepsilon_o + \varepsilon_B + \varepsilon_{ST}\right)^n & \text{for } \varepsilon_B + \varepsilon_{ST} \geq 0 \end{Bmatrix} \quad (2.8)$$

Figure 2.6 shows graphically, the stress-strain characteristics of the material in three regions. In the first region, A, the material actually goes into the plastic compression. It is highly unlikely for a sheet metal part to be in this region, it usually reserved for thicker parts or extrusions. In region B, the compressive forces at the bottom of the part are less, causing only elastic compression. Finally, in the third region, C, the material is being stretched even further, plastically.

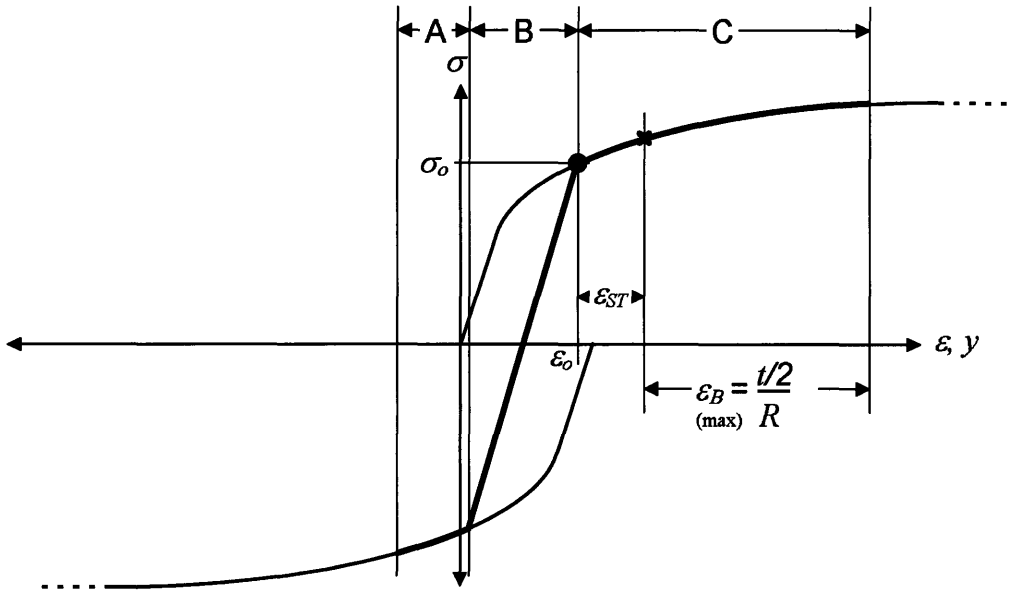

Figure 2.6: Stress-Strain Curve for Three Regions from Equation 2.8

Pre-Stretch and Post-Stretch Forming

Post-stretch is an additional stretch which is added to the material after the part has been formed and before the unloading of the part. The post-stretch induces stresses which depend on the stresses at the end of wrap and the amount of strain, ε_T, added by the post-stretch. The stress equation shown below is for the material in region B, at the end

of wrap, in which the pre-stretch brought the material into elastic compression at the bottom of the part and plastic tension at the top of the part.

$$\sigma_I = \begin{Bmatrix} \text{a}: \ \sigma_i + E\varepsilon_T & \text{for } \sigma_i + E\varepsilon_T < \sigma_o \\ \text{b}: \ K(\varepsilon_o + \varepsilon_B + \varepsilon_{ST} + \varepsilon_T)^n & \text{for } \sigma_i + E\varepsilon_T \geq \sigma_o \end{Bmatrix} \tag{2.9}$$

This is shown graphically in Figure 2.7. If the post-stretch is not strong enough to bring the material into the plastic region, the material would lie somewhere in region a. If the post stretch is strong enough, then the material will be in region b. The larger the post stretch, the further to the right, the material will travel on the stress-strain curve.

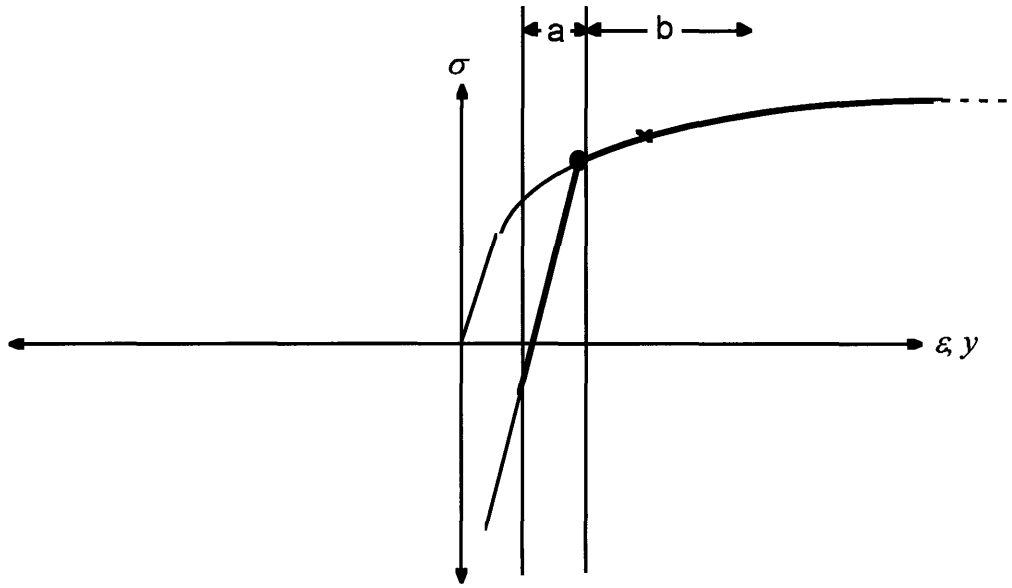

Figure 2.7: Stress-Strain Curve for Two Post Stretch Profiles from Equation 2.9

For the material in region C, a post stretch will simply move the material further along to the right along the stress-strain curve. The stress that this material sees is then given by:

$$\sigma_I = K(\varepsilon_o + \varepsilon_B + \varepsilon_{ST} + \varepsilon_T)^n \tag{2.10}$$

When the material relaxes and springs back, the stresses that the material sees is:

$$\sigma_f = \sigma_I - E\varepsilon_{SB} - E\varepsilon_R \tag{2.11}$$

for elastic recovery, where ε_R is the relaxation strain.

Comparison of Different Stretch Profiles

As described in the previous two subsections, the addition of stretch into a forming operation, whether it be pre- or post-, has a dramatic impact on the forming behavior. While pre-stretching the material and forming alone reduces the springback compared to pure bending, the pre-stretch in combination with a post-stretch reduces it even more. The pre-stretch also serves a secondary purpose, which is to reduce the effect of friction between the workpiece and the die. The effect of friction is reduced because the part does not stretch around the die as much, it is pre-stretched and wrapped around the die at a constant force. If the part were stretched around the die, the interpolator would stick to the workpiece and create various stress inconsistencies within the part and cause varying springback throughout the part. Figure 2.8 shows the effects of simply stretching the material. The □ on the stress-strain curve notes the amount of pre-stretch. In this case there is 1% strain applied to the part.

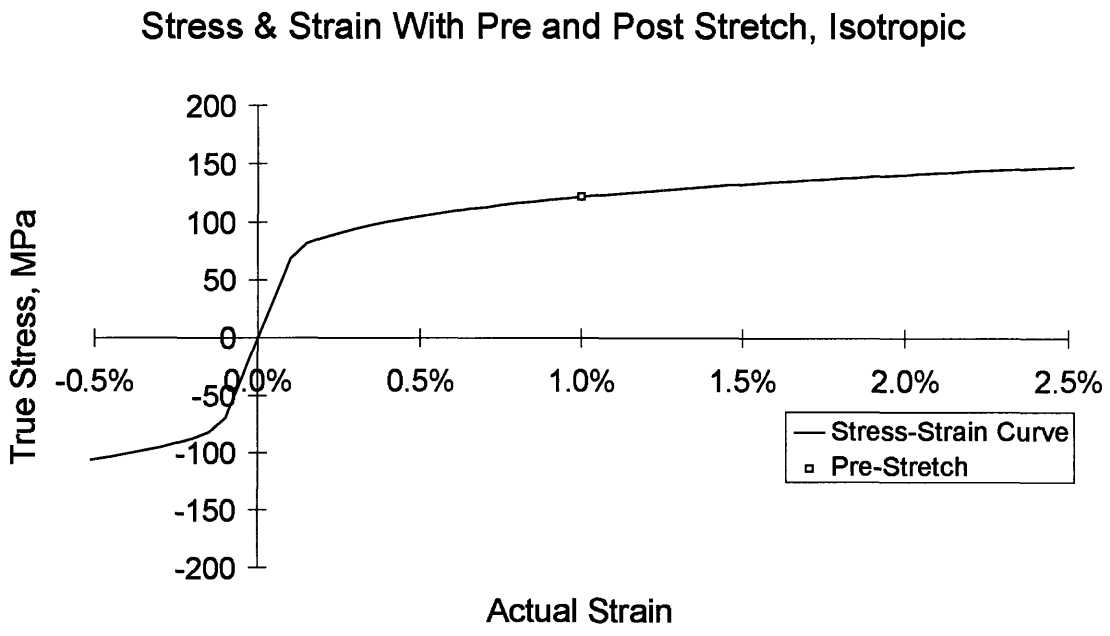

Figure 2.8: Stress and Strain in Pre-Stretch

Figure 2.9 shows graphically the pre-stretch plus bend process. After bending, the top of the part is in tension and thus the strain increases. The top of the part is the furthest right

point of the dark line. The bottom of the part undergoes compression elastically, and thus travels down the stress-strain curve parallel to the linear region. The bottom of the part is the furthest left point on the dark line. The Δ represents the midplane of the part.

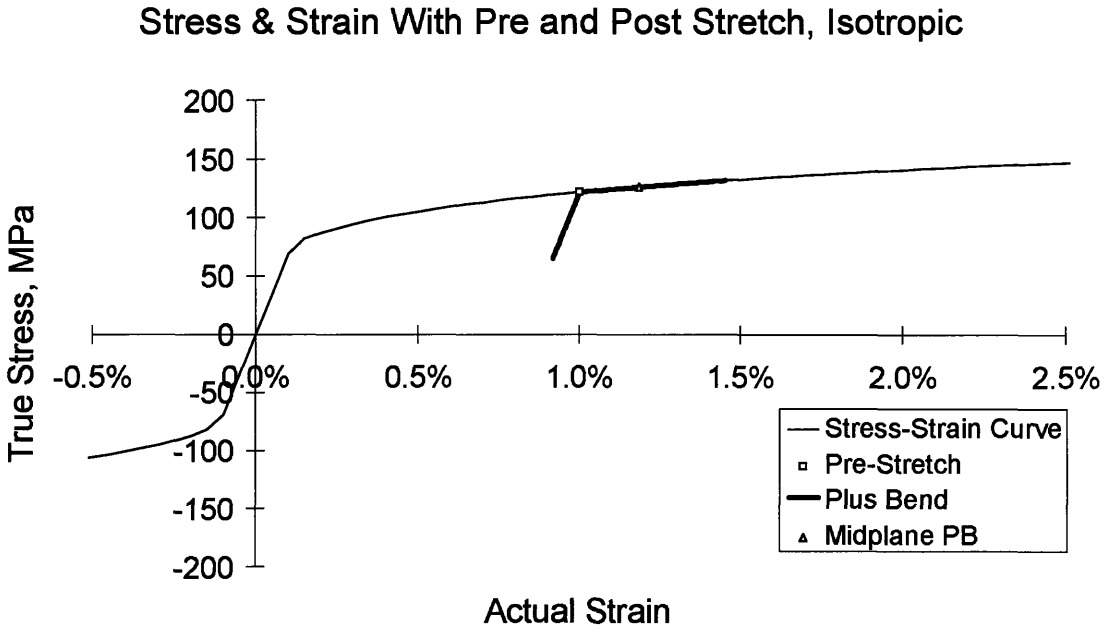

Figure 2.9: Stress and Strain in Pre-Stretch Plus Bend

Finally, Figure 2.10 depicts the pre-stretch, bend and post-stretch process. In this case, notice that the entire part has moved to a higher strain state, due to the post-stretch. Again, the dark line, which extends from the left to the right, depicts the stresses and strains from the bottom to the top of the part.

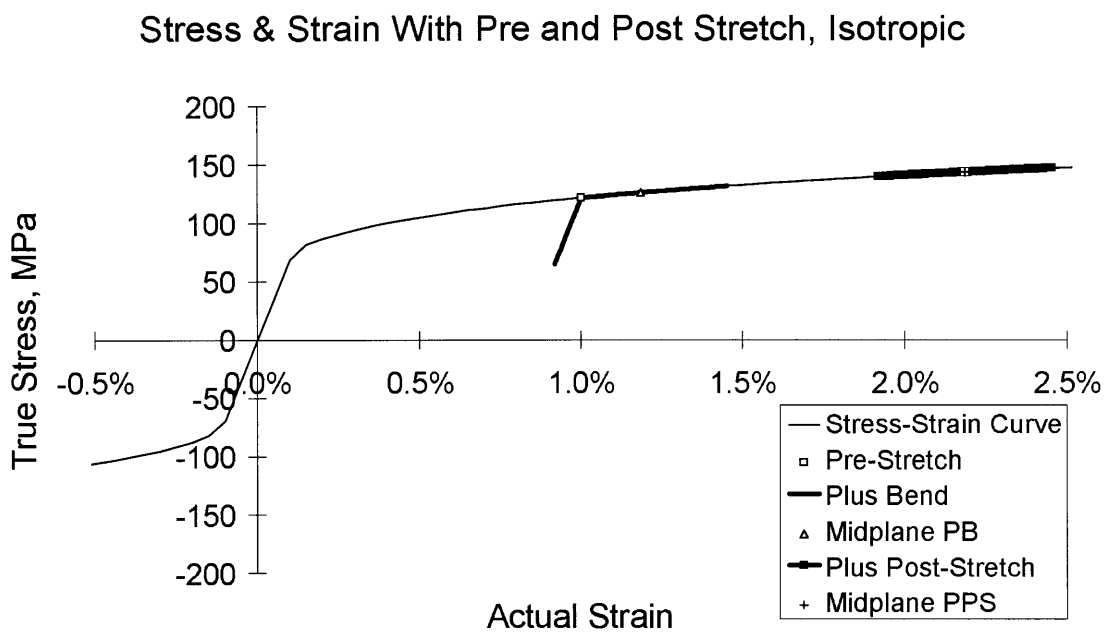

Figure 2.10: Stress and Strain in Pre-Stretch, Bend and Post-Stretch

Observing a pre-stretch, wrap, and no post-stretch process in a stress versus distance from the midplane frame of reference, may better depict the changes occurring within the part. Figure 2.11 shows the stresses within the workpiece at the end of pre-stretch.

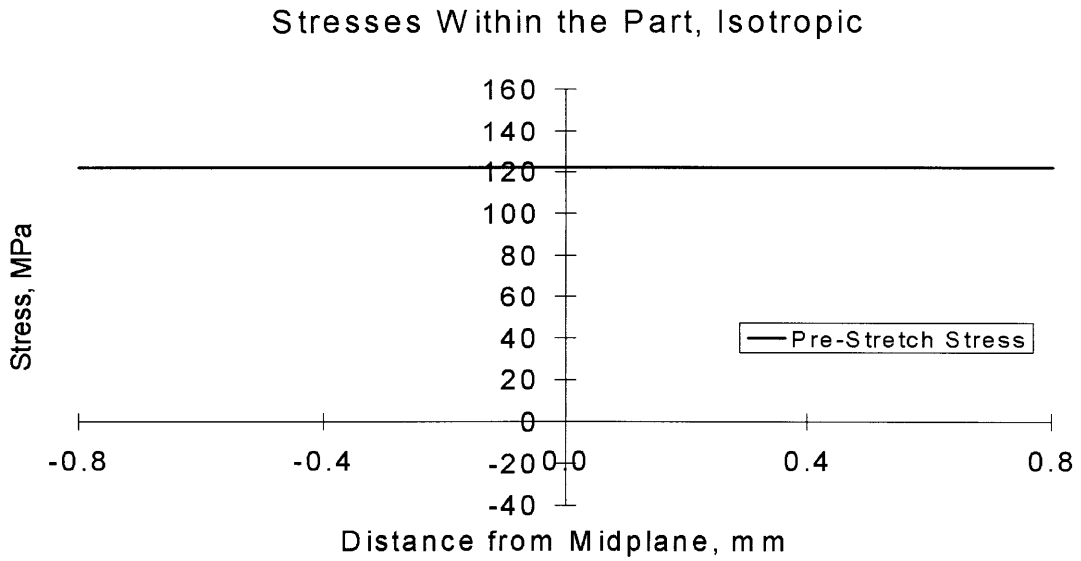

Figure 2.11: Stress Within the Part During Pre-Stretch

Since the part is under pure tension, the stresses within the part are completely uniform through the entire thickness of the part. When the part is then wrapped around the die, as shown in Figure 2.12, the stress within the top portion of the part increases. The very bottom of the part undergoes compression and thus the stresses diminish.

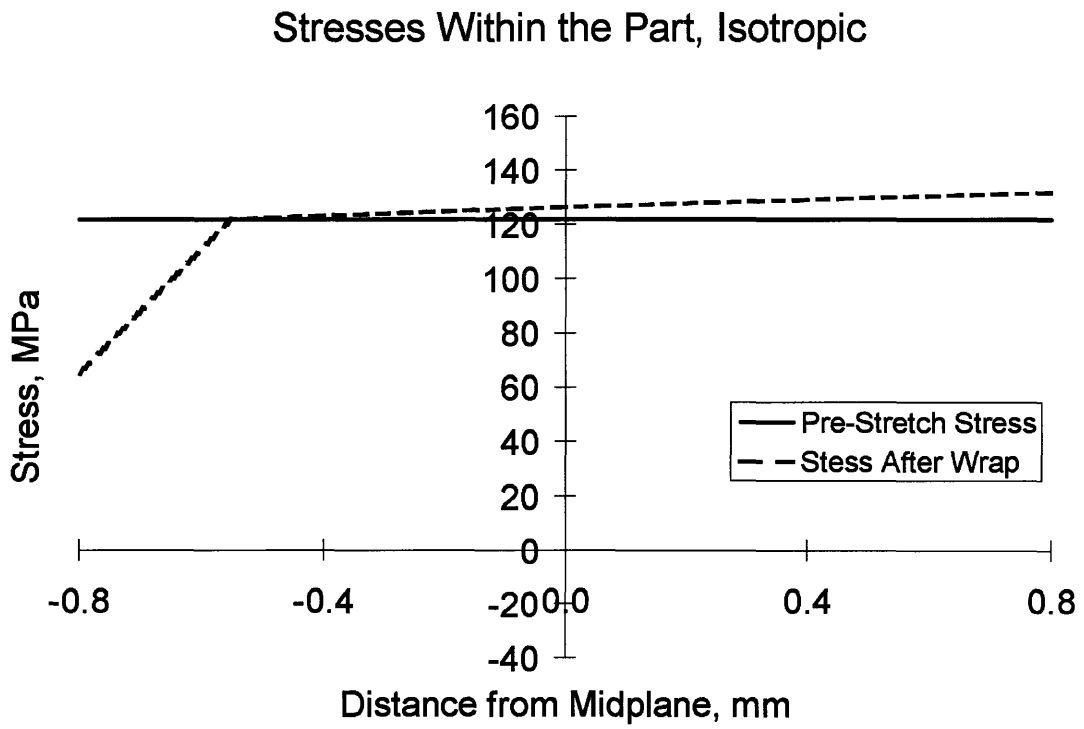

Figure 2.12: Stresses Within the Part During Pre-Stretch and Wrap

Once the part has been wrapped, the part is unloaded and the part springs back such that the internal moments go to zero. The dot and dashed line in Figure 2.13 depicts the residual stresses within the part after unloading. The springback stress is a measure of the amount of stress within the part induced by springback. Notice that the springback stress is at a maximum at the ends of the part where the part springs back the most. The springback stress ranges from -20 MPa to +20 MPa. This range will be diminished greatly when post stretch is introduced to the process.

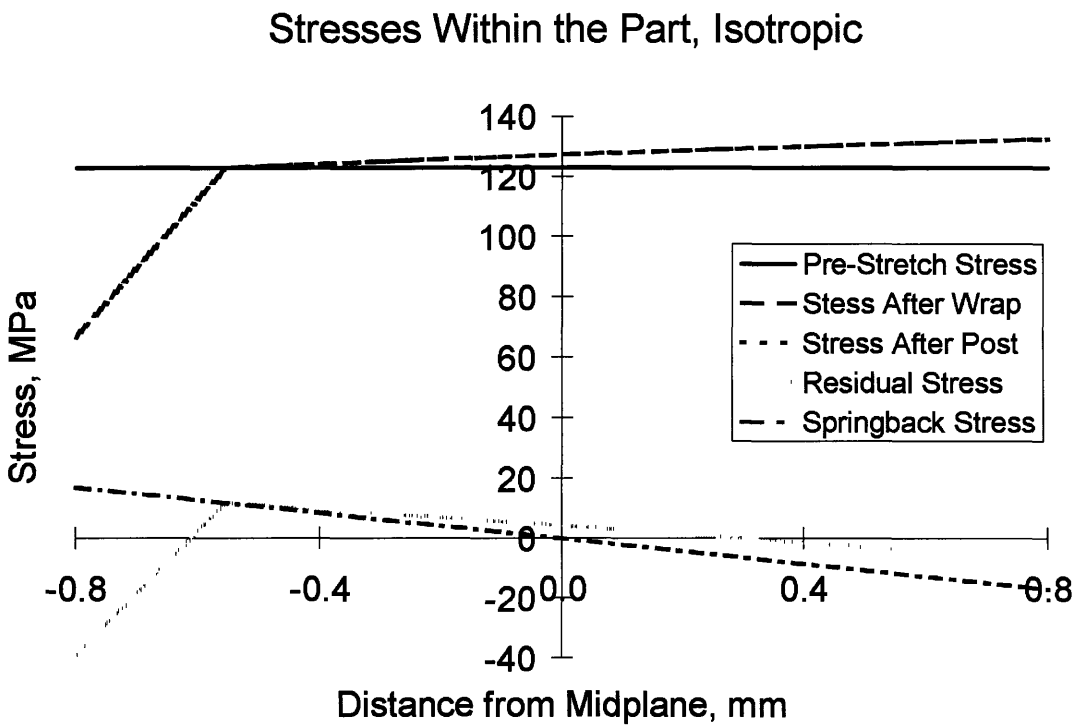

Figure 2.13: Stresses Within a Part Formed With Pre-Stretch and No Post-Stretch

In contrast, Figure 2.14 shows the stresses within the workpiece as well as the residual stresses after unloading and the change in stress due to springback for a part that was made using pre-stretch and post-stretch. In this case, the dotted line depicts the stress within the part after post-stretch. Notice that the residual stresses within the workpiece are now negligible. They are barely visible, even on the ten times scale in the figure. Also, the stresses due to springback are also much lower. By looking at Figures 2.13 and 2.14, it is plainly obvious that the effects of springback are much greater in the case where there is no post-stretch.

Since the main purpose of this thesis is to prove a closed loop shape control function, it is necessary to have significant springback to produce a large error between parts and dies. This large error will allow for easier observation of the control algorithm compensating for the error. If the springback were too small, it would be difficult to observe the control algorithm at work. Therefore, throughout this thesis, all experiments were done using the pre-stretch, wrap stretch profile, without post-stretch.

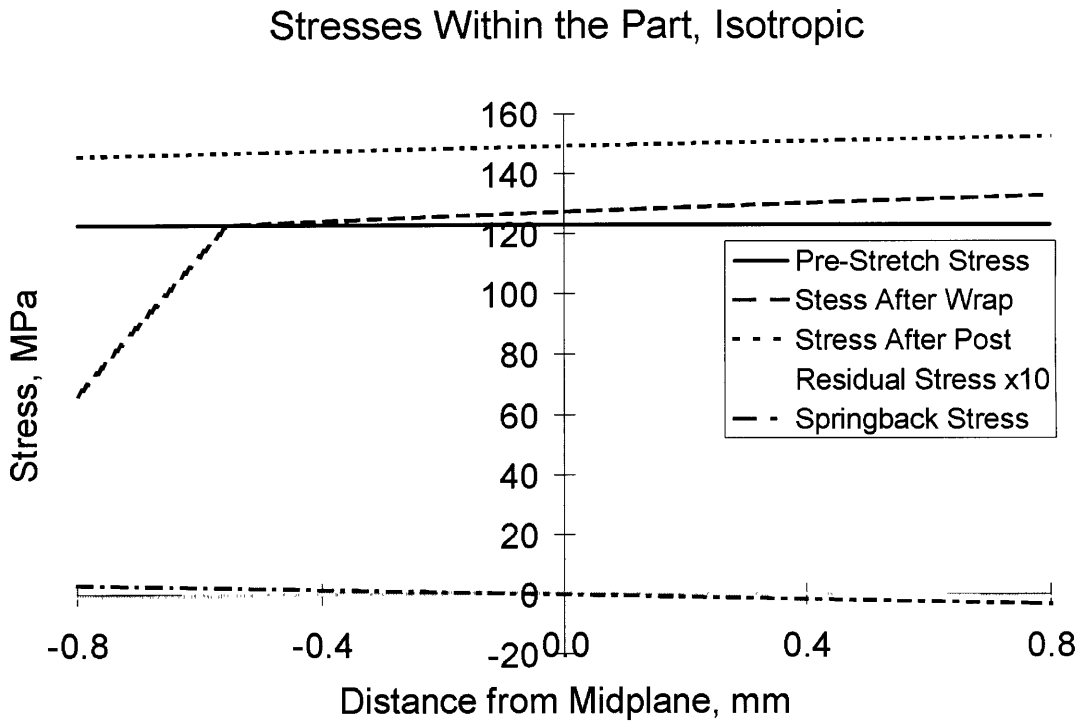

Figure 2.14 Stresses Within a Part Formed With Pre-Stretch and Post-Stretch

Once the algorithm has been proven to work, the future studies can use the pre-stretch, wrap, post-stretch profile. This will lead to less springback, smaller error, and faster convergence to the correct shape.

2.2 Deformation Transfer Function

As mentioned earlier, the closed loop controller went through an evolutionary process before the spatial frequency based control algorithm was adopted as the controller for the stretch forming press. This algorithm has the advantage of making the localized changes to the die through resetting the individual pins, without losing sight of the global nature of the die.

2.2.1 Two-Dimensional Closed Loop Frequency Based Control Algorithm

[The material in this section has been adapted from Ousterhout, 1991]

Figure 2.15 is a basic block diagram of the control system for the stretch forming process. It will be the responsibility of the controller, G_c, to provide necessary compensation to drive the error to zero.

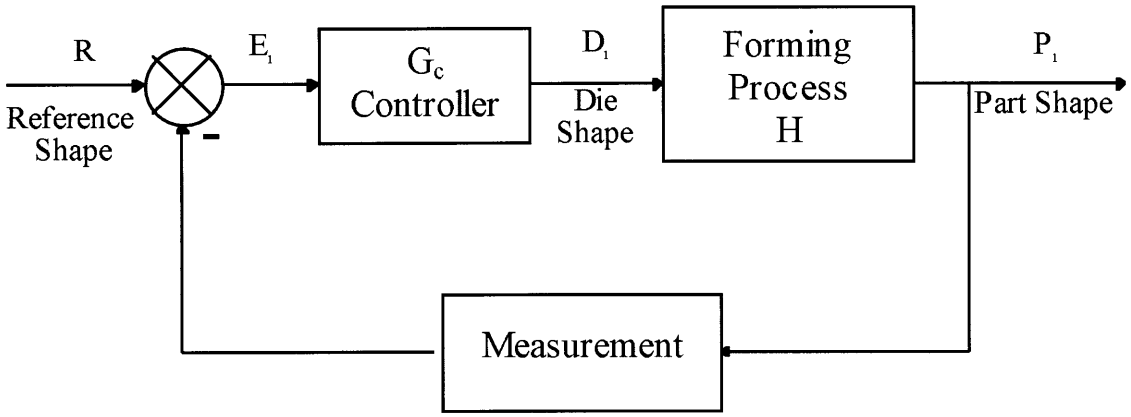

Figure 2.15: Control System Block Diagram

The error, E_1, as with all of the other capital letters in this chapter, represent the variable in the frequency domain, that is, the DFT of the spatial frequency component. The equation for driving the error to zero can thus be represented by:

$$E_1(\omega_1, \omega_2) = 0$$

$$\text{where } E_1(\omega_1, \omega_2) = DFT(e_1)$$

In the control system block diagram, it can be seen that the error can also be represented as the difference between the reference shape, R, and the part shape, P_1.

$$E_1(\omega_1, \omega_2) = R(\omega_1, \omega_2) - P_1(\omega_1, \omega_2) = 0$$

From Figure 4.1, it can also be seen that the part shape is a function of the die shape,

$$P_1(\omega_1, \omega_2) = f(D_1(\omega_1, \omega_2)) = D_1(\omega_1, \omega_2)H(\omega_1, \omega_2)$$

which when substituted into the equation above and expanded into a Taylor series about the operating point, $D_1(\varpi_1, \varpi_2)$, neglecting the second order and higher terms gives:

$$R(\omega_1,\omega_2)-P_i(D_i(\omega_1,\omega_2)\approx R(\omega_1,\omega_2)-P_i(D_i(\varpi_1,\varpi_2)$$
$$-(D(\omega_1,\omega_2)-D_i(\varpi_1,\varpi_2))\frac{\partial P_i(D_i(\varpi_1,\varpi_2))}{\partial D_i(\varpi_1,\varpi_2)}=0$$

This equation can be rearranged into the two-dimensional, frequency based, adaptation of Newton's method for solving a non-linear root.

$$D(\omega_1,\omega_2)=D_i(\varpi_1,\varpi_2)+(R(\omega_1,\omega_2)-P_i(D_i(\varpi_1,\varpi_2))\frac{\partial D_i(\varpi_1,\varpi_2)}{\partial P_i(D_i(\varpi_1,\varpi_2))}$$

The derivative at the end of this equation can be reduced to, the change in die shape over the change in part shape, since there have already been two open loop foaming trials.

$$\frac{\partial D_i(\varpi_1,\varpi_2)}{\partial P_i(D_i(\varpi_1,\varpi_2))}=\left(\frac{\partial P_i(D_i(\varpi_1,\varpi_2))}{\partial D_i(\varpi_1,\varpi_2)}\right)^{-1}=\frac{D_2(\omega_1,\omega_2)-D_1(\omega_1,\omega_2)}{P_2(\omega_1,\omega_2)-P_1(\omega_1,\omega_2)}$$

Therefore, D_1, will correspond to the first open loop die shape and P_1 will correspond to the first open loop part shape formed over D_1. Similarly, D_2 corresponds to the second open loop die shape and P_2 corresponds to the second open loop part shape. Implementing this representation of the derivative into Newton's equation for solving a non-linear equation, and changing it into incremental form will result in the frequency based control algorithm.

$$D_{i+1}(\omega_1,\omega_2)=D_i(\varpi_1,\varpi_2)+(R(\omega_1,\omega_2)-P_i(D_i(\varpi_1,\varpi_2))\left(\frac{D_i(\omega_1,\omega_2)-D_{i-1}(\omega_1,\omega_2)}{P_i(\omega_1,\omega_2)-P_{i-1}(\omega_1,\omega_2)}\right)$$

This equation can be solved to get the next die shape in the frequency domain. In order to get the spatial next die shape, or the new pin positions in the die, an Inverse Discrete Fourier Transform (IDFT) must be applied to the results of the frequency based control algorithm. Once the next die shape has been determined, the discrete die will assume its shape and the next part will be formed over it. This process will continue until the difference between the part shape and the reference shape falls within the limits, set by the forming capabilities of the machine.

CHAPTER 3: THE DISCRETE DIE PRESS & RETROFIT

In this chapter, there will be a brief description of the original MIT Matched Discrete Die Press, and the control system which was used in order to produce a final tool shape, followed by a description of the retrofit to the machine which gave it stretch forming capabilities. There will be discussion of the hardware components that were added and removed, as well as the new software package used to control the press. Finally, the new system for producing a final tool shape will be documented, as well as the forming capabilities of the new press.

3.1 Description of the Matched Discrete Die Press

The matched die press is comprised of six main components, the pin-setting system, the stationary die, the sheet metal binder, the mobile die, the hydraulics and the computer controls, as seen in Figure 3.1. Both the mobile die and the stationary dies were made up of 2160 1 / 4 inch steel pins, arranged in a 45 x 48 matrix in order to create approximately a one foot square die. The lack of symmetry in the die is caused by a 0.010 inch thick piece of sheet metal that was positioned between each column of pins. This sheet metal is necessary so the frictional forces between neighboring rows of pins are eliminated during the setting of the die. It also transmits the shear force from the pins to the back of the stationary die, and thus prevents the pins from sliding during forming. The dies are clamped by a set of three hydraulic rams which clamp the pins firmly within the die housing during forming, and relax during the pin set up. The sheet metal workpiece was held in the blankholder. The blankholder gripped the sheet metal using a series of bolts around the perimeter of the workpiece, and held the interpolator layers in place as well. Since there were two dies in the matched die press, interpolator was fixed on the front and back faces of the workpiece within the blank holder. Once the pins were set and

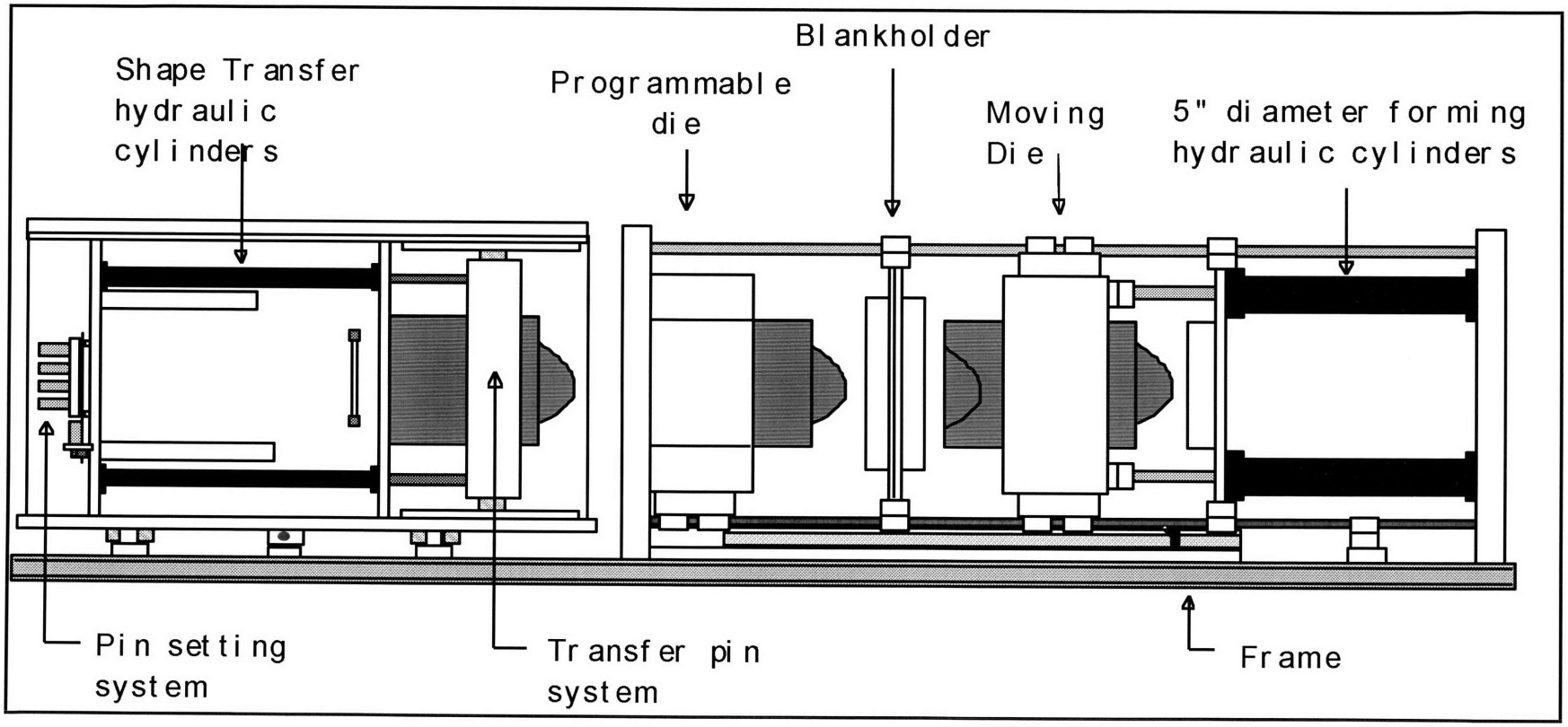

Figure 3.1: MIT Matched Discrete Die Press [Eigen, 1992]

the workpiece was in the blankholder, the mobile die was pushed in the direction of the stationary die by two 60 ton hydraulic cylinders. The pin setting mechanism was originally made so the entire carriage, made up of the shape transfer hydraulic cylinders, the pin setting mechanism and the transfer system, could transverse across the die and set up the pins one column at a time. The carriage, which was located behind the programmable die, housed 48 push pins that were hydraulically clamped into place and pushed into the loose stationary die pins by the shape transfer hydraulic cylinders. The push pins were set up 8 at a time by a system which used DC motors to drive lead screws, which in turn pushed the push pins in and out. The entire set up mechanism, including the carriage, DC servo motors, and hydraulics was set up in a closed loop computer control and was accurate to within ±0.003" [Ousterhout,1991].

The rest of the forming system included a coordinate measuring machine (CMM) and the computer controls. The CMM that was used, was a converted bridgeport milling machine. The Laboratory for Manufacturing Productivity (LMP) has recently acquired a Brown and Sharpe CMM which will be used for all of the measurements for this project and will be discussed further in Chapter 5.

3.2 Description of the Stretch Forming Discrete Die Press

3.2.1 The New Discrete Die

While the machine underwent some major changes to implement stretch forming, the discrete die underwent changes as well. All of the 1 / 4 inch square pins were removed and replaced by longer 1 / 2 inch square pins. The new pins are 40 inches long and have a spherical tip with radius 0.354 inches. This radius corresponds to the length of the diagonal across a one half inch square pin. This change was done for two main reasons: first, the actual production floor stretch forming machine which will be built is going to have a discrete die which will be 4 x 6 feet in size, and comprised of 1 inch square pins. Since the production model is going to have the larger pins, it was necessary to investigate larger pins on the forming process and the use of interpolator layers. Second, the setup time for the 1 / 2 inch pins was drastically reduced from that of the 1 / 4 inch pins. Instead of having 2160 pins to set up there are only 552.

The die is set up as a matrix with 23 columns and 24 rows. Since each pin is 1 / 2 square, the height of the die is exactly one foot. As with the discrete die with the smaller pins, the new die incorporates the 0.010 inch sheet metal dividers between the pins to prevent the translation of frictional forces between columns of pins during setup. Because of the sheet metal dividers and the size limitations of the stationary die, only 23 pins were able to fit across the die housing.

In order to prevent the pins from splaying at the end of the die during forming, and to remove the effect of the sheet metal spacers on the die, a pin alignment clamp was built. The pin alignment clamp is a device which was built to squeeze the pins together and give stability to the discrete die. During forming, frictional and forming forces act in an outward direction at the tips of the discrete pins. Since the pins extend 16 inches out from the clamping area in the stationary die, this force and large moment arm may be enough to cause the outer pins to bend outwards when forming at higher loads. The pin alignment clamp is constructed from two steel plates which are placed on either side of the die and connected by two threaded rods on the top and bottom of the die. Nuts are placed on the outside of the plates and when tightened, squeeze the pins together. Since the sheet metal dividers are located within the die housing, squeezing the outer third of the pins causes the gaps due to the sheet metal dividers within the stationary die to be eliminated at the die face. Thus, the chord length at the edge of the die is exactly 11.5 inches, corresponding to the 23, 1 / 2 inch pins, when the pin alignment clamp is engaged.

The pin alignment clamp also serves a secondary purpose of holding the interpolator in place over the die. Since the discrete die is oriented vertically, it has the problem of holding the interpolator over the die during forming. A second plate is placed over the threaded rods on each end of the die and the interpolator is placed between the plates on each side and around the die. Once the machine begins to form the metal around the die and the interpolator gets taught around the die, the plates can be clamped together using more nuts to hold the interpolator in place.

3.2.2 Removal of Matched Die Hardware

Before much work could be done retrofitting the machine to do stretch forming, all of the extraneous hardware that was necessary for matched die forming but not for stretch forming needed to be removed. Since stretch forming is a process which uses only a single die, all of the pins from the moving die were removed. In the stretch forming process, the workpiece is held by clamps, attached to the stretch cylinders, and the interpolator is held by the pin alignment clamp as described above. Therefore, the blankholder, which had been previously used to hold the workpiece and interpolator, was no longer necessary and was thus removed.

3.2.3 The Clamp

The clamping of the workpiece is a very important process in stretch forming. If the workpiece slips or kinks due to poor clamping, the stresses will be uneven and the part will spring back differently along the length of the part. Uneven springback will cause the workpiece to relax to a different shape after unloading during every forming cycle, thus convergence with the closed loop shape control algorithm would be impossible.

The clamp design is similar to that of the clamps used on an Instron® Universal Testing Machine for tensile tests on sheet metal specimens. They use the self tightening, incline jaw design in which the grippers slide down the tapered clamp and cause the grippers to tighten on the workpiece when the clamps are pulled by the hydraulic cylinders. The grippers are knurled on the face that contacts the workpiece and thus dig into the sheet metal, preventing it from slipping. The grippers are controlled by a threaded bolt which has a large washer welded to the end of it. The bolt goes through a hole in the clamp body and the washer is slid into a groove in the grippers as seen in Figure 3.2. When the bolt is tightened and pushes the grippers down along the taper, the grippers engage the workpiece and tighten against it. When the bolt is loosened, it pulls the grippers up along the tapers and loosens the grippers from the workpiece so it can be removed. The grippers are connected to the clamp via two springs which load the grippers in the closed position so they will always be contacting the workpiece.

The clamp is designed to grip sheet metal blanks which are 12 inches in width and a maximum of 0.100 inches in thickness. The clamp itself is 12.25 inches deep and has

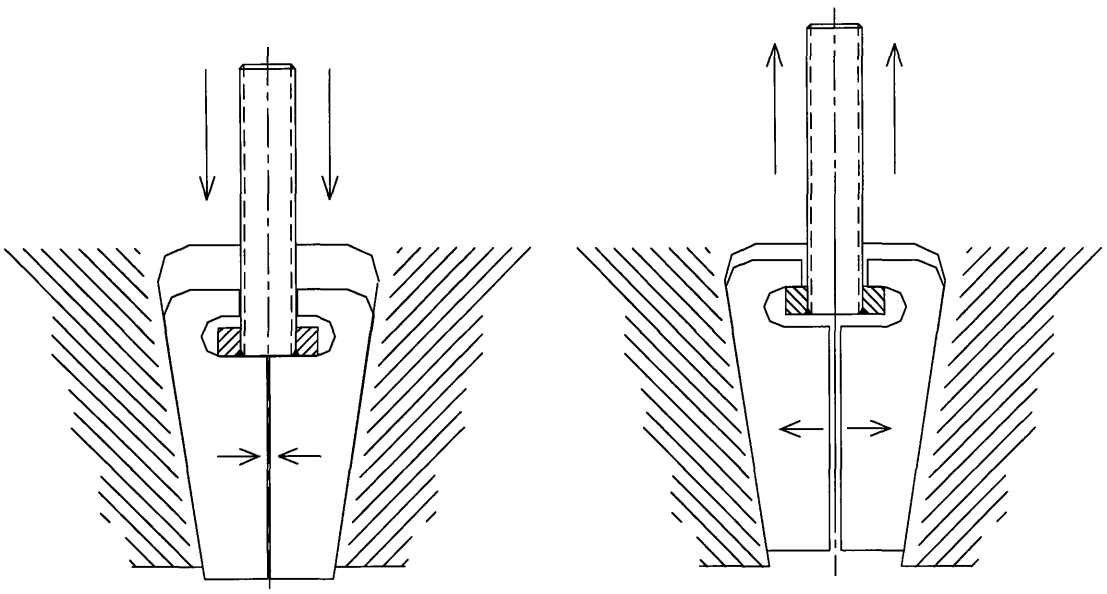

Figure 3.2: Operation of the Grippers Within the Clamp

two metal plates on either end. The plate at the bottom is solid and serves the purpose of centering the workpiece over the die. The plate at the top has a large groove through which the sheet metal is fed. Figure 3.3 is a diagram of the clamp fully assembled from the top view. The threaded bolt is not seen in the figure because the position of the top bolt is an inch and a half down from the top of the clamp. Figure 3.4 is a photograph of the clamp gripping a piece of 0.063 inch aluminum sheet metal.

3.2.4 The Stretch System and Support Structure

The stretch system, shown in Figure 3.5, is made up of the clamps, Parker hydraulic cylinders, Transducer Techniques force transducers, and Celesco optical rotary encoders. The stretch system incorporates both force and position transducers so the machine can form parts using force control, strain control or any hybrid stretch profile which utilizes both force and position. The Parker hydraulic cylinders have a 5 inch bore with 8 inches of stroke and are capable of exerting 50,000 lbs of force. The cylinders are driven by a 75 horse power hydraulic pump which delivers hydraulic fluid at 3,000 psi and 30 gal / min of flow. The Transducer Techniques force transducer has 2.5 pound resolution, but because of signal conditioning and amplifier noise, the actual resolution is

150 pounds.. The Celesco XH25D-SS-12 optical rotary encoders equipped with tensioned cables measure a linear distance to within 0.0001 inches.

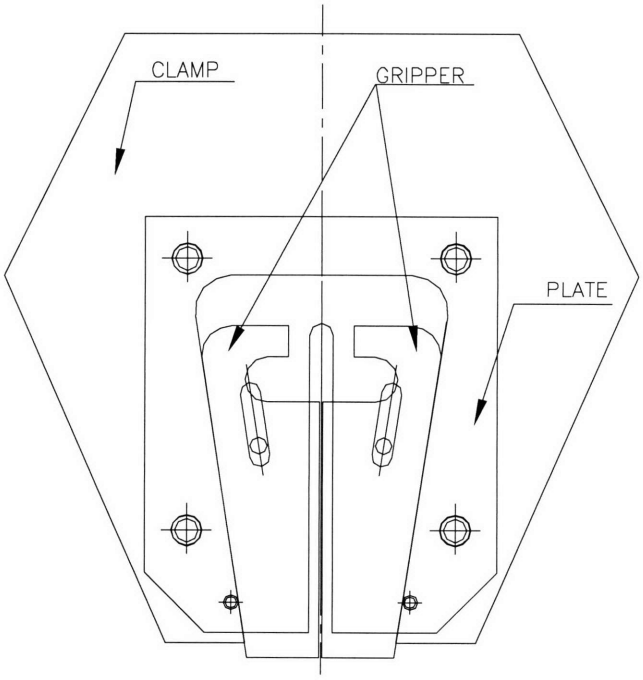

Figure 3.3: The Assembled Clamp

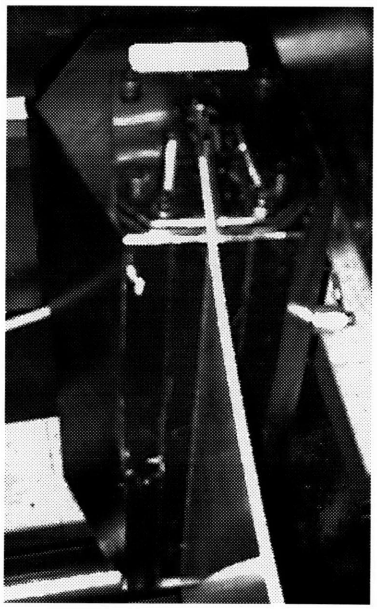

Figure 3.4: Photograph of the Clamp Gripping 0.063 Inch Aluminum

The support structure is made up of 6 large steel beams. Four of the beams are located on the sides of the moving die, two on each side, and serve the purpose of holding the hydraulic cylinders in place. These beams are 5 inch square and extend 17 inches from the die. 3 1 / 2 inches from the end of the beam there is a hole in which the thrust washer bearings lay below the trunions of the hydraulic cylinders. On each side of the die, these beams enclose the cylinder, one on top and one on the bottom, and bolt to the moving die. In addition to the four side beams, there are two stress relieving cross-beams. These beams traverse the gap between the two top side beams and the two bottom side beams. As the hydraulic cylinders stretch a piece of sheet metal, there is a resultant moment inwards on the side beams. The cross beams have steps cut into them, so they are both between the side cylinders, relieving the stress induced by the moment due to stretching, and lay on top of the side beams where they are bolted down. The entire structure is then placed between pillow blocks which are attached to linear bearings that run along the length of the machine. This is done to eliminate any gravitational effects on the support system. The attachment to the upper and lower runners relieve any stresses that would arise due to bending moments induced by gravity. This entire support system can be seen in Figure 3.5. Once the entire machine was assembled, it took the form of Figure 3.6. Figure 3.7 shows the machine after a part has been stretch formed.

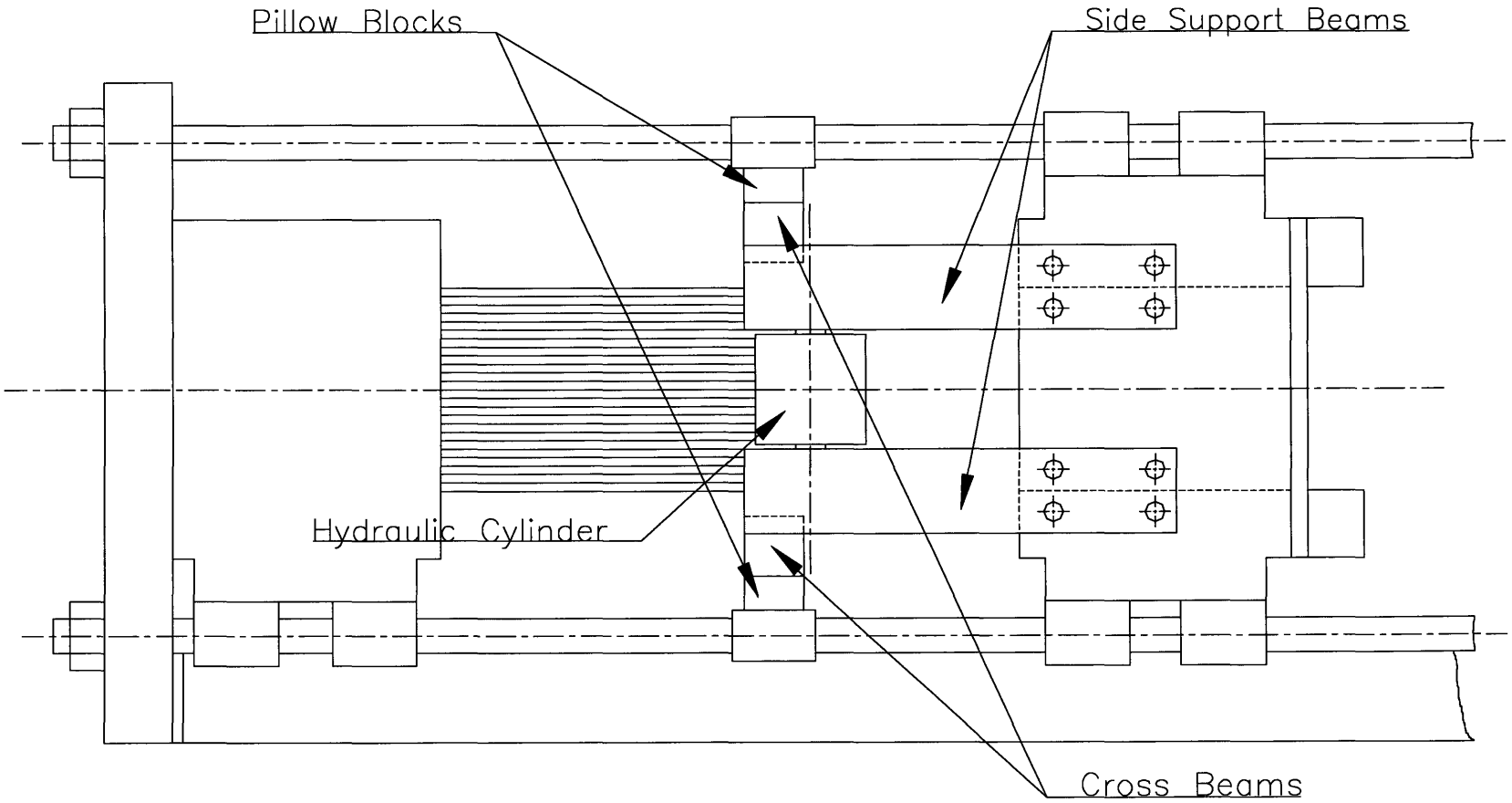

Figure 3.5: Side View of Machine Showing Support Structure Before Forming

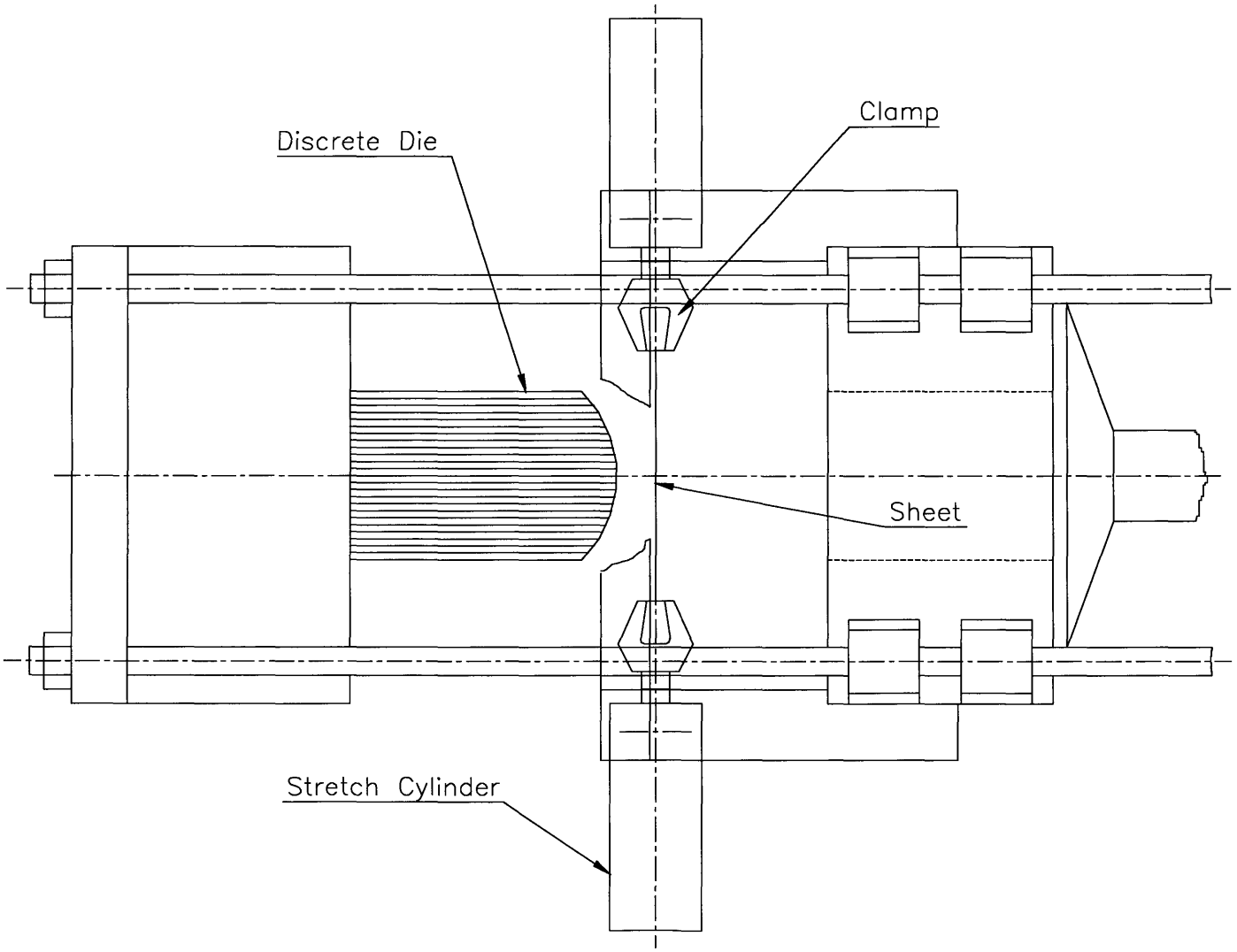

Figure 3.6: Top View of Stretch Forming Machine Before Forming

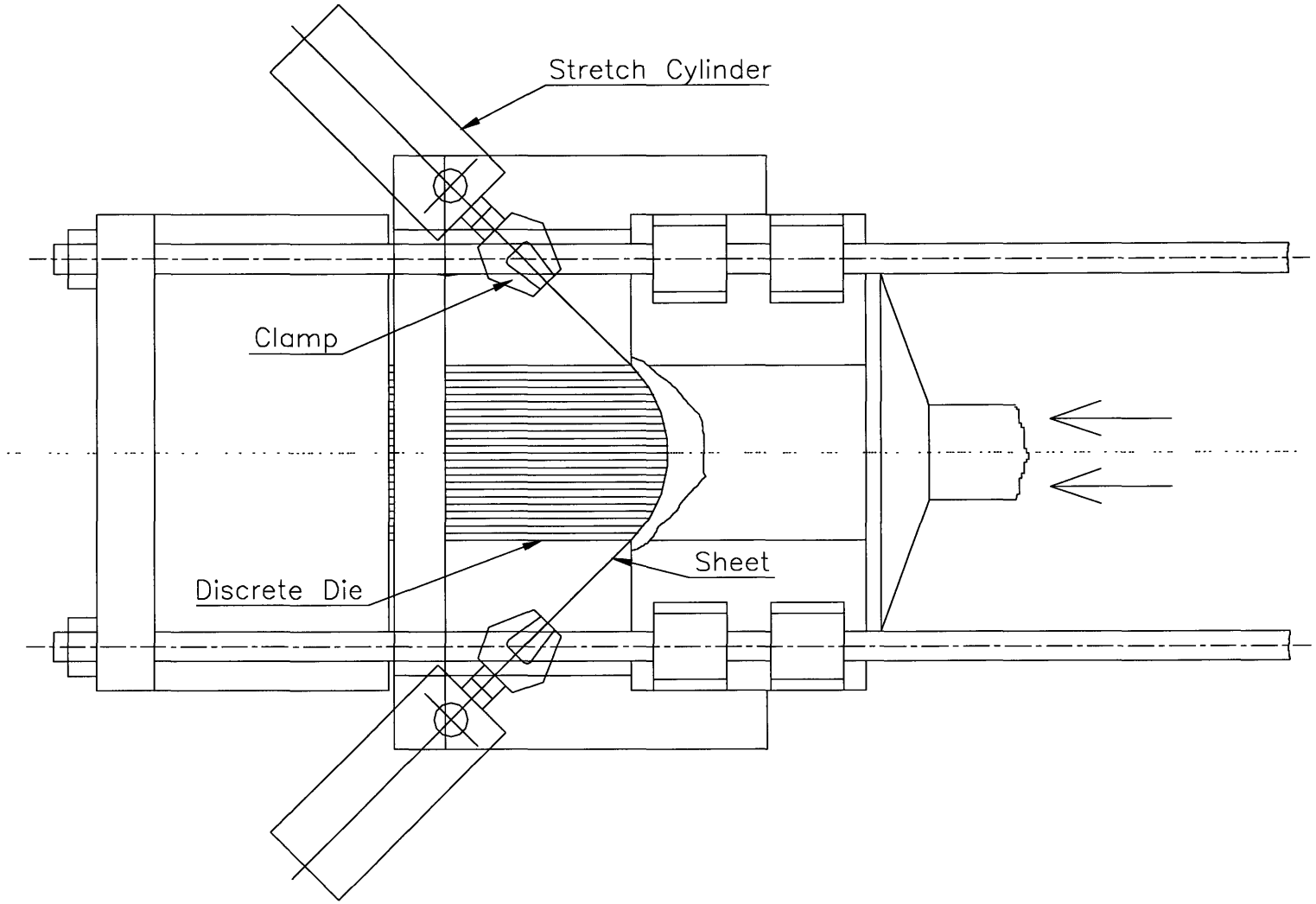

Figure 3.7: Top View of Stretch Forming Machine After Forming

3.3 Software Control

3.3.1 Galil DMC-1000 Motion Control Card and Galil ICM-1100 Interconnect Module

The new software control of the stretch forming machine centers around the use of the Galil DMC-1000 motion control card. The DMC-1000 controls four axes of motion per card and is interfaced to the PC using a high level language which uses a 126 user-defined variables and arithmetic operations and functions to achieve control. Each command is translated into ASCII code and sent down to the 32-bit specialized microcomputer located on the board to execute the command. Encoder feedback of up to 8,000,000 counts / second is permitted, to allow for high speed operation.

The DMC-1000 is connected directly into the ICM-1100 Interconnect module via ribbon cable. The module breaks up the ribbon into individual screw terminals for easy connections to the limit switches, encoders, transducers, and signal conditioners, which are all controlled by the board.

3.3.2 Velocity Control of the Servos

The control scheme which is utilized when forming parts in force control is shown in block diagram form in Figure 3.8. As shown in the figure, the control scheme is fairly simple, with the motion control card directly controlling all of the hydraulics, and receiving feedback of both force and position. The switch in the force feedback loop denotes the ability to change from force control to straight position control on the fly. This control technique is utilized in the forming program which is used to form constant force parts, and is discussed further in Chapter 4. The specific control scheme is as follows: The motion control cards, which are connected directly to the PC bus, connects to the interconnect module as described above. All references to connections to the motion control board are done through this interconnect module. The motion control card connects to the servo valves which control the hydraulics on the machine through the Parker Servo Valve Driver Card. This driver takes the $\pm 10V$ input from the motion control card and changes the voltage signal into a 0 - 20 mA current signal, which drives the servo valves. The four servo valves control the four hydraulic axes of motion; the

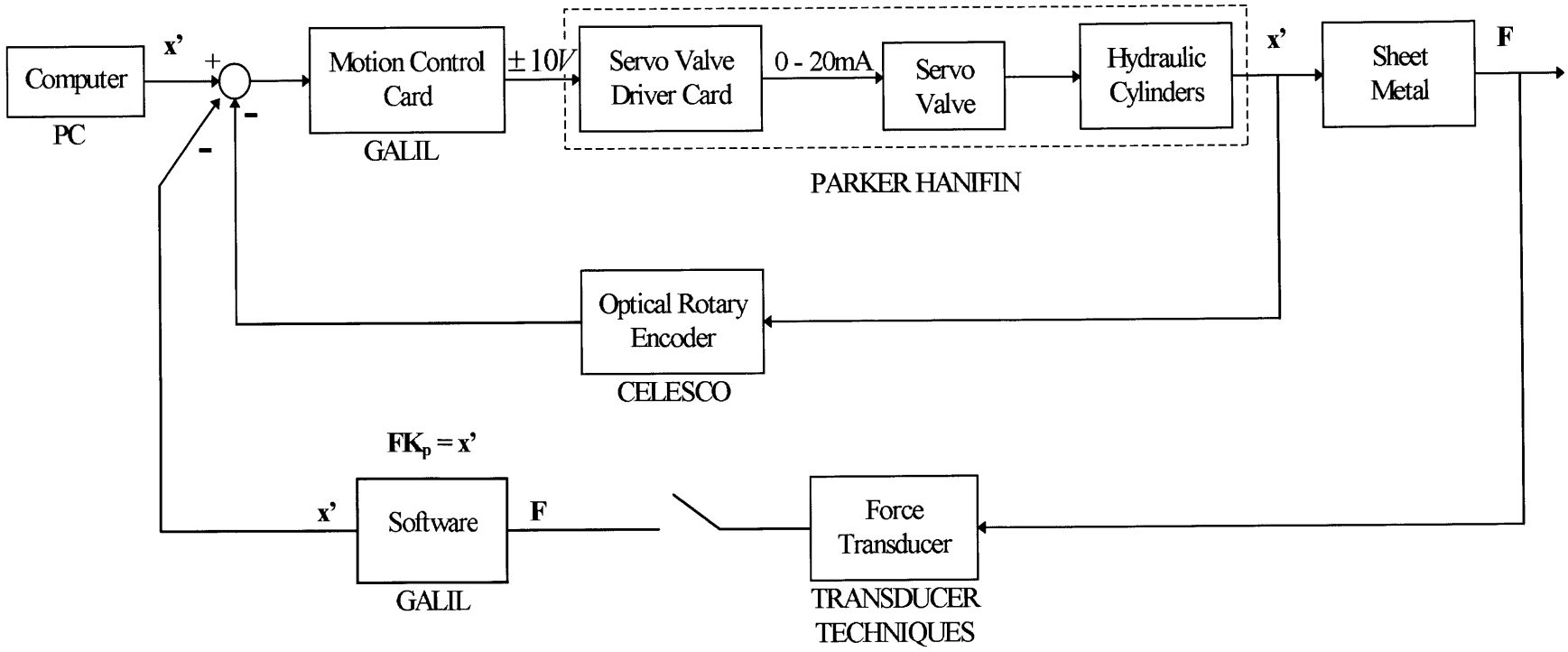

Figure 3.8: Block Diagram of Velocity Control of Servos

motion of the moving die traveling towards the stationary die, the two stretch cylinders, and the pin setting transfer mechanism. All of these four axes of linear translational motion are measured using Celesco Optical Rotary Encoders.

These encoders signals are then fed back to the control card at a sample rate of 8 Mhz. The high speed is necessary to keep the controller updated on the position of the hydraulic cylinders during a continuous forming operation. The motion of the hydraulic cylinders is converted to force through the act of stretching the sheet metal. As the sheet is stretched and wrapped, the force is measured by two Transducer Techniques TLL-50K Force Transducers. The force measurements are fed back to the motion control card after the signal has filtered and amplified by the Transducer Techniques TMO-2 Signal Conditioning and Amplifier Box. That signal converted into velocity in the Galil software using the equation; $x' = FK_p$, where K_p is the proportional gain in the controller.

3.4 The Interpolator

3.4.1 Interpolator Material

One of the major drawbacks of the discrete die is the necessity of an interpolating layer between the die surface and the workpiece to prevent dimpling. Since the interpolating layer causes loss in resolution of the discrete die, it is very important to use the optimal interpolator. The optimal interpolator is a layer which minimizes the loss of resolution while effectively removing all dimples from the workpiece.

The ideal interpolator would initially be soft enough to fill in all of the gaps between the pins, and then become perfectly rigid so that the individual pin pressure would not be translated through to the workpiece causing dimples. The other two requirements, cost and repeatability, really go hand in hand. Since the closed loop shape control algorithm needs parts to be made consistently, the interpolator properties can not change causing part variation. If this were to occur, a new interpolator layer would have to be applied during every forming trial. Even if the cost of an interpolator was extremely inexpensive, the amount of interpolator that would be needed to make many parts would create high costs and a lot of waste. Therefore, it is necessary to find an interpolator

which may be used for many forming trials, while maintaining low cost, and the stiffness profile described above.

Since the choice of interpolator material is such an important one in the forming process using a discrete die, extensive research has been done on the subject by Eigen [Eigen, 1992]. After much experimentation using various interpolator materials, it was shown that Elvax 460 (ethylene vinyl-acetate), produced the best results. It was also shown that the optimal amount of Elvax was between 1 / 8 and 1 / 4 inch for the 1 / 4 inch discrete pin setup. Since this size material would have to be custom ordered and cost thousands of dollars, 1 / 4 inch Elvax was used. Thus, the ratio between the thickness of Elvax and the pin size was a one to one ratio. Since the discrete die now uses 1 / 2 inch pins, 1 / 2 inch of Elvax is used as the interpolator. Because of material availability, this 1 / 2 inch interpolator is made up of four 1 / 8 inch Elvax layers.

3.4.2 Need for Pre-Molding the Interpolator

When parts are stretch formed using the MIT discrete die stretch forming press, the region of the sheet metal part that corresponds to the edge of the die appears to have a kink. A kink is a concentrated bending strain caused by a concentrated moment. Initially, it was thought that this kink was due to over wrapping the metal around the die. It is now known that this is not the case, but rather, it is due to the discrete element nature of the die. Not only do you have to worry about dimpling with the discrete die but also, concentrated bending moments around the individual pins. The concentrated bending occurring in the center of the die can not be seen because the neighboring pins diminish the effect. At the end of the die, there is no neighboring pin, which is why the concentrated bending is visible.

The die can be modeled as a set of line segments which connect the points of contact between the pins and the interpolator layer. Each of these line segments have a finite length and angle from the horizontal. The angle between the second to last pin and the last pin is 28.62 degrees, as seen in Figure 3.9, for a 30 degree die. If the angle between the last pin and the hydraulic cylinder's pivot point is greater than the 28.62 degrees, the metal will "kink" around the end of the die. The angle between the last pin

and the cylinder pivot is the same as the angle defined by the center of the middle pin and the tangent point of the last pin, by geometry. In this case, the die and the angle between the last pin and the cylinder pivot, is defined to be 30 degrees. This phenomenon occurs across the entire die, but since the difference between the angles of the tangent segments get smaller across the die, the "kinks" become less evident. Thus, the kink between the second and third pin is barely evident and the kink between the third and fourth pins is not

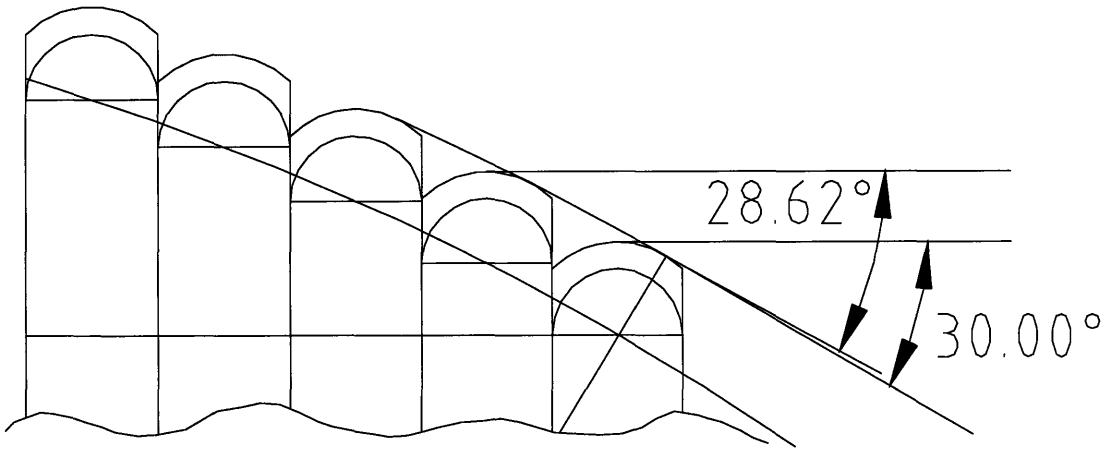

Figure 3.9: Angular Error Between Pins

visible. Though the interpolator layer gets rid of the dimpling effects, the strains due to the kinking effect still translate through, to the part for the large angle differences. The smaller kinks, from the second pin on , are absorbed by the interpolator.

The amount of wrap around the die is determined by the length that the hydraulic cylinder's pivot point travels from the beginning to the end of forming. The travel is determined using a constant curvature, smooth die, and will be discussed in greater detail in Chapter 4. Thus, the machine moves in such a way to wrap a perfect 30 degree part if the die were perfectly smooth.

The most obvious solution to this problem is to make the die perfectly smooth. The only way to do this with the discrete die is to fill the gaps between the pins so the interpolator is supported at the positions at the angle differences and can maintain the smooth surface at the interface with the sheet metal during forming.

3.5 Machine Capabilities

Repeatability between formed parts is of the utmost importance when it comes to trying to control a forming process. If there is significant error between forming trials, then not only will the parts be unreliable, but, it will be impossible to get a control algorithm to cause the part shapes to converge to a reference shape. Also, if the noise margins are too large, the controller will believe that the reference shape has been achieved though the actual part may still be significantly different. Thus, characterizing the machine capabilities and errors is important to know very accurately.

A repeatability study was done by forming seven parts over a single die, without resetting the die or changing the interpolator layer. A second study using the same parameters over a different radius of curvature die shape was then performed for three parts. Once the parts were formed, they were trimmed, using a sheet metal shear, six inches from the center of the part along the arclength. Once trimmed, the parts were measured using the Brown and Sharpe coordinate measuring machine. The measurement process is discussed in detail in Chapter 5. Once the data from the parts was accumulated by the CMM, the data was put into an Excel spread sheet and an error analysis was performed.

The die over which the seven parts were formed was a 30 degree, constant radius of curvature die. Four 1 / 8 inch layers were used to form one half inch of interpolator between the sheet metal and die. All of the parts for both studies were formed using the same material, 0.063" 2024-O Aluminum, the same stretch profile of pre-stretch to 11,000 pounds or ~1.5% strain, and formed under the same constant force control, with no post-stretch. As you can see from Figure 3.10, when the part data has been arranged such that the part heights have been set equal at their maxima, and all of the other points correspond to the points directly above the individual pin positions, it is practically impossible to

discern any recognizable difference between the parts. The error analysis shown in Figure 3.11, is done by subtracting the minimum part height from the maximum part height at each points along the graph. It can be easily seen that the error between parts is much more evident in this form. From the figure it can be seen that the maximum error is 20.4 thousandths of an inch. In the second test, the machine faired even better, with maximum error on the order of 9 thousandths of an inch, as seen by Figures 3.12 and 3.13.

The results from this error analysis were good, even though there was a lot of room for error throughout the forming process. From the start, the trimming process is done by hand, measuring around the arc of the part six inches from the center, which is also marked by hand. Then the trimming is done with a sheet metal shear, marking the trim line by eye. Once the part is trimmed, the part is loaded onto the clamping device used for CMM measurement. The claming device holds down the corners of the part against its base, using four needle points, applied to the part by a threaded rod mechanism. Once the parts are measured the data is processed using MATLAB and Excel, see Chapter 6, which introduces computational noise and 'spline' errors. With all of these possibilities for error to enter the system, it was encouraging to see the actual maximum error was still far less than the industry standard.

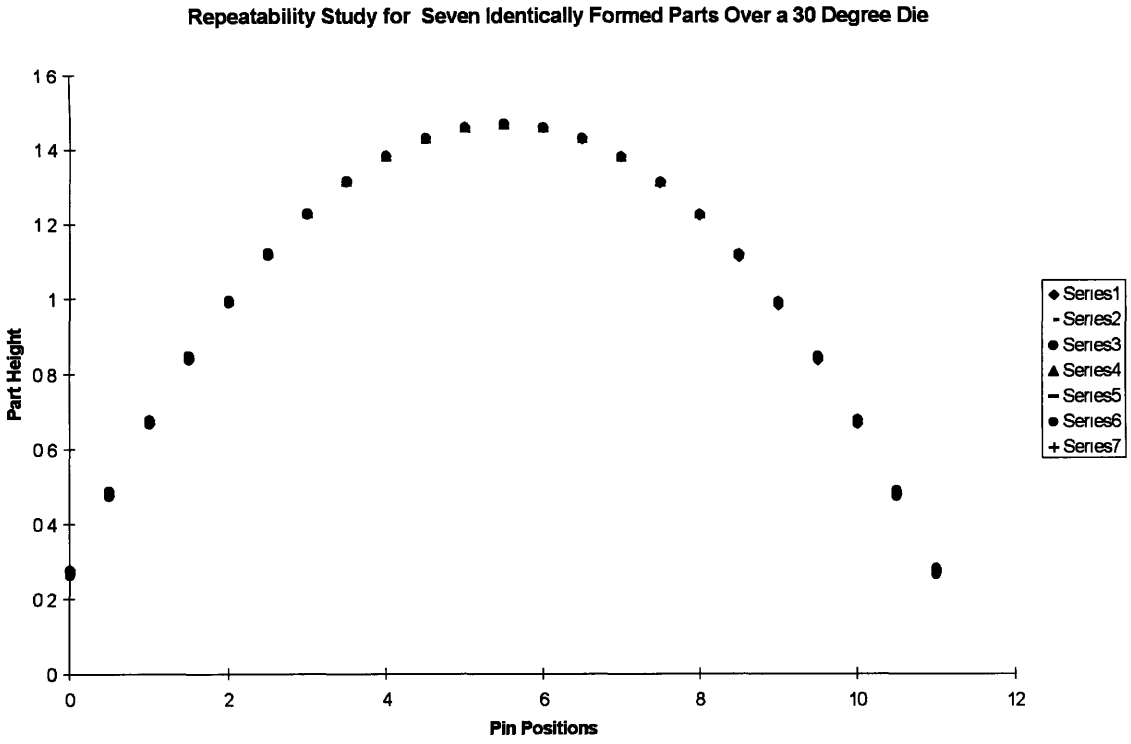

Figure 3.10: Actual Part Data From Seven Measured Parts

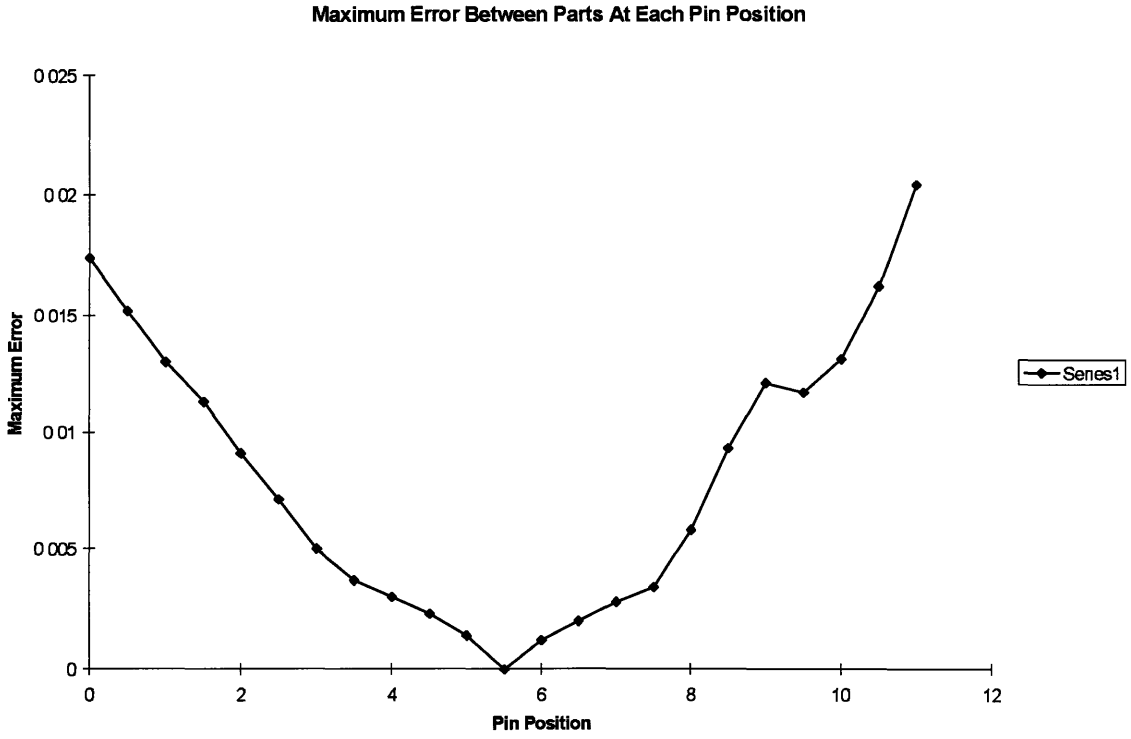

Figure 3.11: Maximum Error Between Seven Identically Formed Parts

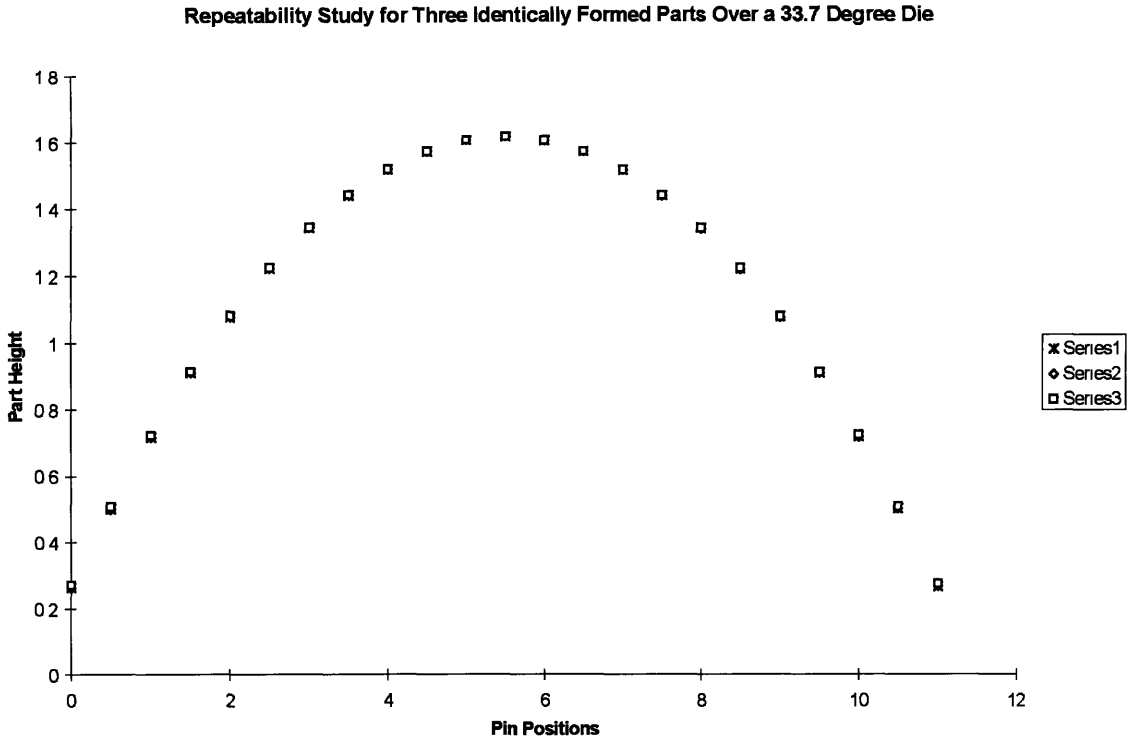

Figure 3.12: Actual Part Data From Three Measured Parts

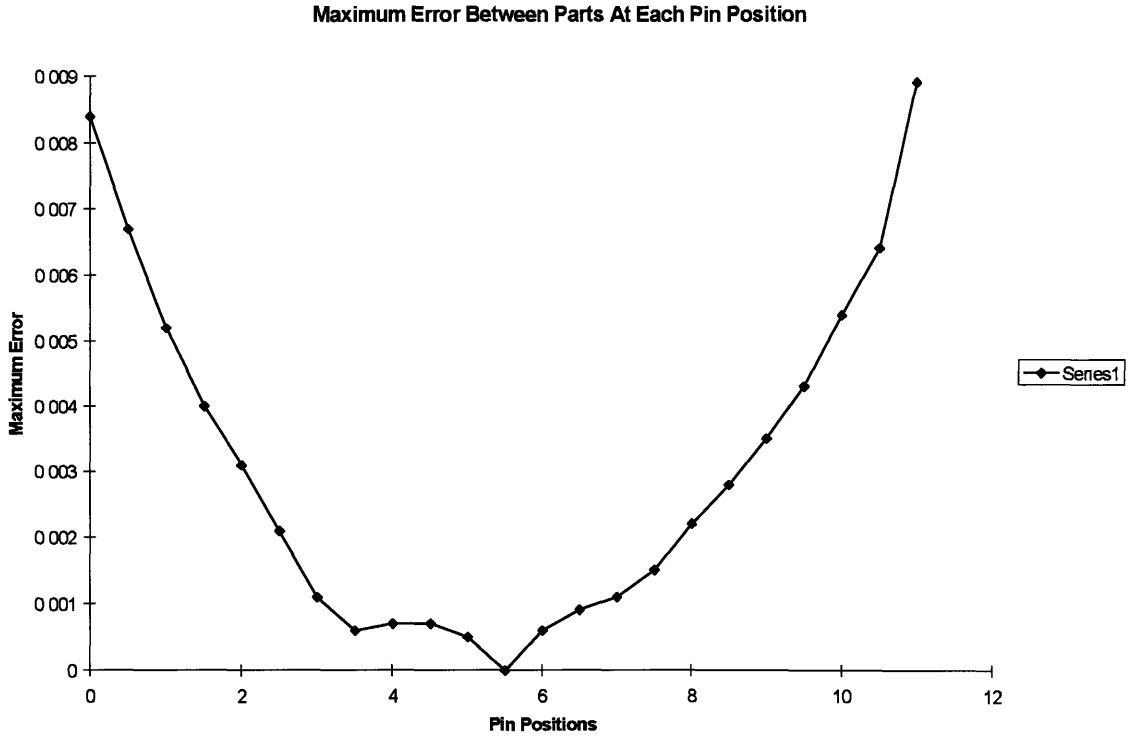

Figure 3.13: Maximum Error Between Three Identically Formed Parts

CHAPTER 4: MAKING A PART

There are many steps that are involved in making a part with the discrete stretch forming machine. They include: setting up the die, applying the interpolator layer, forming the part, and trimming the part. One of the main criteria for the closed loop transfer function to work is repeatable parts. If the parts are made differently each time, the algorithm will adjust for the machine error, instead of the shape error. Therefore, each of these procedures must be done with great care, to assure that the parts are made exactly the same. The following chapter will describe how each of these steps involved with making a part were done.

4.1 Setting Up the Die

4.1.1 Procedure for Setting Up the Discrete Die

Since this thesis is only involved with two dimensional shapes, it is not necessary to employ the use of the setup pin mechanism, which is the device which uses the eight servo motors to change the positions of the setup pins. For a two-dimensional die, the columns of the die will all be at the same position, therefore, the set up pins will all be at the same position.

The first thing that needs to be done when setting up the discrete die is homing the machine. This is done by setting the stretch cylinders and clamps, the discrete pins within the stationary die, and the setup pins to their respective home positions. The homing of the stretch cylinders and clamps is a fairly simple process of executing the *HOME.DMC* program in the Galil software. All of the relevant Galil software programs that were used throughout this thesis will be found in Appendix A. The *HOME* program sends commands to the motion control board, which in turn commands the servo valves to completely retract the cylinders and then extend them a small amount determined by the size of the workpiece. Homing the cylinders serves the purpose of setting the cylinders to

their proper positions for sheet metal loading, and gets them out of the way for the homing of the pins.

The home position for the discrete die is such that the pins form a flat surface, flush with the back of the stationary die. This is accomplished using a one inch thick steel plate which has been attached to the moving die over the hole where the pins used to be. When it is time to home the pins, the valve which controls the clamping cylinders must be turned completely off, and the interpolator layers and pin alignment clamp must be removed from the die. Once the clamping is removed from the pins, the moving die is sent towards the stationary die. As the steel plate contacts the pins, the pins begin to slide back towards the rear of the stationary die. Once the pins are flush with respect to the back of the stationary die, the moving die is brought back to its home position which is located at the end of its travel away from the stationary die.

The setup pins are homed using the back of the stationary die as a homing surface. The setup pin carriage is moved all the way across the back of the die to its furthest right position, when looking at the back of the die. Once the carriage stops, due to the tripping of the limit switch, the setup pins must be homed. In order for this to occur, the valve that controls the clamping of the setup pins must be closed. Once the setup pins are able to move freely, the pins are pulled out and placed against the back of the stationary die. Since the back of the stationary die is a large, flat steel block, it can be used as a reference surface. Once all of the setup pins are homed, the clamping valve is opened again and the hydraulic cylinders that control the motion of the setup pins are retracted approximately one inch. This is done so the setup pins do not scrape against the back of the stationary die or the ends of the pins, when the carriage is moved to its setup position. The setup pins are not very sturdy, thus, any moment applied to their tips may bend or damage them.

Once the entire machine is homed, the hydraulics for the process of setting the pins must be set. In order to prevent the neighboring columns of pins from moving freely due to frictional forces during setup, a small force must be applied from the clamping cylinders. The valve that controls the fluid flow to the pin clamping hydraulic rams must be opened and then closed so that only ~ 100 lbs. / $in.^2$ is acting on the pins. The hydraulic booster must then be applied with the pressure adjusted to ~ 2000 lbs. / $in.^2$.

Once the pin setup carriage and the hydraulics have been positioned properly, the discrete die is then set by one of the setup programs in the Galil software.

Each of the setup programs written using the Galil software, use the same procedure to set the pins, while using different pin height arrays to create different die shapes. The setup programs first move the setup pin carriage such that the setup pins are in line with the first row of pins. Once the setup pins are lined up, they are driven into the first row of pins a distance corresponding to the first number in the measurement array, plus an offset. The offset is used to ensure the setup pins contact the pins. As mentioned earlier, the setup pins are retracted approximately one inch from the back of the stationary die during homing, and thus the offset must account for that distance. Each of the next columns are set up the same way. The program instructs the carriage motor to move to the next column of pins and then instructs the pin setting cylinders to extend to the appropriate length, according to the position in the measurement array. Once all of the pins have been set, the program ends and the pin clamping valve should be opened once again, to clamp the die in place.

4.1.2 Determining Pin Positions

The most important element for the closed loop shape control algorithm to work is accurate die shapes, which for a discrete die means accurate pin positions. Although the pin positions for the closed loop die shapes are all output by the shape control algorithm, the open loop die shapes are determined by the operator. Since all of the parts formed are two-dimensional and constant curvature, the equation for a circle is used as a governing equation for the pin positions. A problem arises since each of the pins have spherical tips. A circle can not be simply fit to the tips of each pin; instead, the circle must be fit to the point in which the circle would touch the pin, the tangency point. In order to accomplish this, the circle that defines the die shape, Rd, goes through the center of the circles defined by the tip of the pins, as shown in Figure 4.1. The actual pins are positioned using the procedure described above and require a measurement array. The values of the measurement array give the positions of the centers of the circles defined by the pin tips, which lie along a larger "die defining" circle. These values are set using the

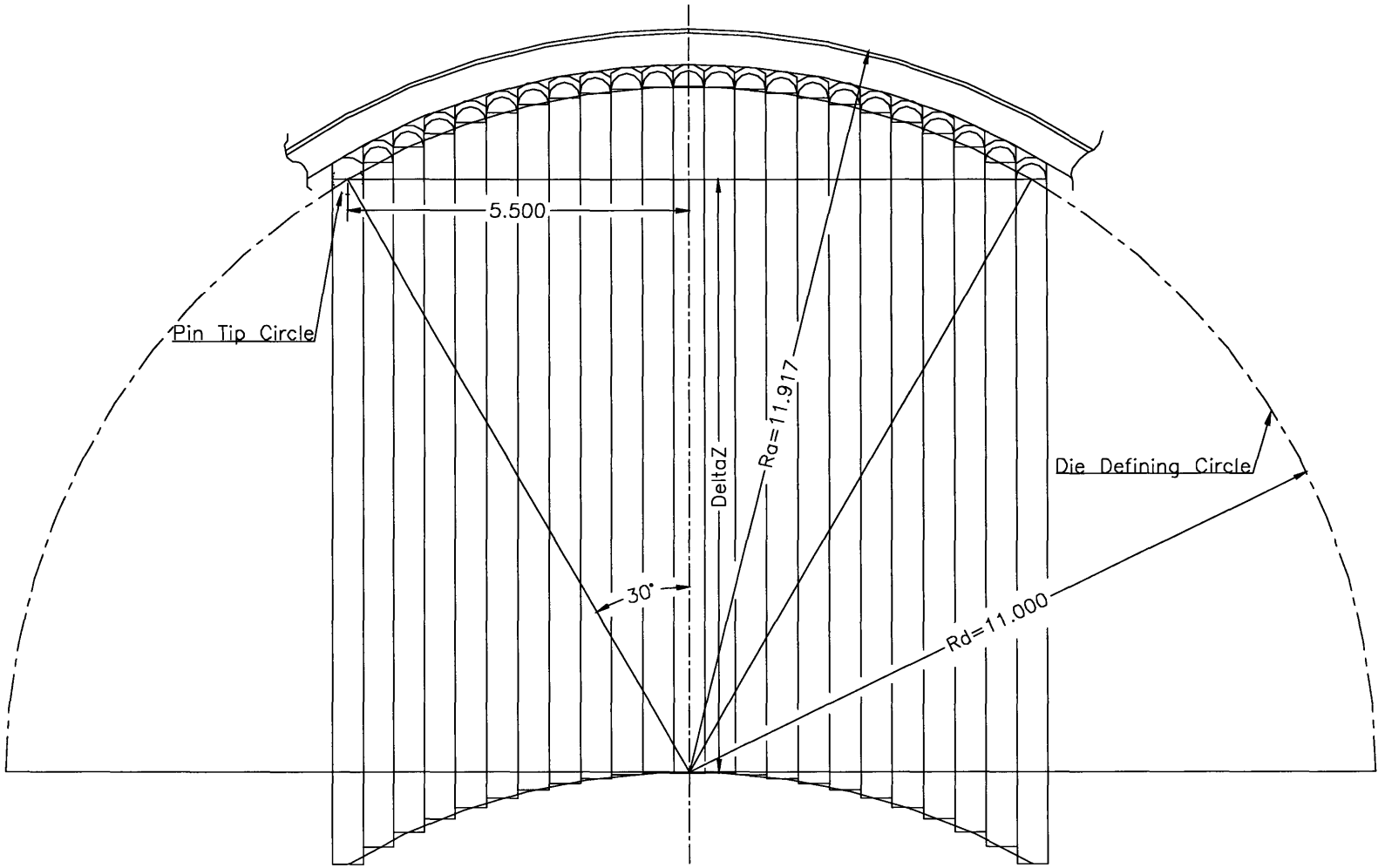

Figure 4.1: Geometry for Setting the Discrete Die

center of the last pin as a zero reference for x and y. The larger "die defining" circle is determined by the radius of curvature for the die shape desired.

The actual values for the pin positions are found using the equation for a circle:

$$Z = \sqrt{R^2 - X^2}$$

Shifting the center point to the middle of the first pin involves both an X and a Z shift. The X shift is accomplished by simply subtracting the distance of the desired shift, 5.5 inches, from the X term in the equation above. The value 5.5 will always remain constant since it is determined by the thickness of the pins. The Z shift is upwards, a distance of ΔZ, as shown in Figure 4.1. This distance is determined by the geometry of the die, through the relationship:

$$\Delta Z = Rd * \cos\Theta$$

where Θ is defined by:

$$\Theta = \sin^{-1}\left(\frac{5.5}{Rd}\right)$$

Θ is 30° in the figure. Once all of the shifts have taken place, the equation which governs where the pins are positioned is as follows:

$$Z = \sqrt{Rd^2 - (X - 5.5)^2} - \Delta Z$$

where X is defined to be an array of numbers from 0 to 11 in 0.5 inch increments. Thus, X locates the center of each pin, and Z gives the height the pin should be at in order to create the specified die shape.

4.2 Applying the Interpolator Layer

Applying the interpolator layer is a two step process in which the pin alignment clamp must first be applied, and then the interpolator attached to it. The application of the

pin alignment clamp should be done with low hydraulic pressure running throughout the system. This will cause the pin clamping cylinders to hold the pins tight while the pin alignment clamp is applied. This is necessary because the pin alignment clamp must be clamped very tightly around the pins. Tightening the pin alignment clamp is accomplished by tightening the bolts on the threaded rods. The bolts require a lot of torque to tighten, which could move the pins if they are not clamped by the hydraulic rams.

Once the pin alignment clamp is in place, the second plates are put on the threaded rods on the pin alignment clamp to hold the interpolator layer. The four layers of 1 / 8 inch Elvax are placed between the two plates on the pin alignment clamp around the die and held in place by tightening the second set of bolts on the threaded rods, outside the plates. The bolts should only be hand tightened, so the interpolator can then be moved to cover the die. The bolts should remain hand tightened during forming, so as the sheet presses the interpolator against the die the interpolator can flow between the plates. Once the forming process is finished, and before the pressure has been released, the bolts can be tightened to hold the interpolator snug against the die.

4.3 Forming a Part

To concentrate on identifying machine, measurement, and forming error, one forming profile was used to form every part. The parts were made under force control, with a stretch profile that involved an 11,000 lbs. pre-stretch, constant force wrap and no post-stretch. The material which was used was 0.063 inch 2024-O Aluminum, thus the 11,000 lbs. stretch corresponded to about 0.75% strain within the material. As shown in Chapter 2, this stretch profile yields the most amount of springback of any of the stretch forming profiles. This was an intentional procedure and not an oversight. Since the purpose of this thesis is to examine the performance of the closed loop shape control algorithm, it is necessary to have significant springback so the change caused by the algorithm is visible. Once the algorithm is proven to work, the stretch profile should be changed to include post-stretch in order to make parts which springback less and thus converge faster to the reference shape.

The forming program, *WRAP.DMC* in Appendix A, requires two values as input; pre-load force and y-travel. The pre-load force is defined to be the amount of stretch that will be applied before the forming of the part. The y-travel is defined to be the distance that the center of the trunions on the hydraulic stretch cylinders will travel from the point when the material just comes into contact with the die, until the wrap is complete.

4.3.1 Defining the Y-Travel and Stopping Criterion for Forming

The y-travel of the machine is probably one of the most important and difficult variables to control in the forming process. Since the machine is not capable of making angular measurements on the stretch cylinders to determine the angle of wrap, a linear distance must be computed to determine when a particular angle has been achieved. This distance is the y-travel of the machine. The difficulty lies in determining when the part comes into contact with the die, to start counting the y-travel. This problem was temporarily solved by attaching a limit switch to the cross beam of the stretch cylinder support structure. The central pin on the die has a half-moon shaped piece of plastic that trips the limit switch as it passes over it. The problem is that the plastic had to be adjusted by eye to trip the limit switch when the part hit the die. Therefore, though the machine will travel the proper distance, it may start counting that distance too early or too late. This will cause under or over wrapping, which will affect the accuracy of the formed part.

For a two-dimensional, constant radius of curvature part, the angle formed by hydraulic stretch cylinder and the y-axis should be the compliment of the angle formed internally in the die, by the center of the middle pin and the center of the last pin, in order to wrap a part tangent to the die. This can be seen in Figure 4.2.

In order to determine the y-travel for a particular radius of curvature, some machine measurements must be known. Those measurements are, the distance between the center of the middle pin and the center of the trunion on the hydraulic cylinder, D, and the distance between the center of the middle pin and the center of the last pin. These two measurements characterize the cylinder to die relationship, and characterizes the size of the die.

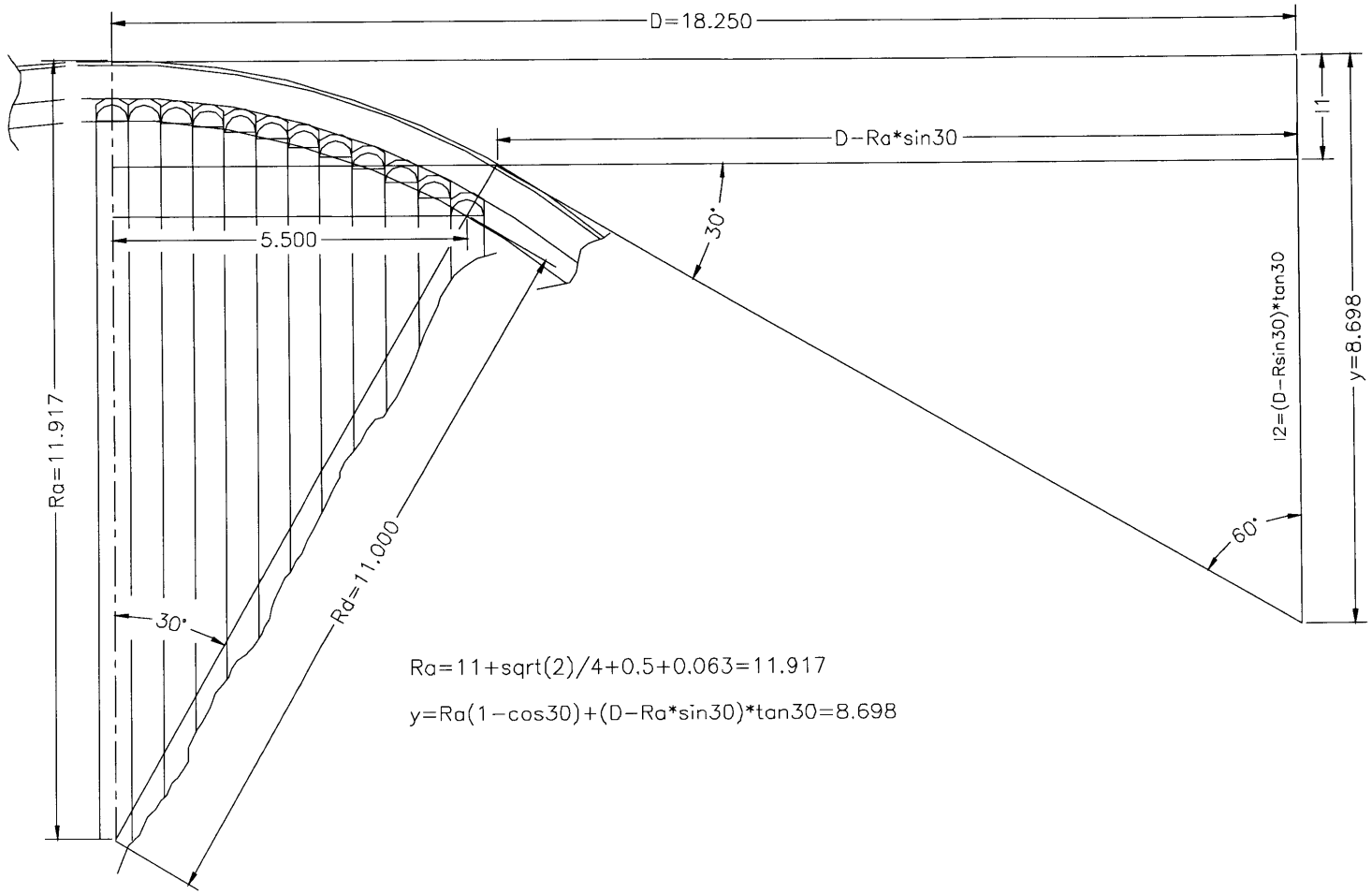

Figure 4.2: Geometry for Computing Y-Travel

The y-travel is computed by breaking the total travel into two smaller lengths that are easier to solve, using trigonometry. The first length, l_1, is the distance between the top of the sheet over the die and the projection of the tangency point onto the central axis. In Figure 4.2, l_1 is computed by subtracting the projection from the distance from the center of the die to the top of the sheet, *Ra*, and is shown below, where Θ is 30°.

$$l_1 = Ra*(1-\cos\Theta)$$

The second length, l_2, is the distance between the tangency point, and the intersection of a straight line extended from the tangency point and the position of the center of the trunion of the stretch cylinder. This length requires solving for the distance between the tangency point and the center of the trunion when it is perpendicular to the tangency point. This distance is:

$$D - Ra*\sin\Theta$$

where D = 18.25 inches, is the distance between the center of the middle pin and the center of the trunion on the stretch cylinder, and Θ is 30°. Now l_2 can be found by:

$$l_2 = (D - Ra*\sin\Theta)*\tan\Theta$$

Knowing l_1 and l_2, the y-travel is simply the addition of the two terms.

$$y = l_1 + l_2 = Ra(1-\cos\Theta) + (D - Ra*\sin\Theta)*\tan\Theta$$

This equation for the y-travel can be used for any constant radius of curvature, two-dimensional die.

4.3.2 Control Scheme for Forming a Part

Once the inputs, pre-load force and y-travel, have been determined, the *WRAP.DMC* program can be run. The *WRAP* program is divided into three sections; pre-load, one cylinder position control wrap, and full force control wrap. The motion control cards have many axes of motion under its control, the stretch cylinders are the Z and W axes. The pre-load is done by retracting the two stretch cylinders, Z and W, until they reach their stopping conditions. Each cylinder begins to retract at a velocity of 150 encoder counts per second, and then slow down, proportional to the difference between the input pre-load force and the force being feedback through the force transducers. When the Z cylinder reaches 95% of the pre-load force, the program enters the one cylinder position control wrap phase.

Up until this point, the two cylinders have been retracting together at the same rate. Once the Z cylinder reaches 95% of the pre-load force, that cylinder locks its position and waits until the wrap around the die begins, before reentering force control. When the Z cylinder stops, the W cylinder continues to pull until the pre-load force is achieved. Once the force transducers feedback the pre-load force, the moving die begins to travel toward the discrete die at a rate of two inches per minute. This speed can probably be increased with some adjustment to the gain of the controller. Once the limit switch is tripped, the Z cylinder waits for seven seconds, which translates to approximately one quarter of an inch of y travel, before engaging the force control again. This force and position control scheduling is necessary to prevent the stretch cylinders from fighting each other and going unstable or "walking" across the face of the die with the workpiece. When the part begins to be wrapped around the die, the frictional forces prevent the "walking" of the cylinders, and true force control can be achieved.

As the full force control wrap progresses, the cylinders must move at a faster rate to adjust for the change in force as the angle of wrap increases. Because of this need for more velocity, the gain of the controller is scheduled so that it increases as the wrap progresses. Thus, as the part nears the end of wrap, the gain is at its peak, trying to adjust for the large change in force which results from small movement in the y direction. The gain schedule in the program works better than if the gain were kept constant, but, by

watching the force throughout the wrapping of a part, it can be observed that the force varies by approximately 500 pounds towards the end of the wrap. That is, the force begins at 11,000 pounds and begins to increase as the cylinders can not keep up with the change in force, and peaks at about 11,500 pounds, before the motion stops and the fluid within the cylinders relaxes and the force drops back down to 11,300 pounds. This 4% steady state error has shown to show very little affect on the repeatability of forming parts. Better gain scheduling could be investigated should the need for a more accurate force control present itself.

4.4 Trimming the Part

Once the part has been wrapped around the die to completion, the part is moved away from the die, the pressure is released and the part is removed. The area of the part of interest is the region that was directly over the die, therefore, the rest of the material must be trimmed away. Since the parts are two-dimensional and constant curvature, the area to be trimmed away is flat. This shape lends itself very well to trimming and was able to be done on a conventional sheet metal shearer. As secondary curvature is introduced to the forming process, the sheet metal shear will not longer be a viable option for trimming. Research will have to be done in the areas of laser and water jet cutting, as a replacement method for the sheet metal shear.

In order to trim the part, the center position must be marked on the part during forming. This is accomplished by lining up the mark on the center of the middle pin with the part during forming and marking the part as accurately as possible. This mark is only the approximate center, since it is drawn by hand, but is good enough for the purposes of trimming the part. Once the part is trimmed, the exact center is found in software and the part data is interpolated and splined to get the useful data from it. This process is described in detail in Chapter 6.

The part is trimmed six inches from the center along the arc of the part on each side. This length was determined because it exceeds the edge of the die, therefore all of the important data is included in the trimmed part.

CHAPTER 5: MEASUREMENT

Perhaps even more important than the repeatability of the forming process is the reliability of the measurement technique. The only means of communication between the actual formed part shape and the closed loop shape control algorithm is the shape measurement. Therefore, a good measurement technique must be employed so that the measurement error is negligible compared to the error caused by incorrect part shape.

The apparatus employed to measure the part shapes is a Brown and Sharpe mm4 Coordinate Measuring Machine (CMM). There are two main concerns when using the CMM: fixturing and measurement spacing. The fixturing device should allow for quick clamping and provide good reference surfaces but not distort the part. The ideal measurement spacing would be the minimum number of measurements needed to accurately describe a part. The curve fitting method in software is very closely related to the measurement spacing and thus must be addressed as well. An in-depth discussion of measurement spacing and curve fitting is in section 5.2.

5.1 Fixturing the Part for Measurement

The need for a good fixturing device when measuring on a CMM is of the utmost importance. Since the CMM is accurate to within a few ten thousandths of an inch, the part should always be clamped to the CMM the same way, and should always use the same surfaces for referencing the measurements. In addition to having good reference surfaces, the fixture must be able to clamp the part without distorting it. If the shape of the part is changed due to fixturing, the algorithm will compensate for measurement error rather than die error. These are the properties that a good fixturing device should have, to minimize measurement error.

Since the parts being measured are two-dimensional, and have a constant radius of curvature, the fixturing device was constructed to clamp down normally on the corners of the part. The clamps have three degrees of freedom in order to insure normal clamping: vertical translation, rotation about the y-axis, and radial translation. There is also a fine adjustment to the radial motion, achieved by a threaded rod moving within the clamp. The interface between the fixture and the part is a needle point. This point allows for minimal clamping surface, so the CMM measurement ball can reach a maximum area on the part. The clamps are all attached to a machined base plate which is used to support and provide a reference plane for the part. In order to facilitate the loading of the part, three locator pins are attached to the base plate. There are two pins that align the part in the y-axis, and one that aligns the x-axis. This kinematic fixture assures repeatable placement of the part on the fixture every time. The fixture holding a part is shown in Figure 5.1.

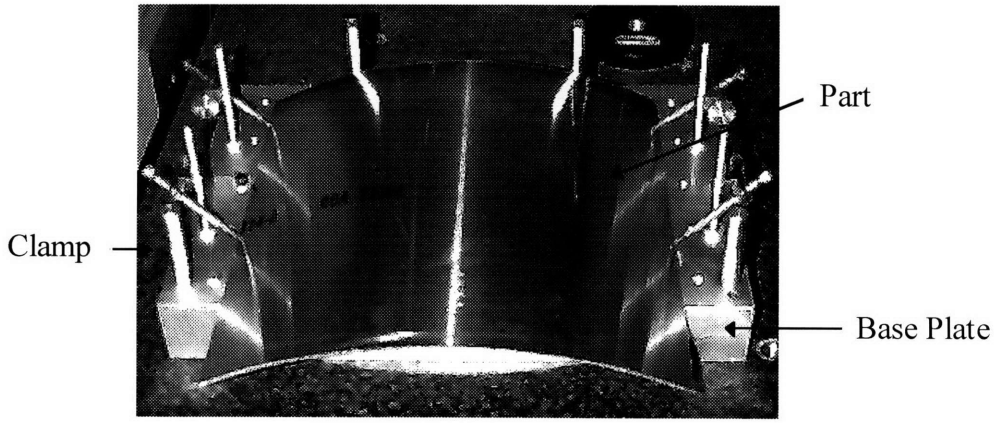

Figure 5.1: Fixture with Part on CMM

5.2 Choosing Measurement Increments and an Interpolation Method

Once the part is fixtured, it is important to create a measurement technique in which the least amount of data points are taken to accurately describe the part. Obviously, the more points taken, the more accurate description of the part the

measurement will yield. The main drawback of taking more data points is the length of time the measurement takes. Since the part is two-dimensional and constant curvature, and the ability to adjust for secondary curvature during forming is not yet available, it is not necessary to measure the entire part. Only one strip across the length of the part is necessary. In this case, when only one measurement strip is being taken, time is not really a factor, but when the entire three dimensional part must be measured, measurement time will become a much larger issue.

Once the points are taken, a curve fitting method must be chosen to recreate the shape given the discrete measured points. Cubic spline interpolation and nth order polynomial fit are two interpolation methods that were investigated for this purpose. The polynomial fit requires the order of polynomial to create the least square error fit with the data. After checking the least square error of the polynomial data versus the actual data, the order that gave the minimum error in a reasonable amount of time was 8. Therefore, an eighth order polynomial was compared with a cubic spline interpolated curve for different measurement increments to determine the optimal measurement spacing and curve fit method. The measurement intervals that were used were 1 / 32", 1 / 16", 1 / 8", and 1 / 4". The 1 / 4" spacing was chosen as the maximum measurement increment for the test because the time saved between going to larger intervals was not significant. Therefore, if it turned out that taking measurements every quarter inch still output good data, it would not be significantly beneficial to go to larger measurement intervals..

The following eight figures, Figure 5.2 - 5.9, show the analysis of the eighth order polynomial curve fit to the measured data points at varying measurement increments. For each measurement increment, the first figure shows a plot of the actual measured part data at the specific intervals, and the corresponding eighth order polynomial curve fit. The second figure shows the error between the curve fit data and the actual measured data for each point along the length of the part.

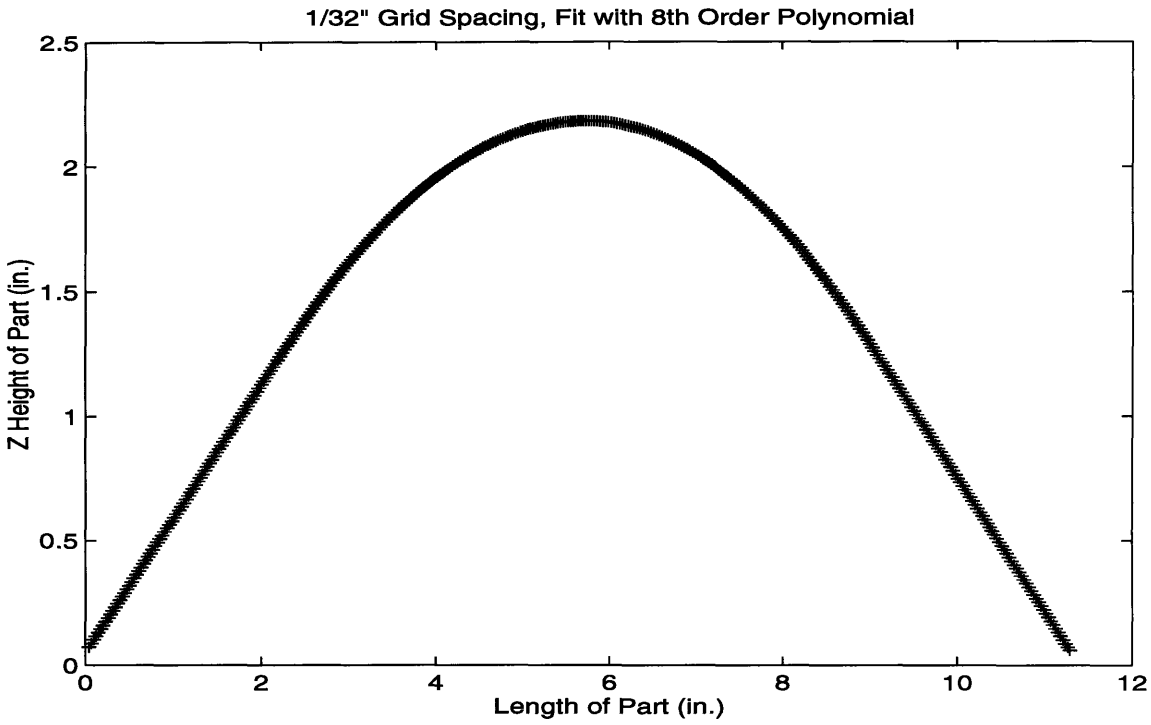

Figure 5.2: 1 / 32 Inch Grid Spacing, Fit with 8th Order Polynomial

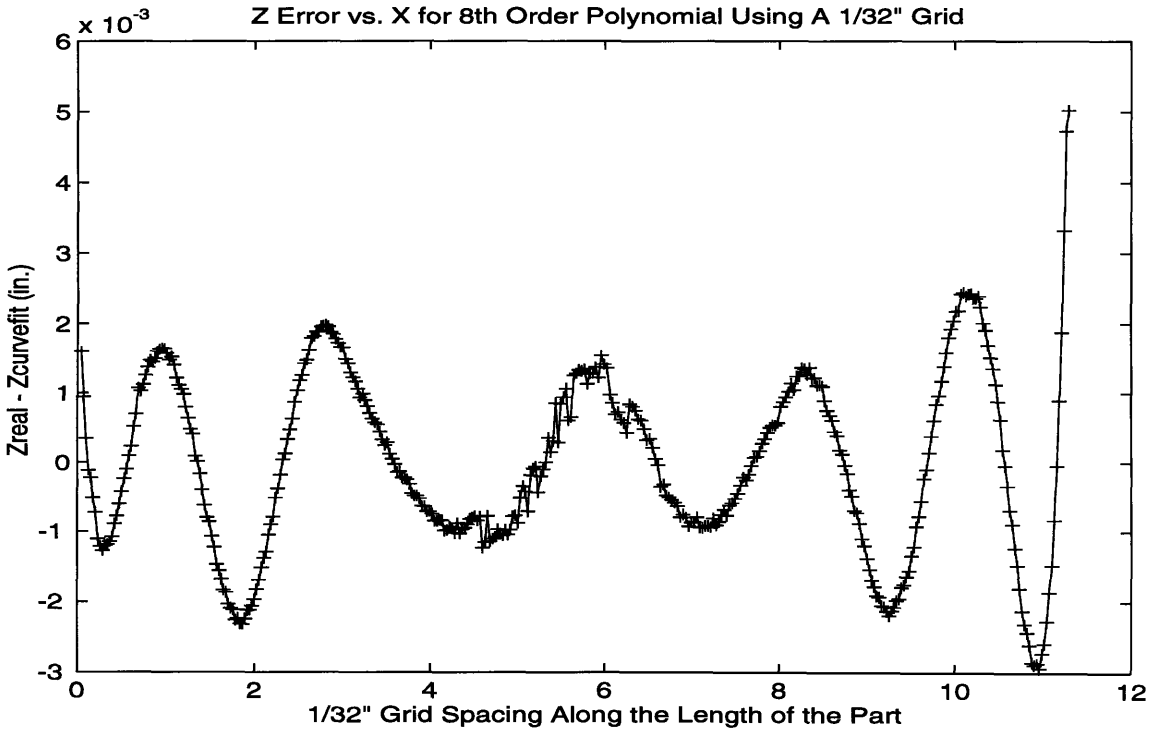

Figure 5.3: Z Error vs. X for 8th Order Polynomial Using 1 / 32" Grid Spacing

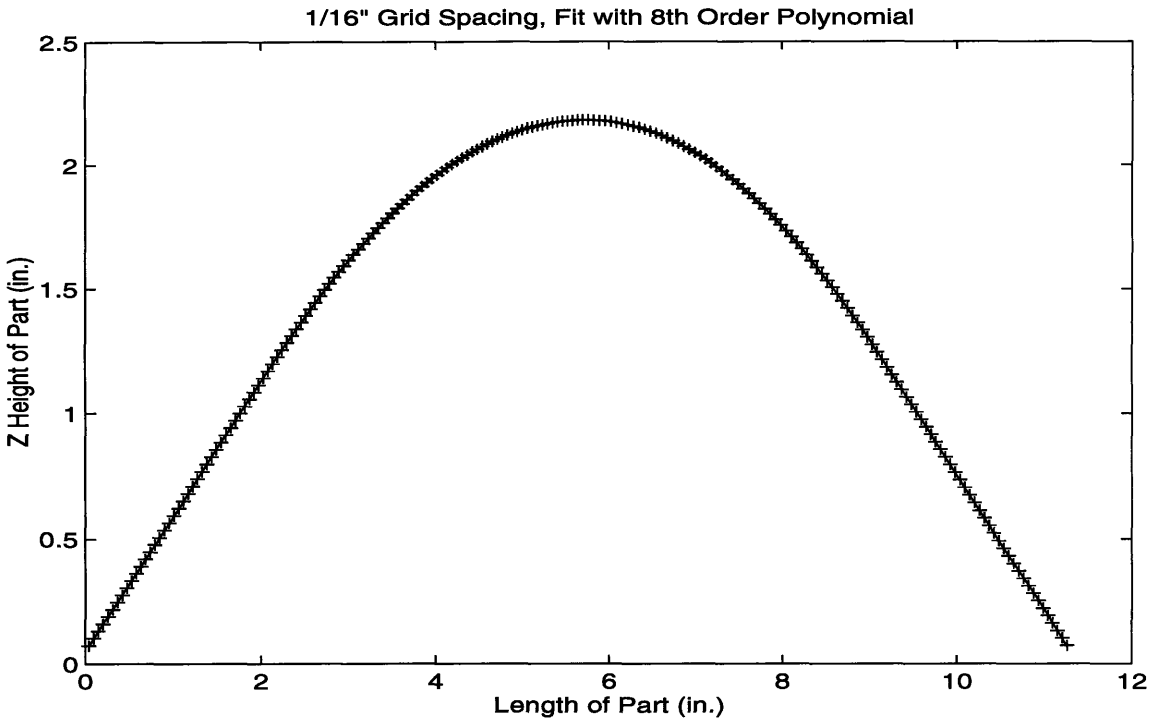

Figure 5.4: 1 / 16 inch Grid Spacing, Fit with 8th Order Polynomial

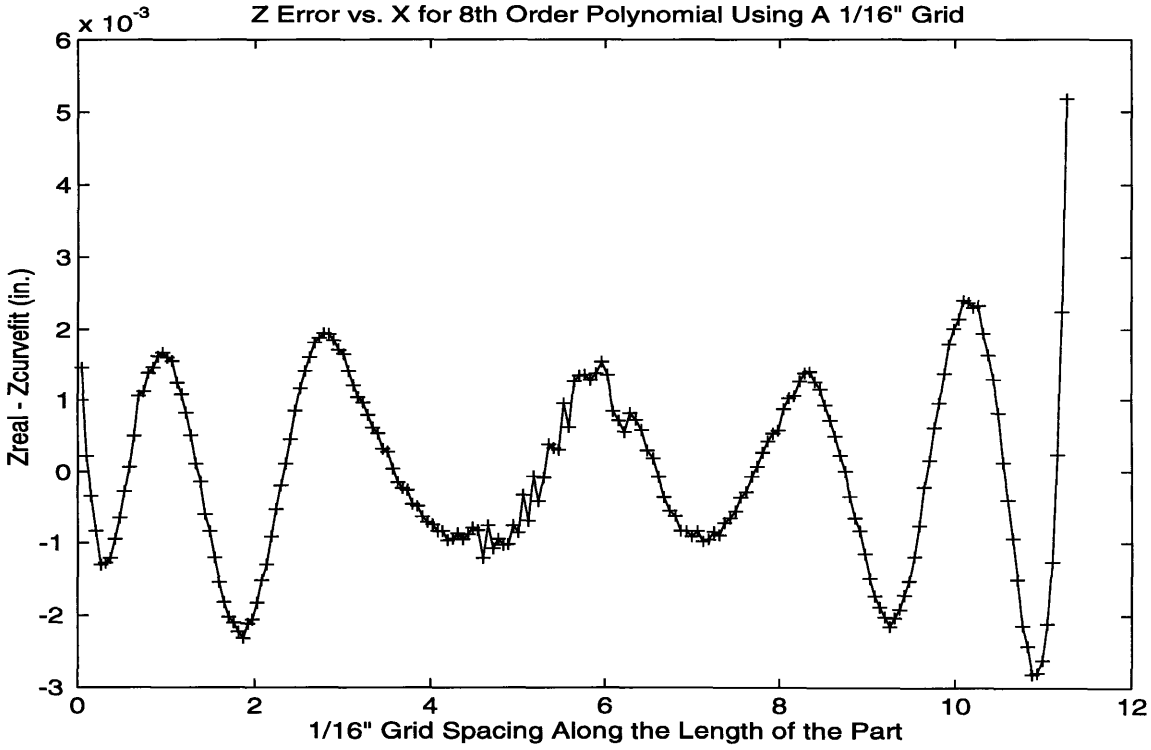

Figure 5.5: Z Error vs. X for 8th Order Polynomial Using 1 / 16" Grid Spacing

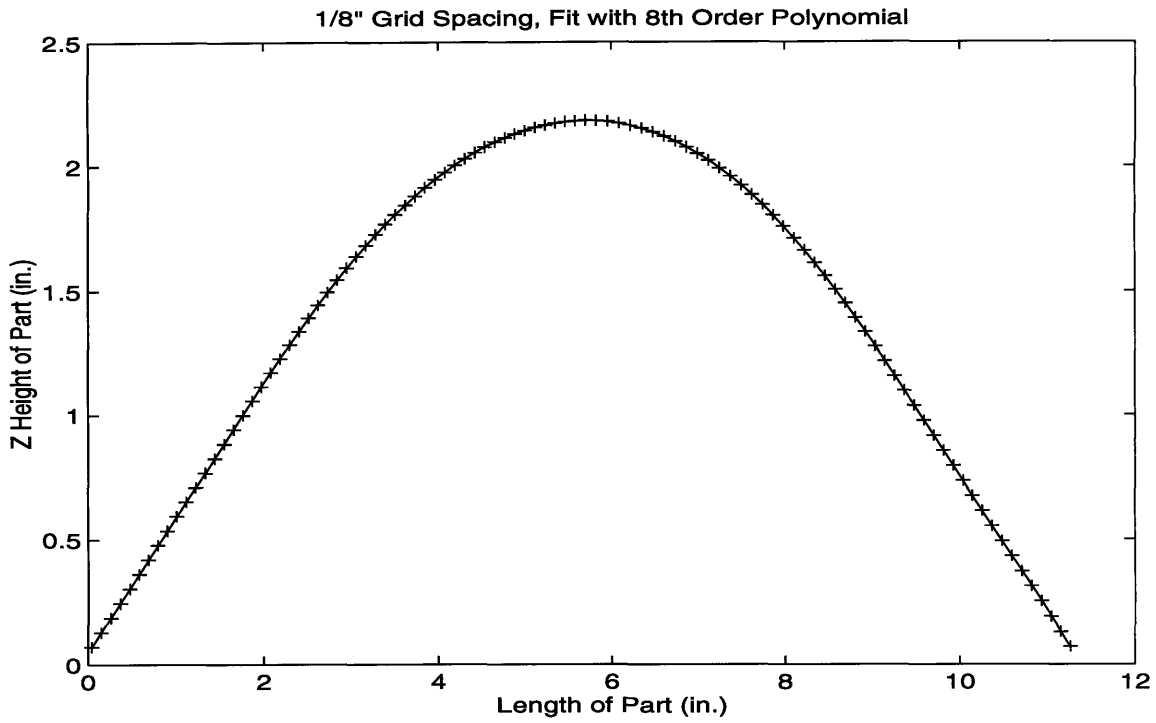

Figure 5.6: 1 / 8 inch Grid Spacing, Fit with 8th Order Polynomial

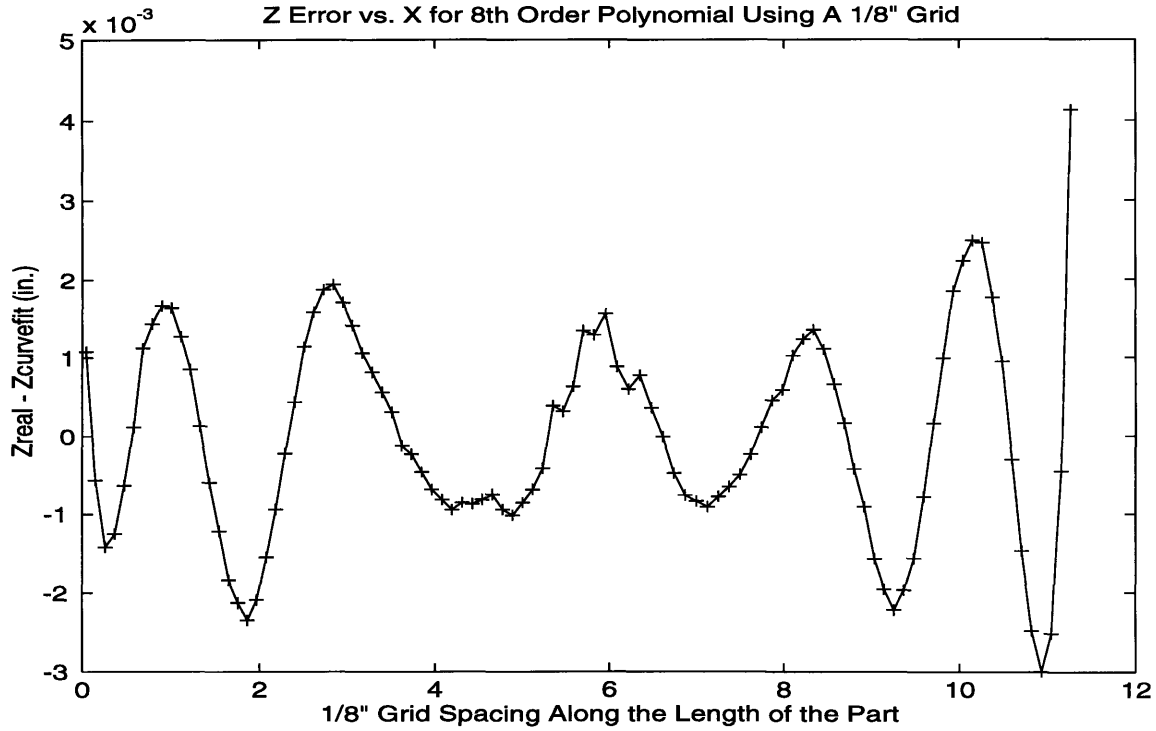

Figure 5.7: Z Error vs. X for 8th Order Polynomial Using 1 / 8" Grid Spacing

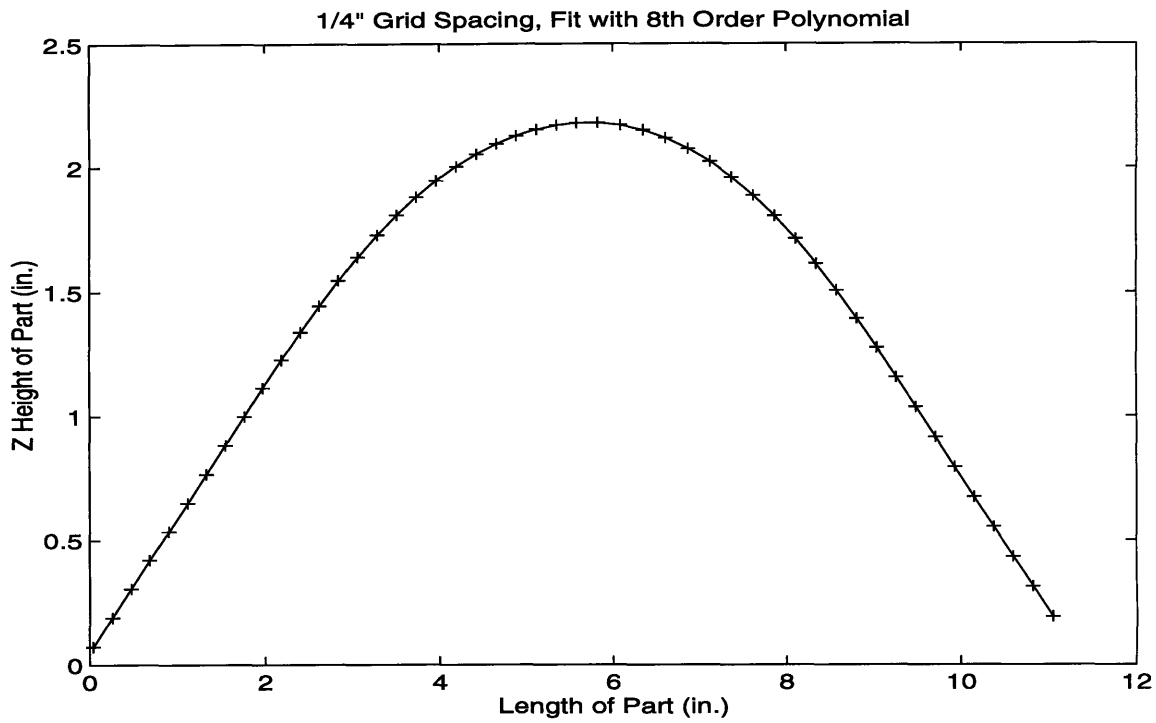

Figure 5.8: 1 / 4 inch Grid Spacing, Fit with 8th Order Polynomial

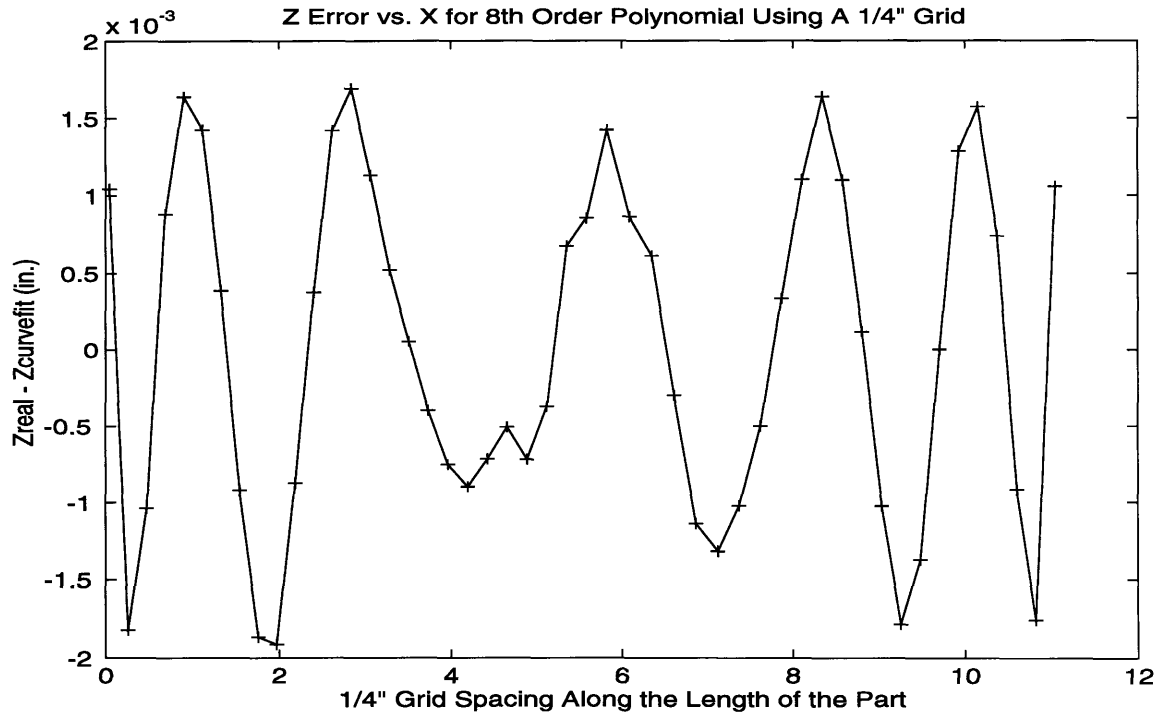

Figure 5.9: Z Error vs. X for 8th Order Polynomial Using 1 / 4" Grid Spacing

It can be seen from the data above, the error between the actual measured data and the polynomial curve fit data runs on the order of 0.002 inches and larger. It can also be seen that the measurement spacing at the different intervals had little impact on the error. Compared to the CMM, a machine which has accuracy within a few ten thousandths of an inch, this measurement error of ±0.002 and up is unacceptable.

The second type of curve fitting tested was cubic spline interpolation. Rather than trying to fit a high order polynomial to the measured data, it fits a low order piecewise polynomial with the data as its endpoints. That is, it takes each of the data points and fits a third order polynomial between them, and makes sure the first and second order derivatives of the curve are equal on either side of the data point to assure continuity in the curve. Therefore, the error between the spline data points and the measured data points will always be zero, while the error of the cubic splined curve in between the data points and the actual measured data will be non-zero.

The following six figures, Figure 5.10 - 5.15, show the analysis on the cubic spline interpolation curve fitting method for varying measurement spacing. Figures 5.10, 5.12 and 5.14, show the measured part data for varying measurement increments. It also shows the intermediate data between these points, spaced every 1 / 32 inch, generated by cubic spline interpolation. Figures 5.11, 5.13, and 5.15 show the error between the actual measured data at 1 / 32 inch intervals and the cubic spline interpolated data at this measurement interval.

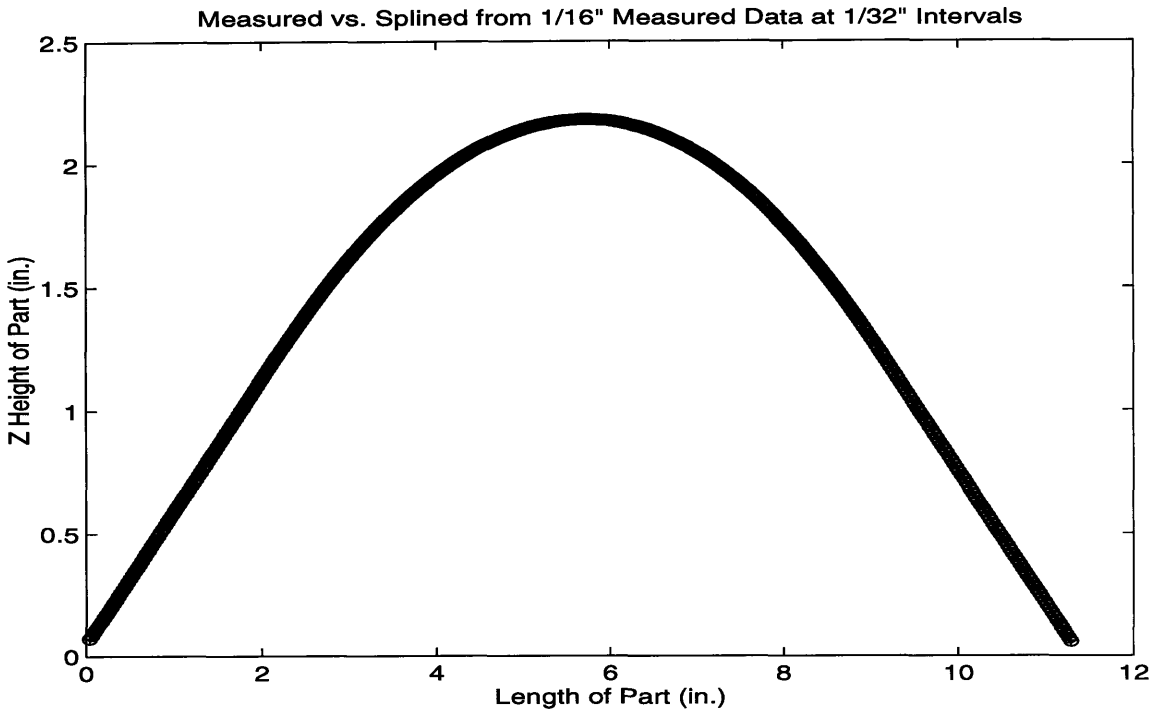

Figure 5.10: Measured vs. Splined Data from 1/16" Measured Data at 1/32" intervals

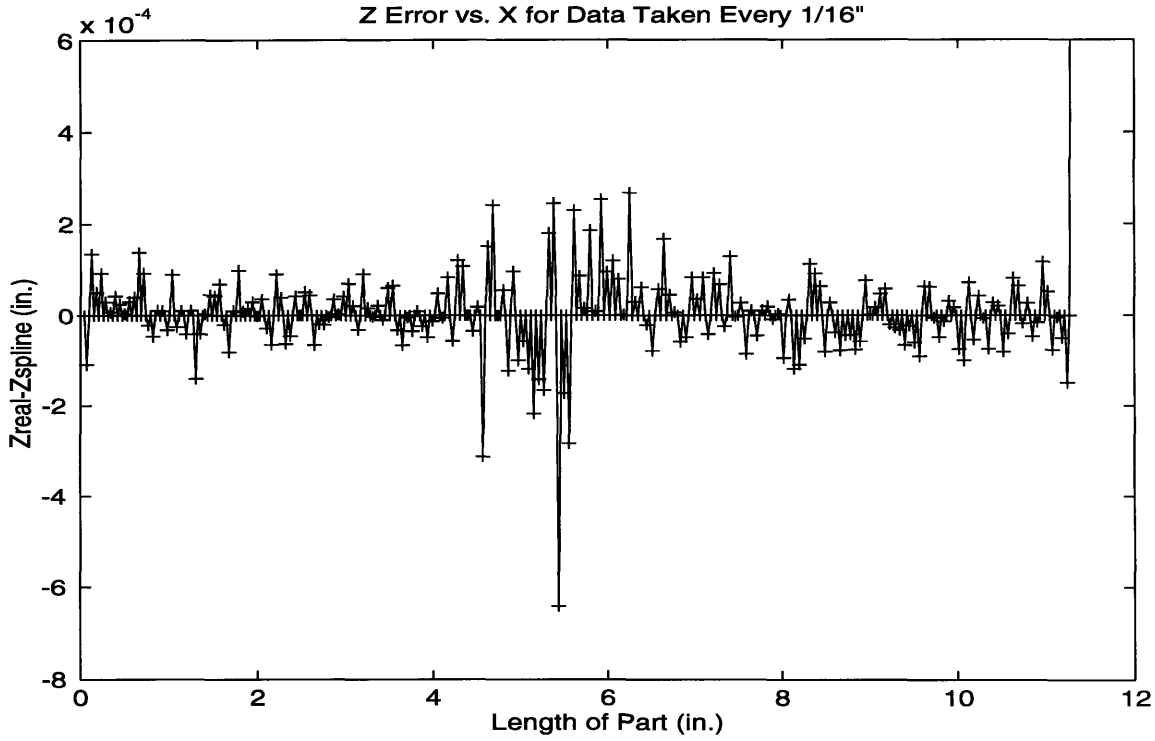

Figure 5.11: Z Error vs. X for Data Taken Every 1 / 16"

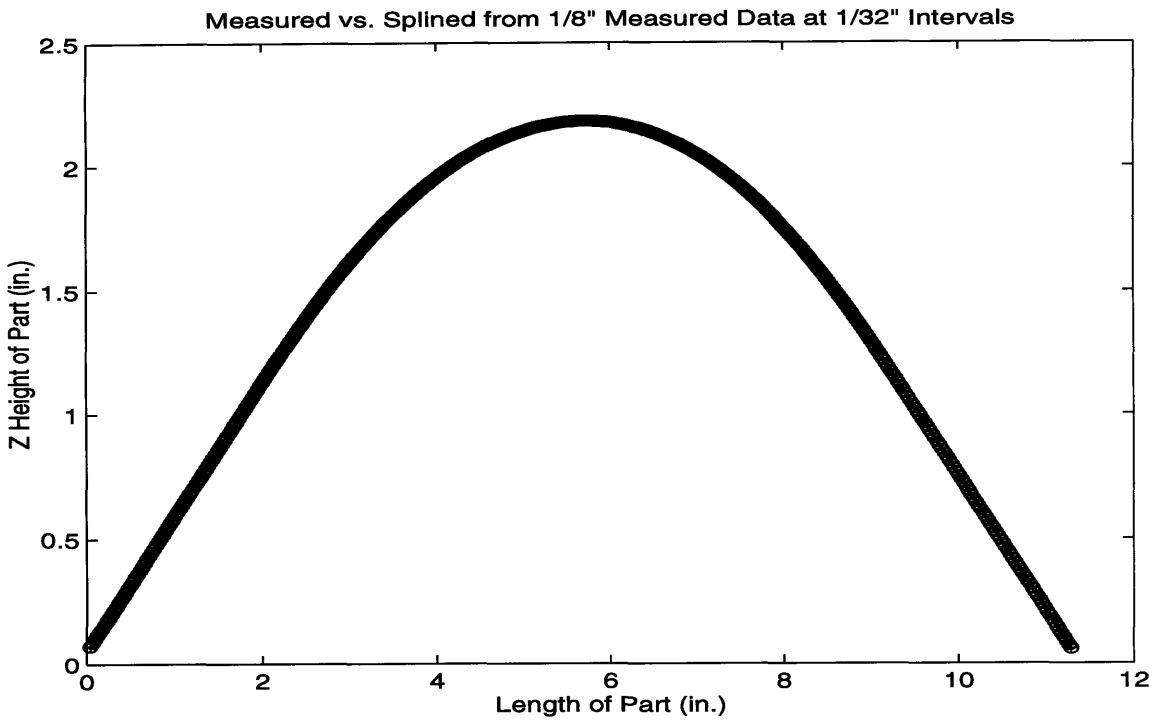

Figure 5.12: Measured vs. Splined Data from 1/8" Measured Data at 1/32" intervals

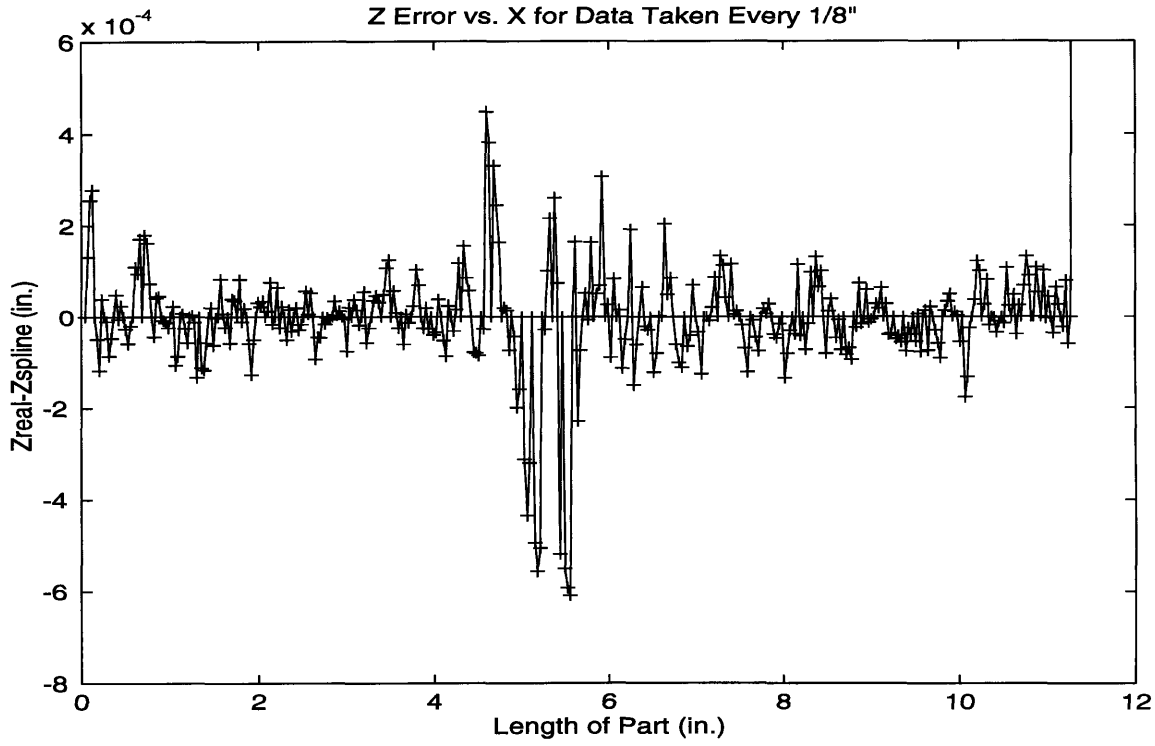

Figure 5.13: Z Error vs. X for Data Taken Every 1 / 8"

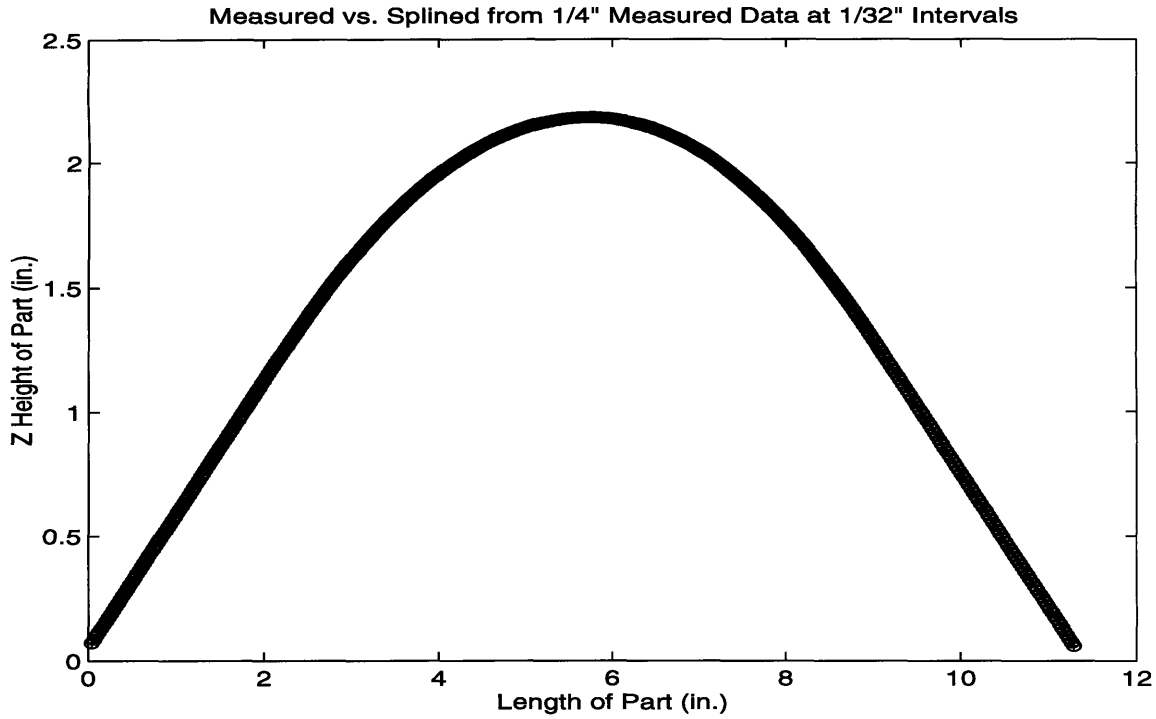

Figure 5.14: Measured vs. Splined Data from 1/4" Measured Data at 1/32" intervals

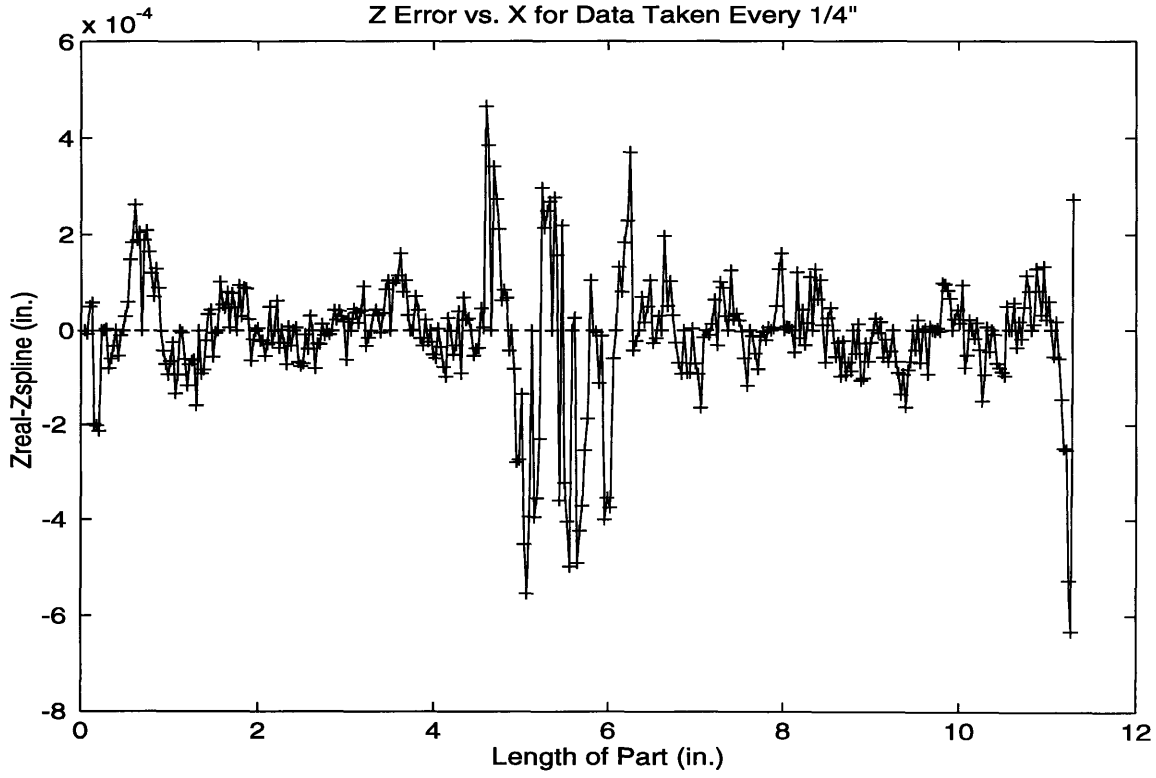

Figure 5.15: Z Error vs. X for Data Taken Every 1 / 4"

From the data in the figures, it can be seen that the error between the actual measured data and the cubic splined data is practically negligible. The error is on the same order as the CMM's accuracy, 0.0003 inches. It is also shown that the measurements every 1 / 4 inch will suffice to recreate the die shape.

5.3 Making Measurements

The actual measurement on the Brown and Sharpe mm4 CMM is very easy using the Brown and Sharpe software. The data points are taken every 1 / 4 inch along the arclength, through the center of the part. The center of the part is defined to be an imaginary line which runs along the length of the part, six inches from the top of the twelve inch part. The data is then sent into the computer controlling the CMM. Once in the computer, the data is collected for analysis. Figure 5.16 shows a close-up shot of the CMM taking data on a fixtured part. Figure 5.17 shows the entire Brown and Sharpe CMM setup.

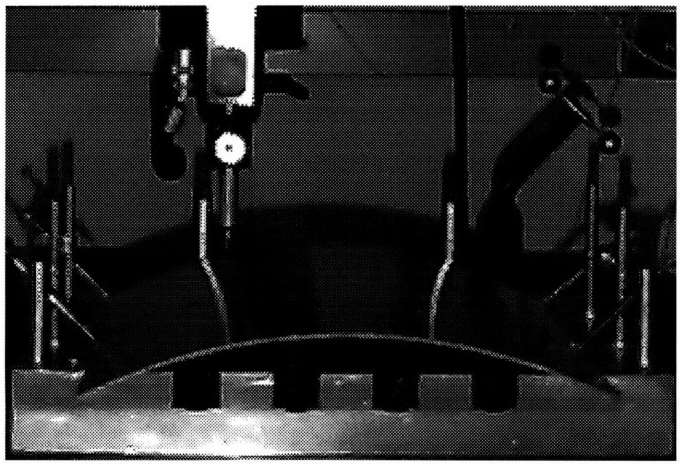

Figure 5.16: CMM Taking Data on a Fixtured Part

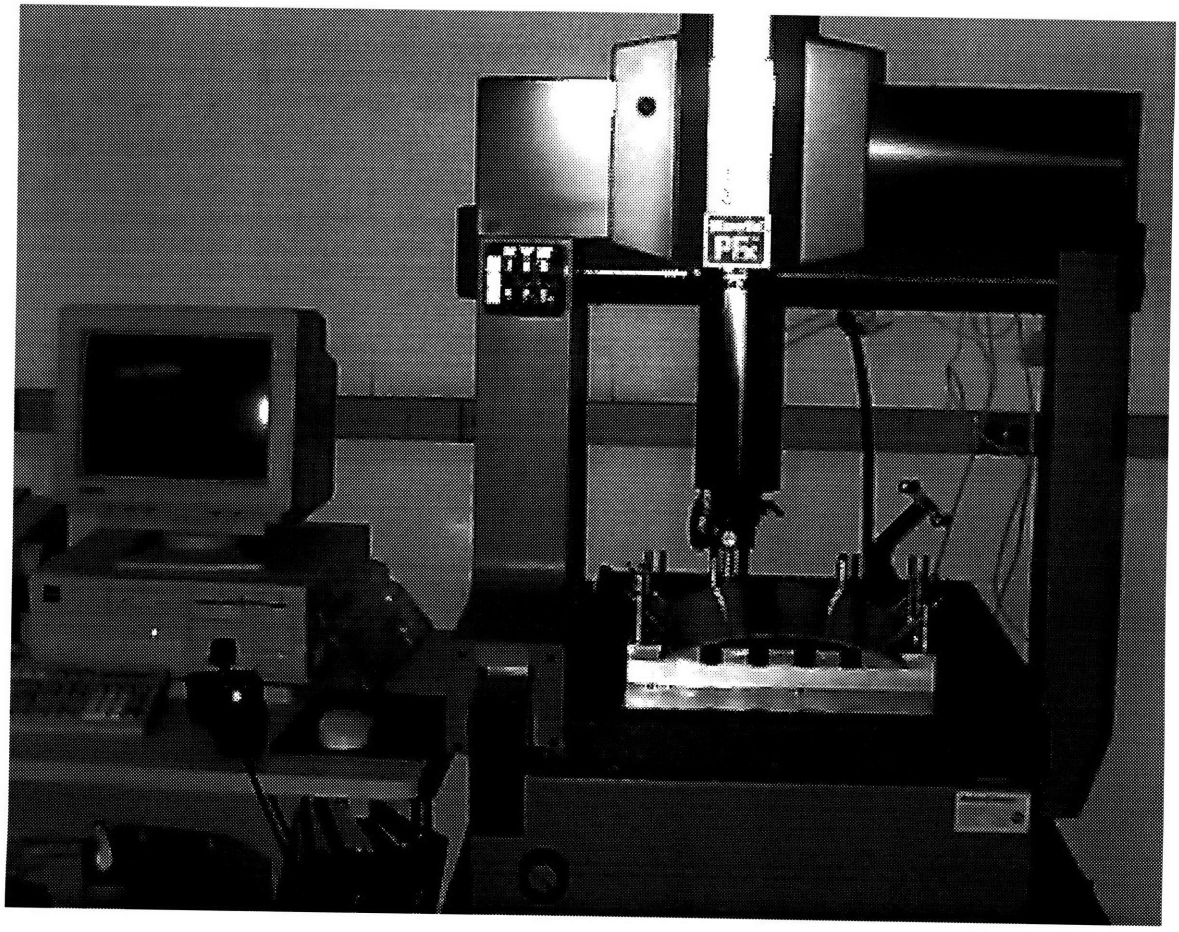

5.17: Brown and Sharpe mm4 CMM with Controlling PC

CHAPTER 6: EXPERIMENTATION

Having finalized the forming and measurement techniques, we now intend to investigate whether the closed loop shape control algorithm can be used, for stretch forming processes, to obtain a series of part shapes converging toward a predetermined reference shape. We begin with an overview of the closed loop shape control algorithm and proceed to describe actual forming trials in which the algorithm was used to obtain the desired part shape. It will be shown how the data for the measured part used in the control scheme is extracted from the raw data output by the CMM and how the data for the previous die and part shapes are aligned into the same frame of reference. Next, the capability of the algorithm to attain convergence of the part to the reference shape will be demonstrated.

A comparison will then be made between the results of numerical simulations modeling the forming process and actual experimental data. Once it has been shown that the simulation software accurately models the process, the "spring forward" algorithm will be used to obtain a new die shape which will bring the part shape closer to the reference shape. Finally, we will compare the die shape obtained with the spring-forward algorithm with the shape obtained with the closed loop shape control algorithm.

6.1 Closed Loop Shape Control Algorithm

As derived in Chapter 2, given two open loop die and part shapes, the shape control algorithm will construct a die shape that will bring the part, closer to the defined reference shape. Figure 6.1 shows the first step in this process. Two "open loop" die shapes must be constructed and two parts must be formed to create $\hat{H}_1$, the closed loop transfer function.

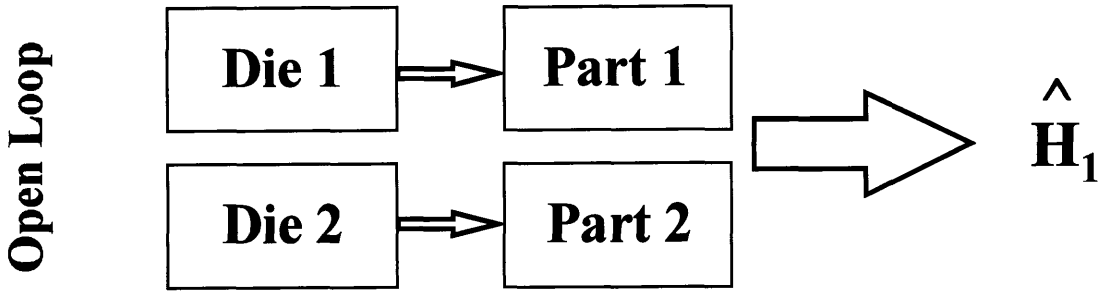

Figure 6.1: First Step in Shape Control Algorithm

$$\hat{H}_1 = \frac{P_2 - P_1}{D_2 - D_1}$$

Once again, P_i and D_i are the part and die shapes in the spatial frequency domain. The derivation for the following equation can be found in section 2.2.1. The closed loop transfer function is used to create the next die shape, using the closed loop shape control algorithm equation:

$$D_{i+1} = D_i + (Ref - P_i)\hat{H}^{-1} = D_i + (Ref - P_i)\left(\frac{D_i - D_{i-1}}{P_i - P_{i-1}}\right)$$

When $i = 2$, the algorithm solves for the first closed loop die shape, Die 3, as shown in Figure 6.2.

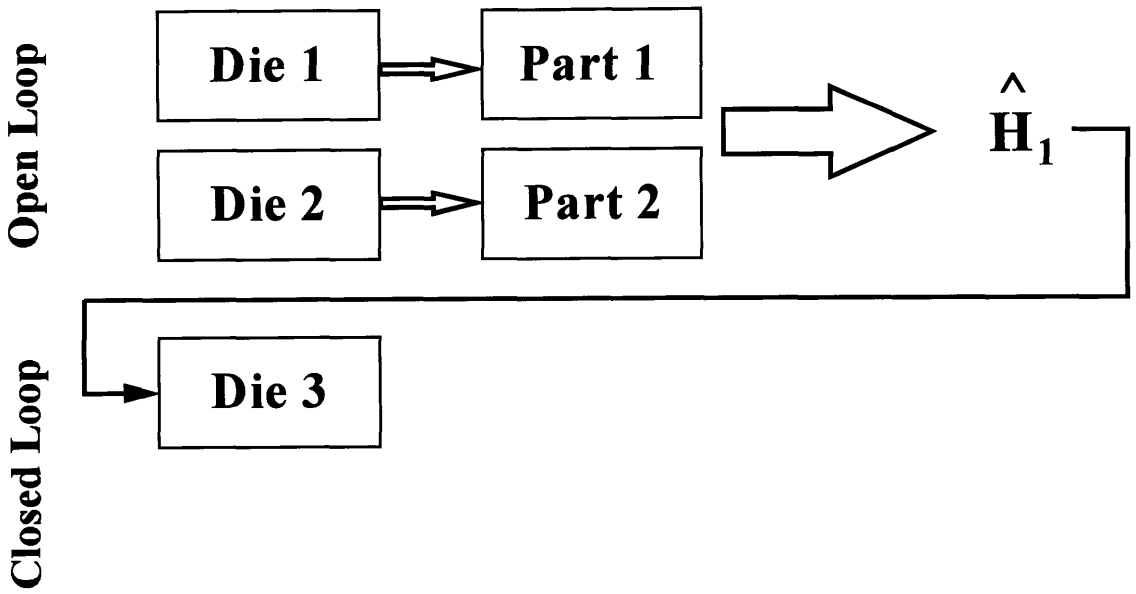

Figure 6.2: Creating the First Closed Loop Die Shape

Once the third die shape, or first closed loop die shape, has been constructed, a part must be formed over it. That part shape is then compared to the reference shape. If the error between the part and reference shape is less than the error margin ε, the convergence test is complete. If not, the next transfer function, $\hat{H}_2$, must be constructed and used to create the fourth die, or second closed loop die shape, as shown in Figure 6.3.

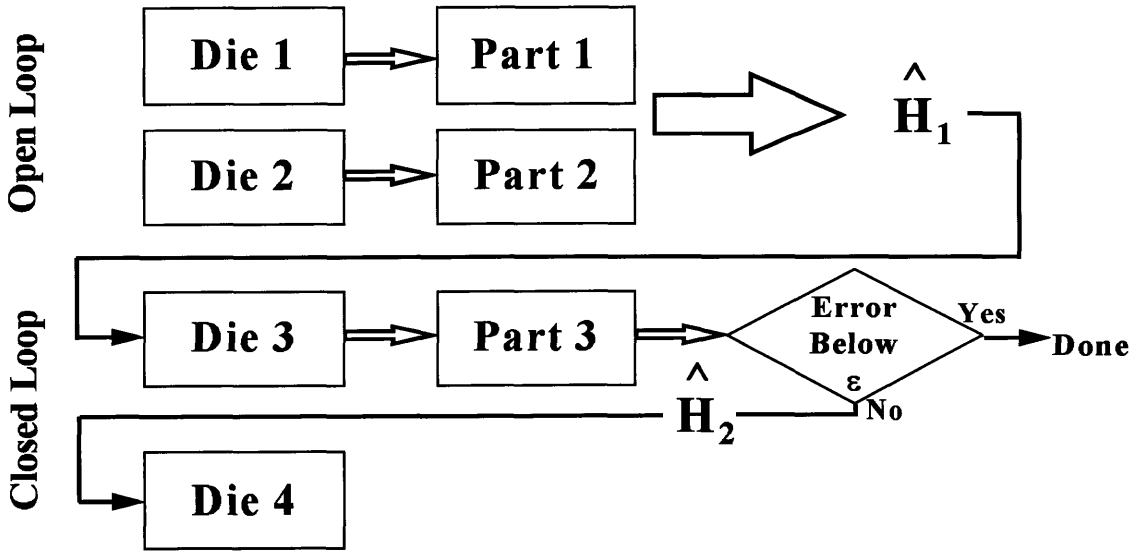

Figure 6.3: Third Part Comparison and Fourth Die Shape Construction

The procedure of creating a new part over the new die, is iterated until the convergence requirement, i.e. the conditions that the error between the part shape formed and the reference shape less than the error margin, ε, is met. This is shown in Figure 6.4.

For the forming trials described in the following sections, the error margin was set to 0.020 inches. This was the magnitude of the worst error recorded during the seven part repeatability study described in Chapter 3. The part error can be when the parts are formed and trimmed consistently, as seen in the three part repeatability study discussed in Chapter 2. The 0.020 inch criterion was chosen to allow wider margins for convergence.

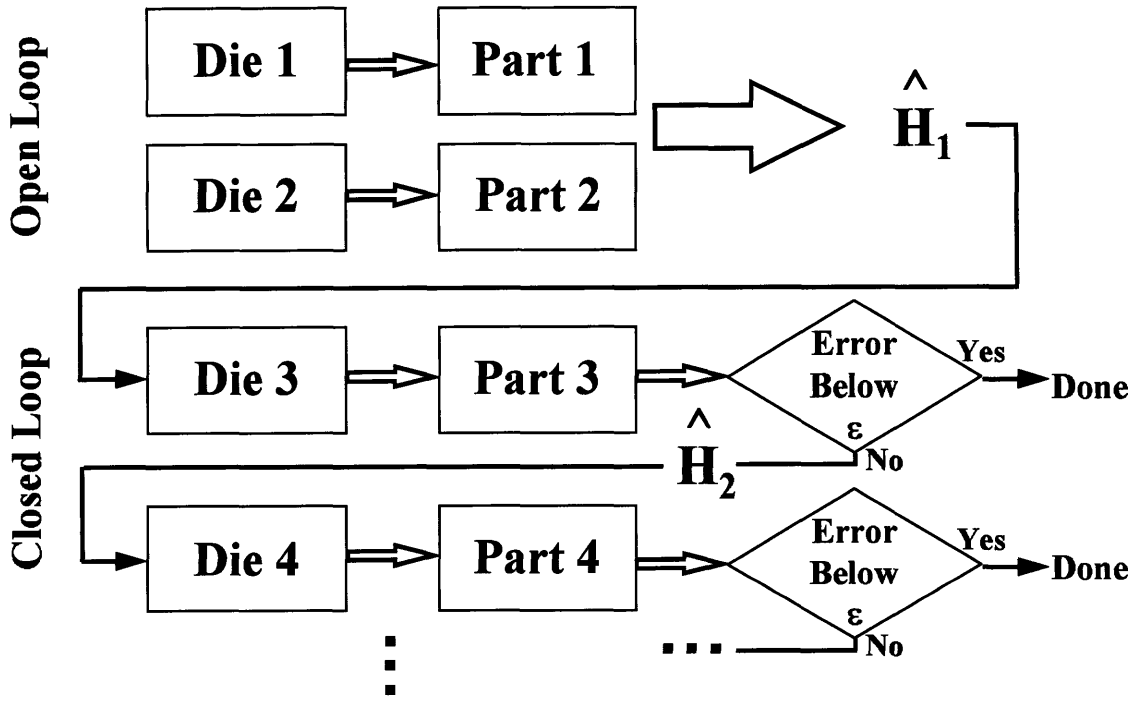

Figure 6.4: Fourth Die Shape and Algorithm Iteration

6.2 Data Manipulation to Create Consistent Frame of Reference

As evident from the closed loop shape control algorithm equation given in the previous section, in order to obtain a new die shape, it is necessary to evaluate the differences between part shapes, die shapes, and part and reference shapes. It is then necessary to have all the data in the same format, i.e. each of the data files describing the

shapes must contain the same number of data points, the frame of reference that is used for all of the parts, dies and reference shape must be unique.

6.2.1 CMM Data Acquisition and Manipulation

The data files created by measuring parts on the CMM using one quarter inch measurement intervals along the arclength of the part includes 49 (x, z) data points. The x coordinate corresponds to the length traveled from the edge of the part and the z coordinate corresponds to the height from the reference plane. For the measurements, the origin is set to be the upper left hand corner of the part, and the reference plane is set to be the base plate of the CMM fixturing device.

Since the dies are described by 23 data point arrays, corresponding to the positions of each pin, it is important to be able to describe the parts formed in this same format. The process of changing the part shape data file, containing a 49 element array, to a format which includes 23 elements corresponding to the exact positions of the part above each of the die elements when wrapped around the die, is a complex one, which requires several steps.

As a first step, it is necessary to find the exact center of the part shape and "trim" the part to the exact dimensions of the discrete die in software. When the part shape is measured, the starting and ending points may be at different heights, as measured from the base plate, as seen in Figure 6.5. This phenomenon occurs because the start and end points of the scan for the CMM are determined by manual positioning of the CMM measurement probe.

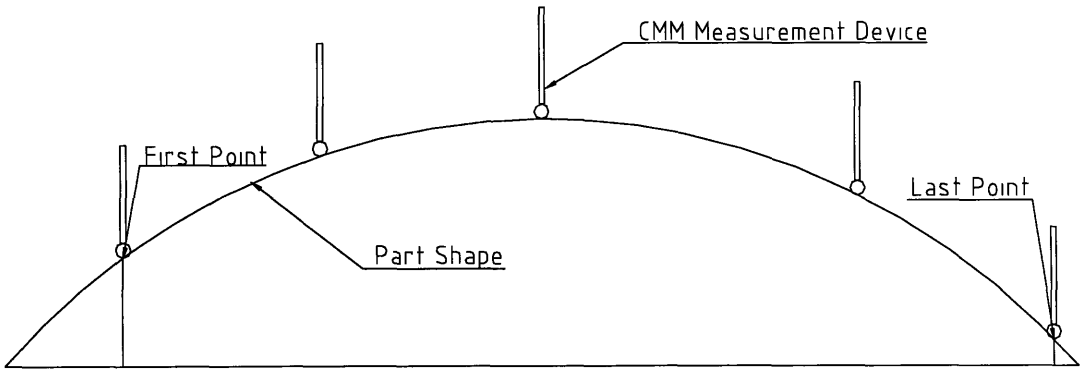

Figure 6.5: Varying Heights During CMM Measurement

Since the first and last data points are at different heights, the row data from the CMM describes a non-symmetric part, as seen in Figure 6.6. The point that is necessary for referencing purposes is the actual center of the part, which is the point that lies directly on top of the center of the middle pin during forming. The geometric center of the part, corresponds to the midpoint of the line created by connecting the first and last points, is easier to find but serves no purpose for referencing.

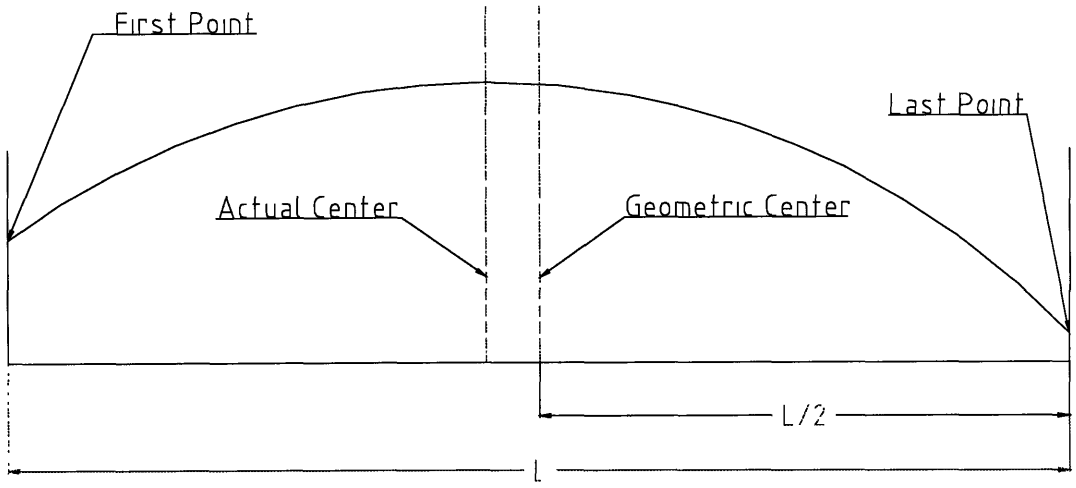

Figure 6.6: CMM Data Acquired From Part Shape

The actual center could be easily determined if the part had constant curvature. However, the part, even if formed over a constant curvature die, does not have a constant curvature. When the part is formed on the die, the interpolator at the actual center of the die, corresponding to the peak of the curve, compresses more than it does at the periphery of the die. This is caused by uneven pressure distribution imposed by the sheet metal on the interpolator, which is maximum at the center. This uneven compression of the interpolator during forming causes a variation in the radius of curvature throughout the part.

The actual center of the part shape is found by fitting an arc of a circle to the part data. By minimizing the mean square error between the circle and the part data, a "best fit" circle is found. Figure 6.7 shows an actual part data and the corresponding circular curve fit. Figure 6.8 portrays the flattening of the part shape due to the uneven interpolator compression. Notice that Figure 6.8 is a detail of the central part Figure 6.7.

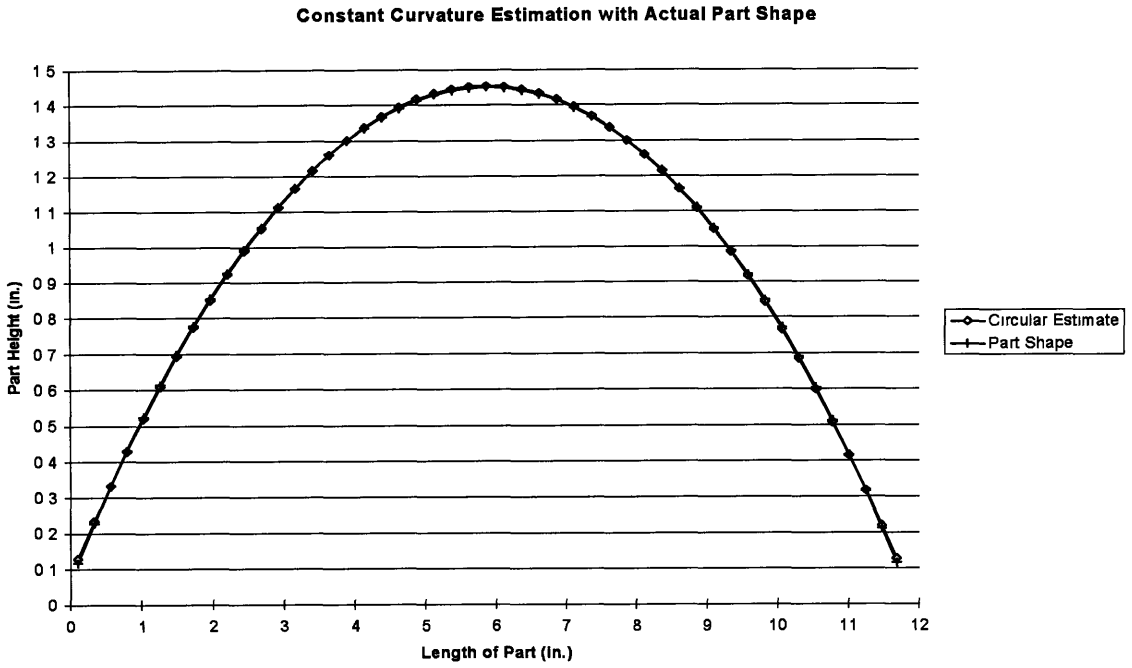

Figure 6.7: Constant Curvature Estimation with Actual Part Shape

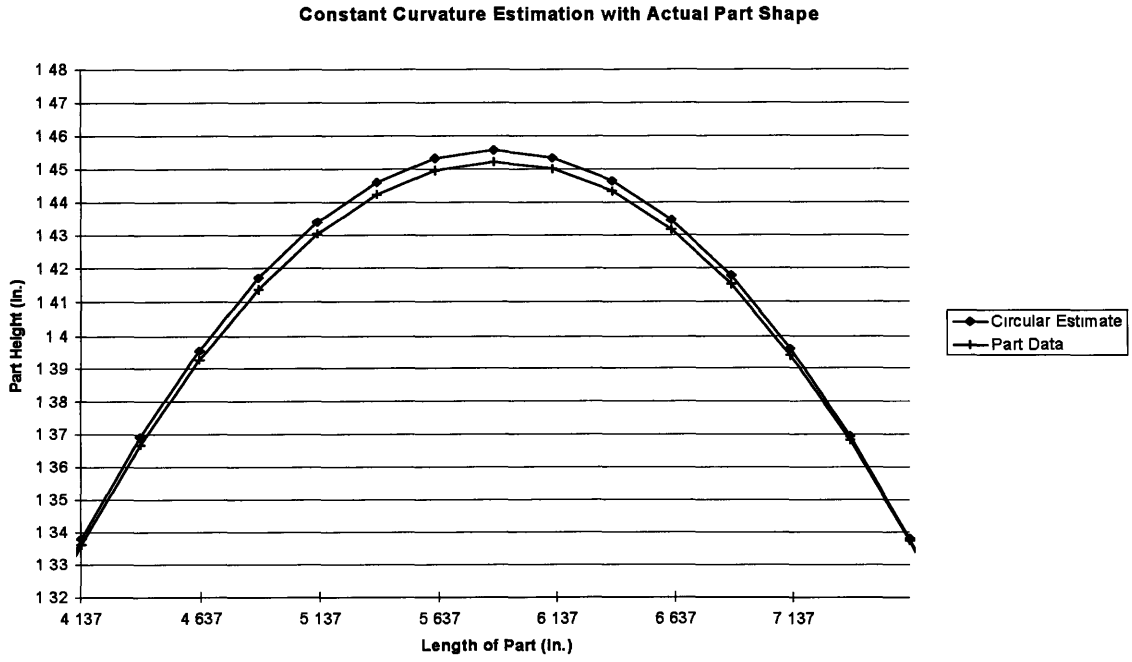

Figure 6.8: Flattening of Part due to Uneven Interpolator Compression

As can be seen from the figures, the variation between the constant curvature shape, and the actual part data is very slight, so that the center of the constant curvature estimate can be used to offset the part data, positioning the actual center of the part at x = 0.

The next step is to "trim" and interpolate the data so that the part described by 23 data points corresponding to the positions directly above the center of each pin. This is accomplished using cubic spline interpolation. A new x axis vector is formed, ranging from -5.5 inches to +5.5 inches, in increments of 0.5 inches. The point at x = 0, corresponds to the center of the middle pin on the discrete die, while positions at -5.5 inches and +5.5 inches, correspond to the center of the first and last pins respectively. The part data is then interpolated to create the height data for the part using the new x data matrix. The part data which lies outside of the 11 inch area is "trimmed" away. The data that is left represents the part shape with data points corresponding to the pins over which they were wrapped. The data is then offset +5.5 inches, so the x dimensions of the part data range from 0 to 11 inches, which corresponds to the x-vector describing the die. Figures 6.9 and 6.10 show the new x vector and interpolation of the part data and the final result of the software trimming operation, respectively.

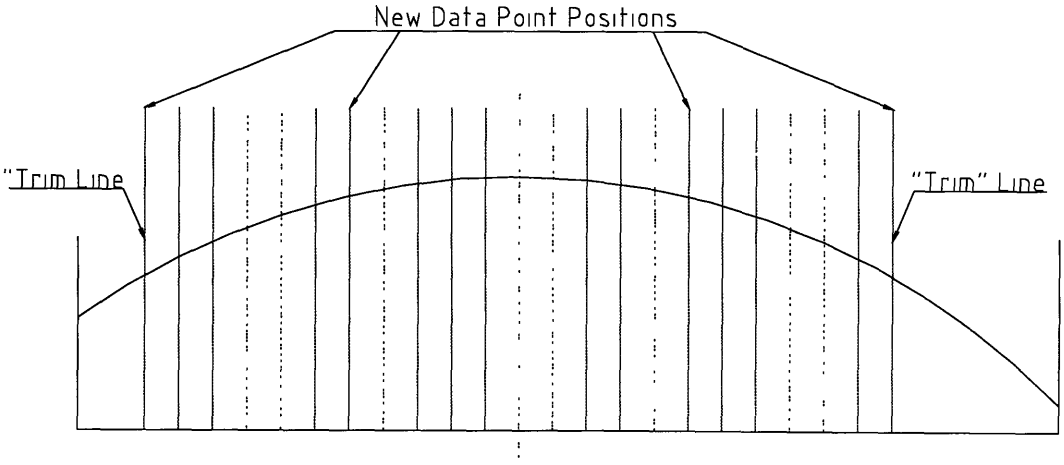

Figure 6.9: New X-Vector and Interpolation of Part Data

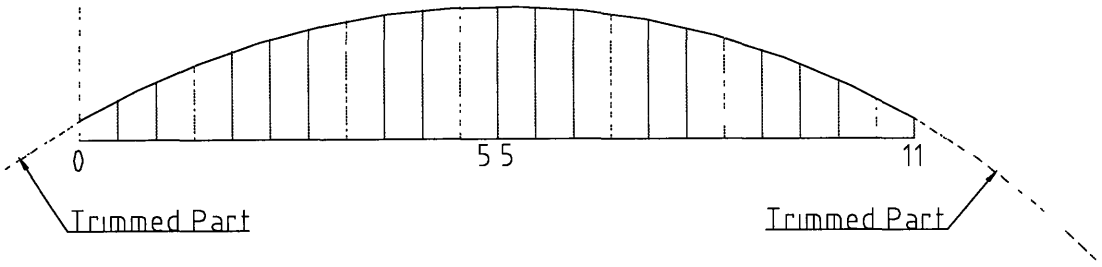

Figure 6.10: Trimmed Part With New Coordinates

6.2.2 Comparison Between Parts, Dies and Reference Shapes

The procedure described in the previous section has been applied to every part formed, and measured on the CMM, so that every part is described in the same frame of reference. as every other part. The die shapes are also described in this same frame of reference, and thus parts can also be compared to dies. The reference shape is defined as a constant curvature part, with data points calculated for the same x-positions used for parts and dies.

Once the data is aligned in the x direction, the curves are all set to the same z reference by adjusting the maximum z heights to the same value. Thus, the differences between any parts or dies, at the x = 5.5 inch mark, the actual center, will always be zero, while the maximum error will occur at the edges of the parts

6.3 Closed Loop Shape Control Convergence Test

6.3.1 Parameters for Convergence Test

In the following sequence used to test the effectiveness of the closed loop shape control algorithm, the two open loop die shapes were significantly different from the reference shape. This choice was meant to assure that more than one iteration would be

necessary to converge to the reference shape. Once the algorithm has been proven to be effective, the open loop shapes can be chosen more wisely.

As described in Chapter 5, the die is set according to a given radius of curvature, which corresponds to the length from the center of the circle to the center of the sphere at the tip of the pin. This radius is called the die radius and denoted by Rd in Figure 6.11. Though this is the radius to which the die is set, it is not the radius that the part, which is stretched over the die, actually sees. The part sees a die with a radius of curvature equivalent to the die radius, Rd, plus the radius of the sphere on the tip, Rp = $\frac{\sqrt{2}}{4}$ inches, plus the thickness of interpolator, d = 0.5 inches. As the CMM measures the top surface of the part, the radius of curvature of the part includes the thickness of the sheet as well, which for this set of experiments was t = 0.063 inch. Thus the actual radius of curvature of a part, Ra, wrapped around a die, is:

$$Ra = Rd + Rp + d + t \quad \text{in.}$$

For the convergence test, the first open loop die was set to have a radius of curvature, Rd = 11 inches. This translates to an actual radius of curvature, Ra = 11.917 inches, for the part wrapped around the die. The second open loop die shape was set to have a 9.9 inch radius of curvature, 110% of the curvature of the first die. This die shape translates to an actual radius of 10.817 inches for the part measurement. The reference shape is always defined using Ra, as radius of curvature, since the reference shape is only used as term of compensation for the part shape to confirm convergence. For the convergence test, the reference shape was set to have a radius of curvature, Ra = 11 inches.

The condition for convergence was determined from the repeatability study done on the stretch forming machine. From that study, the maximum error recorded was 0.020 inches at the edge of the part. Although this error is slightly higher than the capability of the machine, it is a good value for testing the algorithm. Once it has been determined that the part shape will converge to within 0.020 inches of the reference shape, the convergence criteria can be decreased.

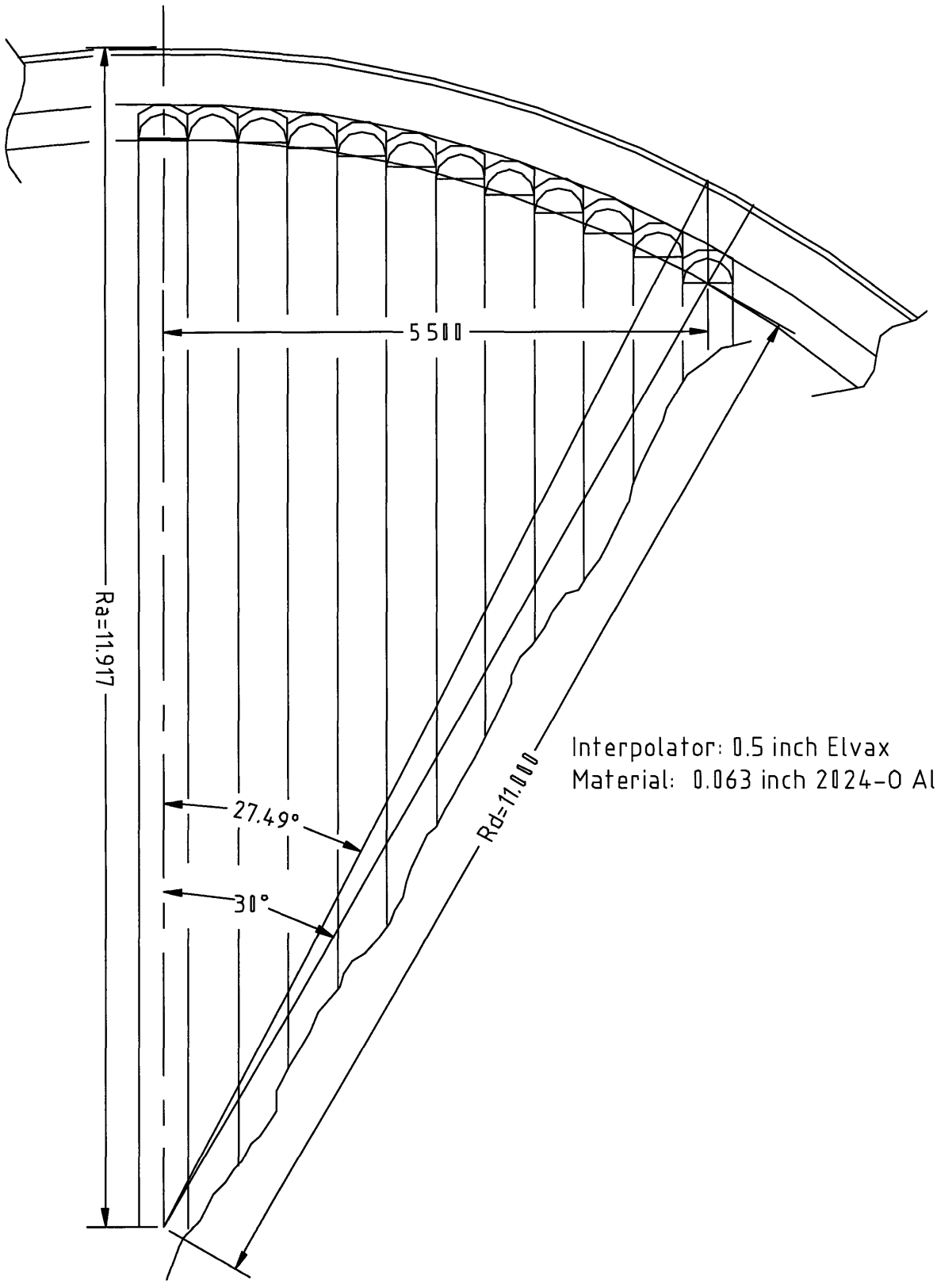

Figure 6.11: Description of Die and Part Radii. Geometry of the First Open Loop Die

6.3.2 The Convergence Test

As described in the first section of this chapter, the first step for the algorithm involves forming two open loop parts over the two open loop die shapes. Figure 6.12 and 6.13 shows the two open loop die shapes and the two open loop part shapes, respectively. It can now be graphically seen how the maxima of the two dies and parts are set to the same point to eliminate the translation of the next die shape due to the difference in z positions. Since the center of the part shape was determined by fitting a circle to the part data, the approximate radius of curvature of the part shape can be determined from the circle. Remember, the actual part formed is not constant curvature and the radius of curvature determined is only an average.

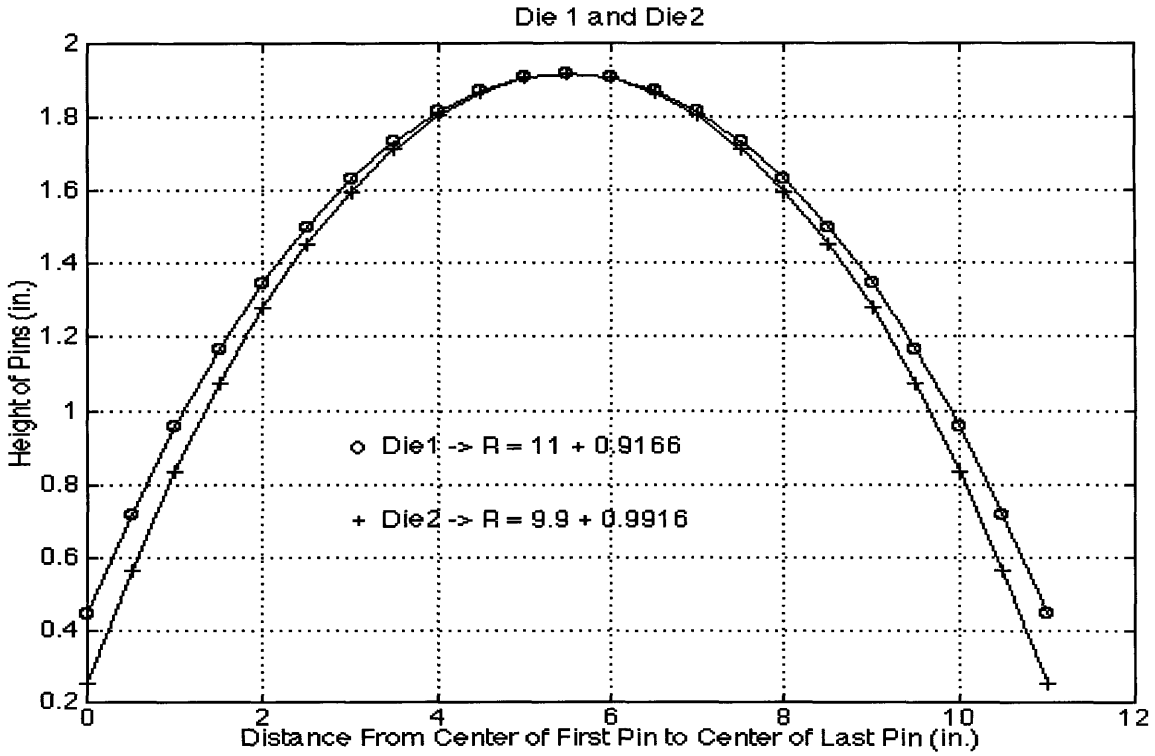

Figure 6.12: The First Two Open Loop Dies

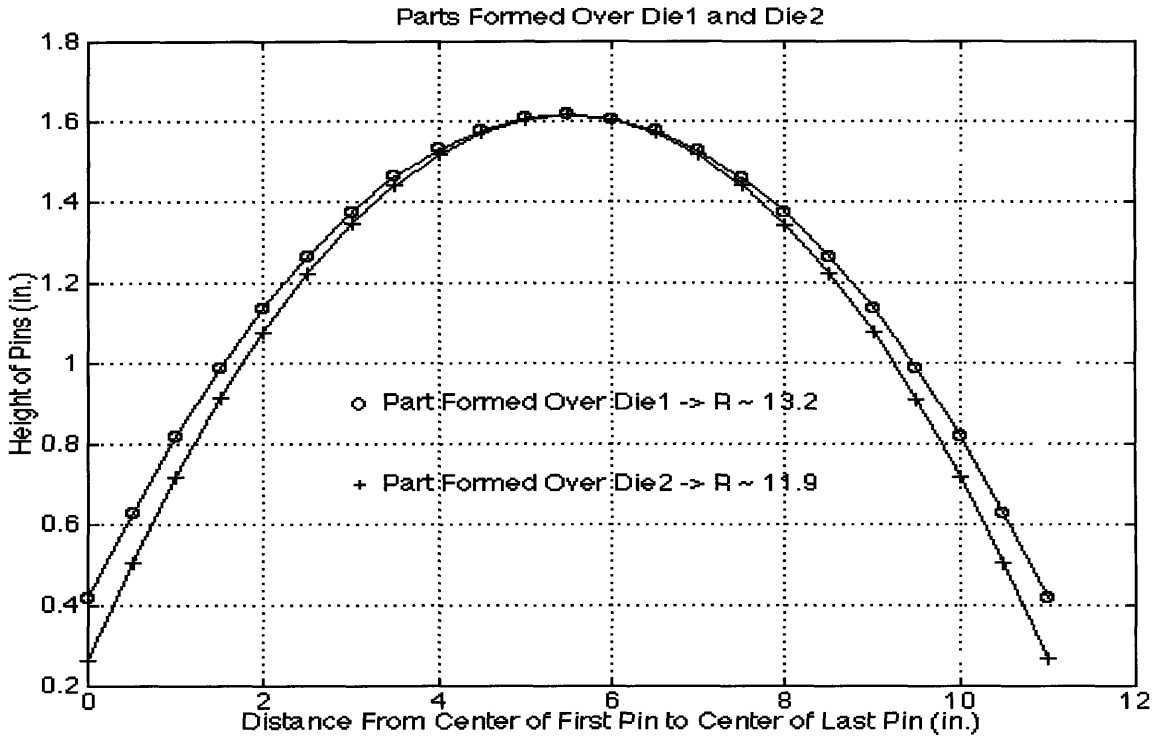

Figure 6.13: The First Two Open Loop Parts

Once all the die and part data for the two open loop trials, and the reference shape have been determined, the closed loop shape control algorithm can be run to determine the next die shape. This is only done if the error between the second part shape and the reference shape is above the error margin. The reference shape was defined such that the error between it and the second part shape would be significant. Figure 6.14 shows the second part shape which has an approximate radius of curvature, Ra = 11.9 inches, and the reference shape which was defined to have a radius of curvature of, Ra = 11 inches. The error between these two curves can be seen in Figure 6.15, note the maximum error is well above the error margin. Therefore, a next die shape must be produced and a new part must be formed to compare with the reference shape. Figure 6.16 shows the first two die shapes and the new die which compensates for the error between the part shape and the reference shape.

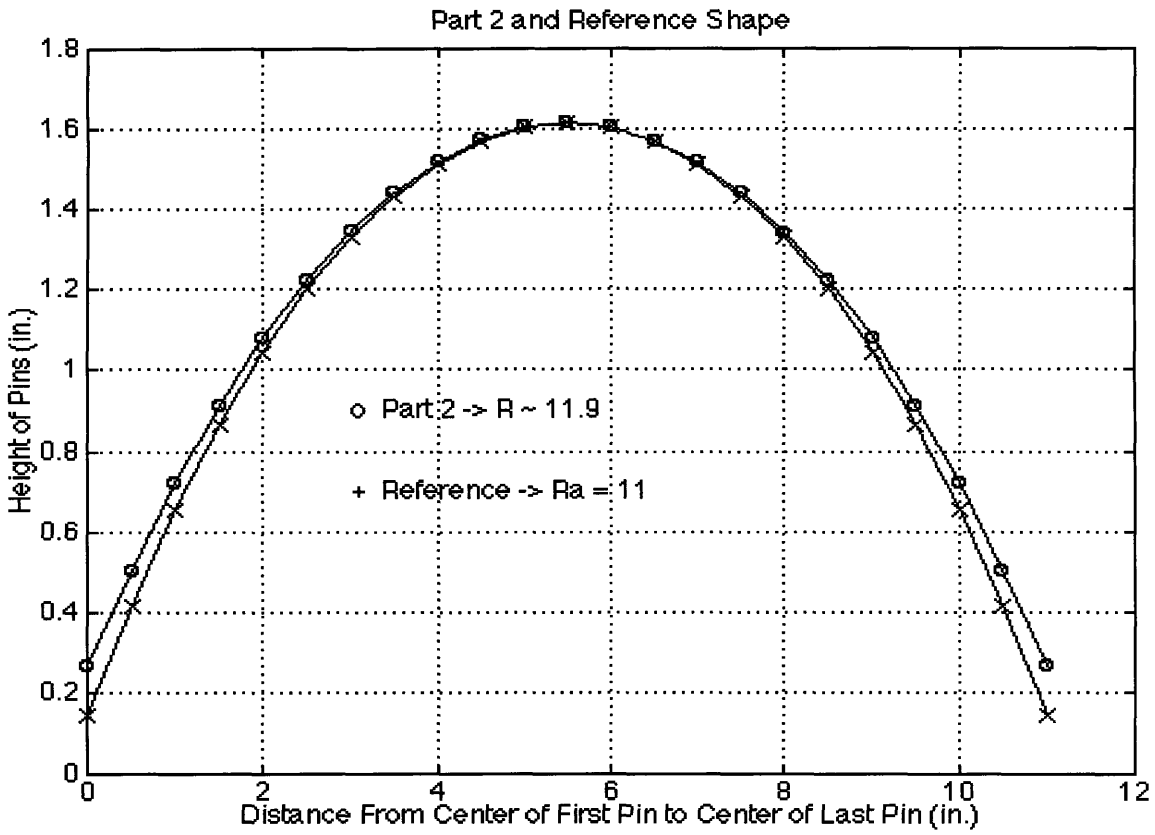

Figure 6.14: Second Part Shape and Reference Shape

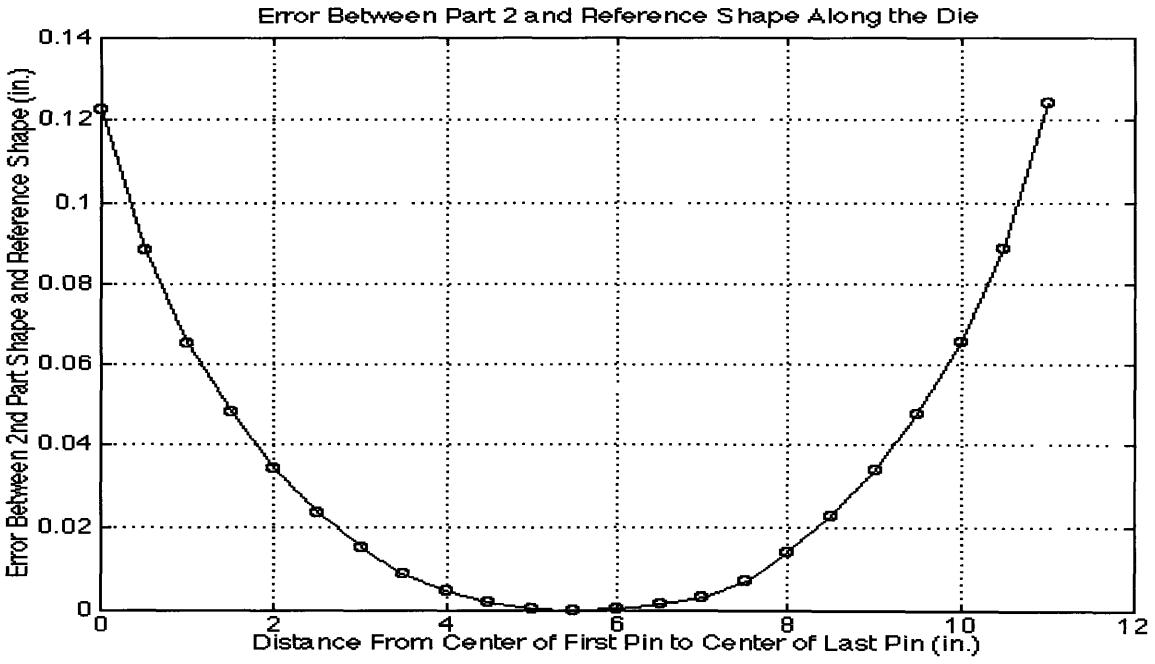

Figure 6.15: Error Between the Second Part Shape and the Reference Shape

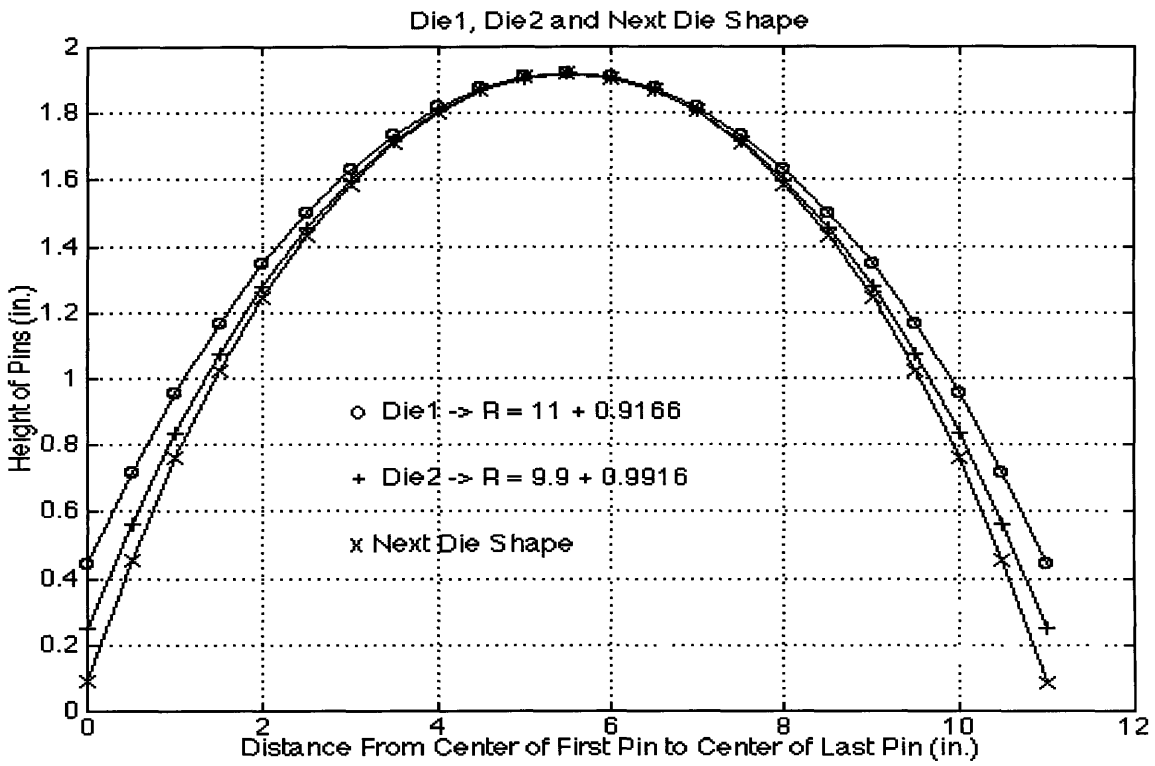

Figure 6.16: Two Open Loop and Next Die Shape

The next step is to form a part over the first closed loop die shape and compare it to the reference shape. If the error is still above the error margin, a second closed loop die shape must be formed. If not, the part has converged and the test is done. Figure 6.17 and 6.18 show the part shape and the reference shape and the error between them, respectively. Figure 6.18 shows that the error between the part and the reference shape is still too large and thus another closed loop die shape must be formed as shown in Figure 6.19.

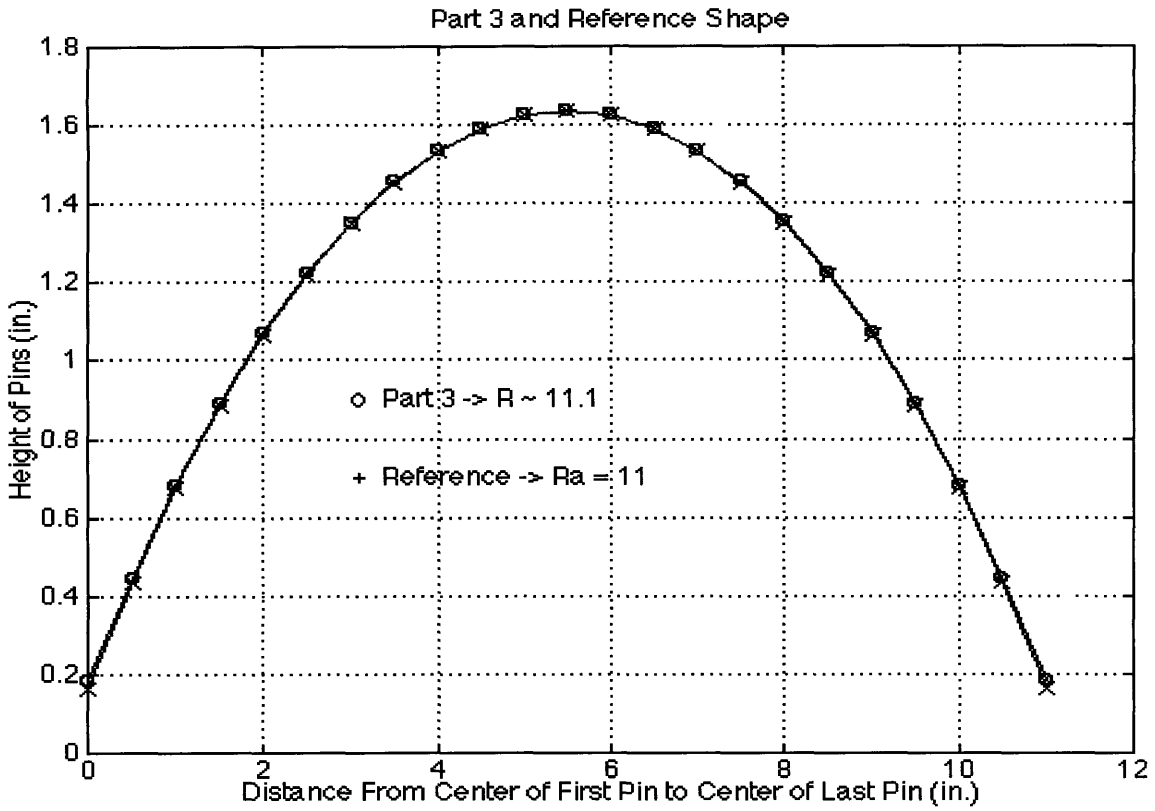

Figure 6.17: Third Part Shape and Reference Shape

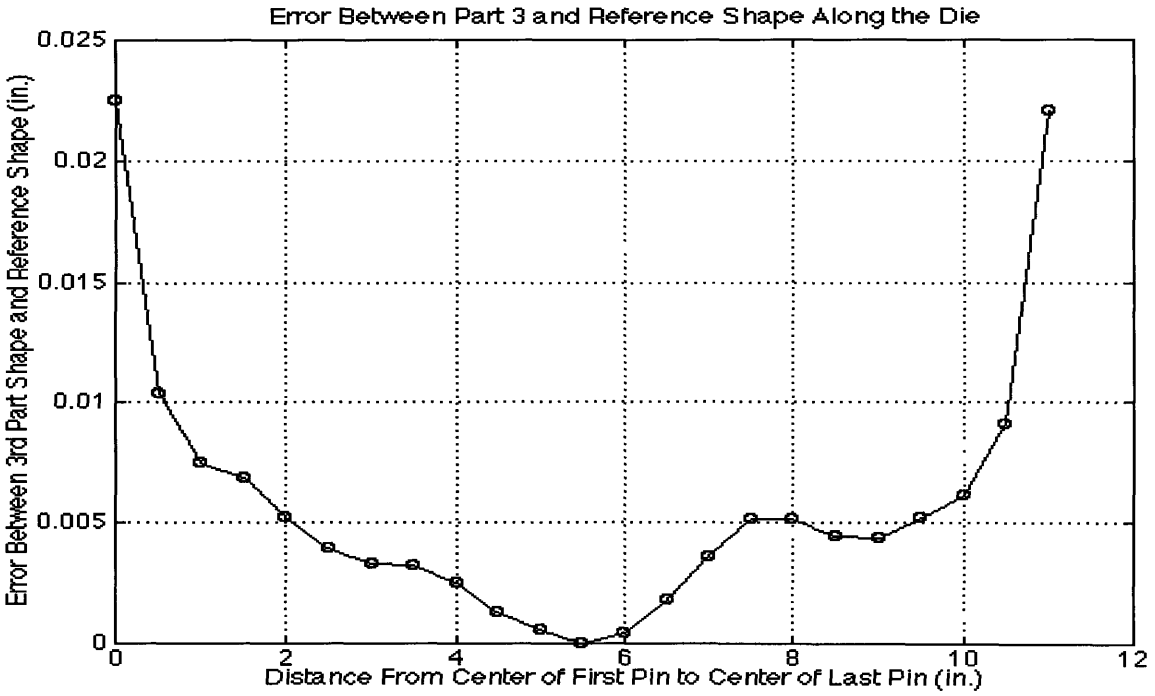

Figure 6.18: Error Between the Third Part Shape and Reference Shape

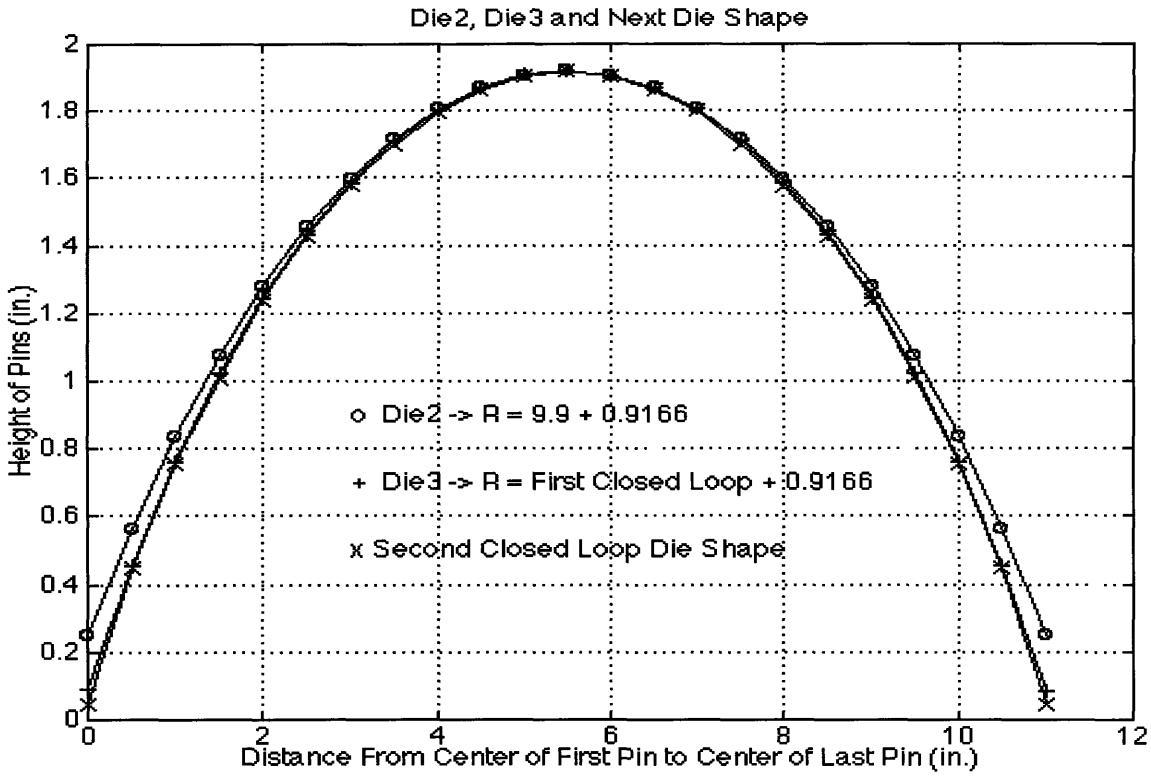

Figure 6.19: Die 2, Die 3 and Second Closed Loop Die

Once again, a part must be formed over the new die shape. This time the error between the fourth part shape and the reference shape is entirely below the error margin, as seen in Figure 6.20. Thus, the part has converged to the reference shape and the procedure is completed.

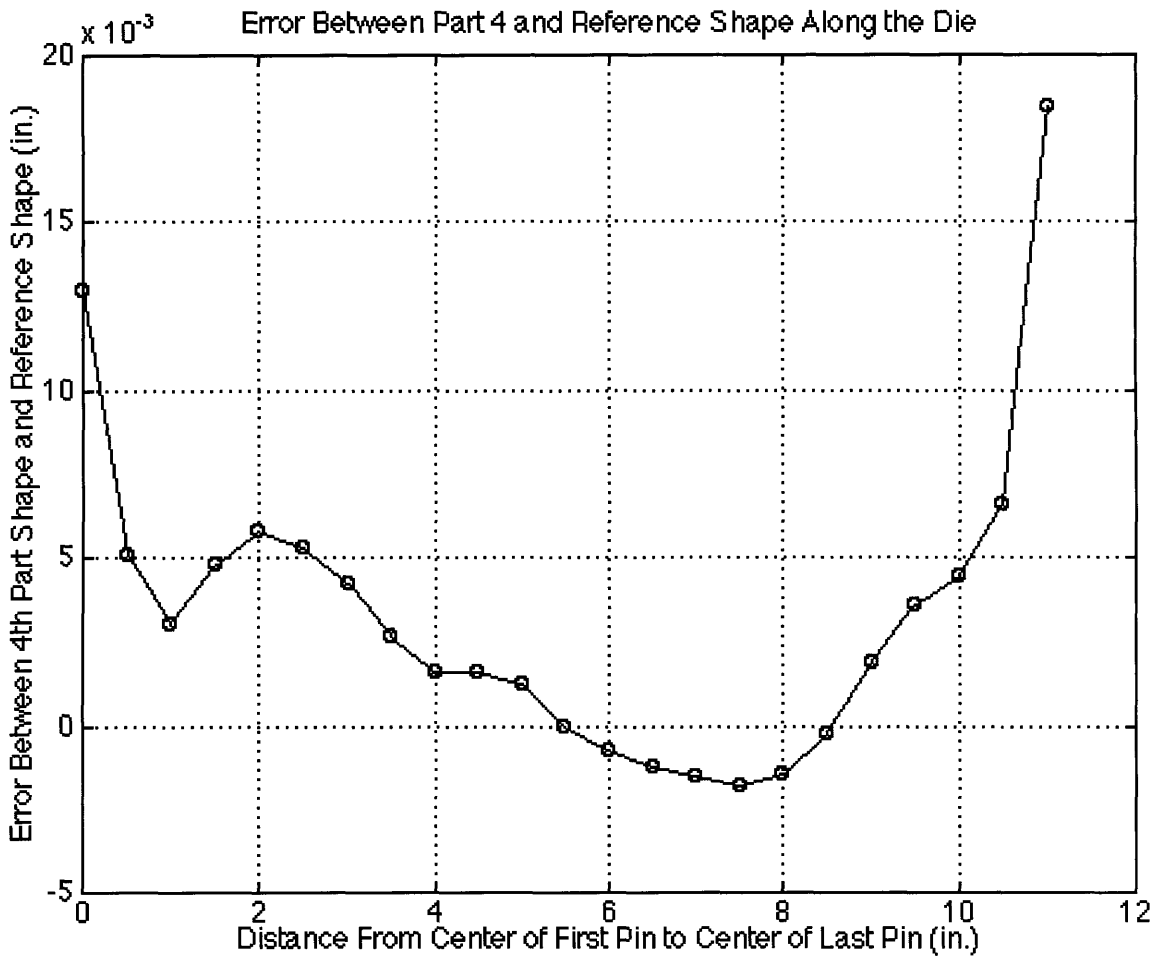

Figure 6.20: Error Between the Fourth Part and Reference Shape

6.3.3 End Effects

It can be seen in each of the figures, which show the error between a part shape and the reference shape, that the error suddenly jumps at the first and last data points. This can be caused by a number of different end effects. The part trimming was done by using a metal shear with a the clamping bar which holds the sheet during trimming. This clamping could have deformed the part at the edges. Also, the kink around the end of the die described in Chapter 4 could be a factor in creating a larger error at the end of the part. Although the error does increase significantly as compared to the error in the mid portion of the part, the magnitude of that error still drops below the error margin and thus the part is acceptable.

6.4 Comparison With Simulation

The following section documents simulation work by Dr. Simona Socrate of MIT, it is involved here to show its relationship to the actual forming experiments done by the author.

The commercial finite element program ABAQUS has been used to simulate forming operations on the discrete die with an interpolator. The overall model of the forming process is constructed by "assembling" submodels of specific elements that compose the system: sheet metal, interpolator, discrete die, contact conditions between interpolator and die, contact conditions between sheet and interpolator, and boundary conditions imposed by the grips.

A simulation of a forming operation over the first open loop die shape (R_d = 11") has been carried out and a comparison between the predicted part shape and the experimental measurements is given in Figure 6.21.

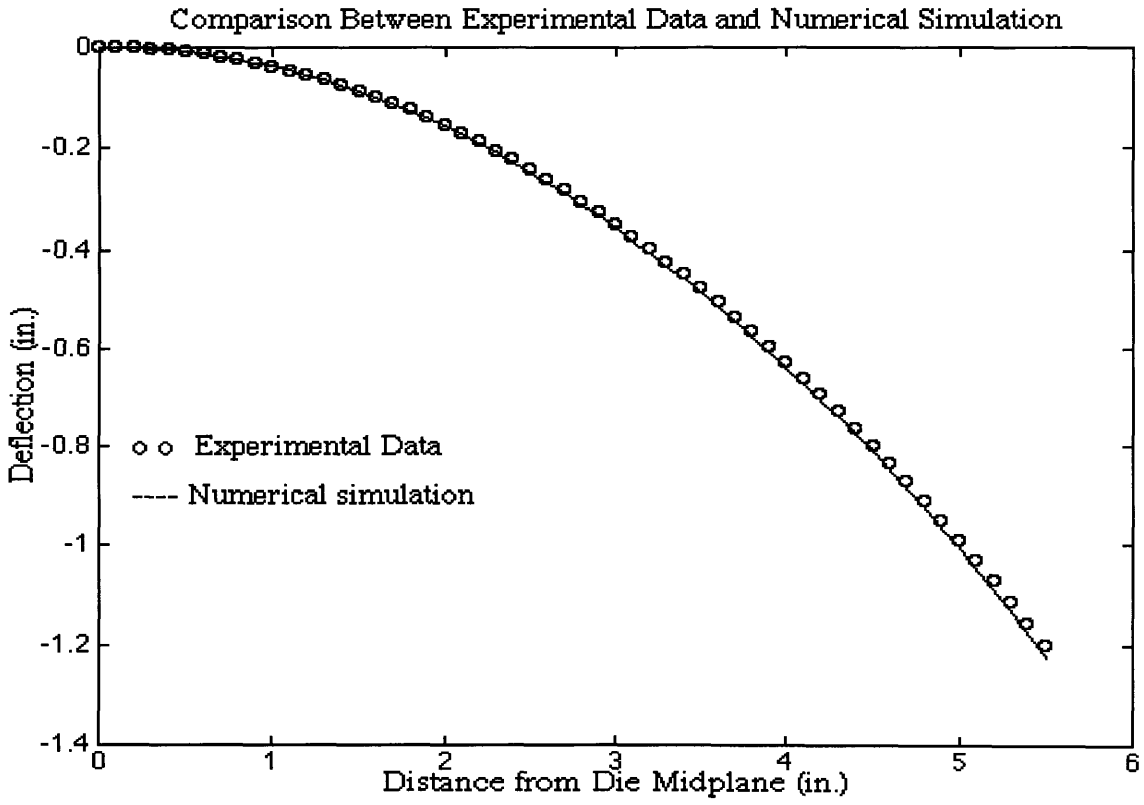

Figure 6.21: Comparison Between Experimental Data and Numerical Simulation

It appears that for the particular choice of model parameters used for this simulation, the springback observed upon unloading was slightly underestimated. It is interesting to observe that the numerical model provides a good estimate of the deviation in part shape from constant curvature, as shown in Figure 6.22, where the difference between the local part radius and the average part radius is plotted for both the actual part, and the numerical model. The flattening of the part in the central section of the die, and the slight kink around the edge of the die, described in Chapter 4, is well captured by the numerical model.

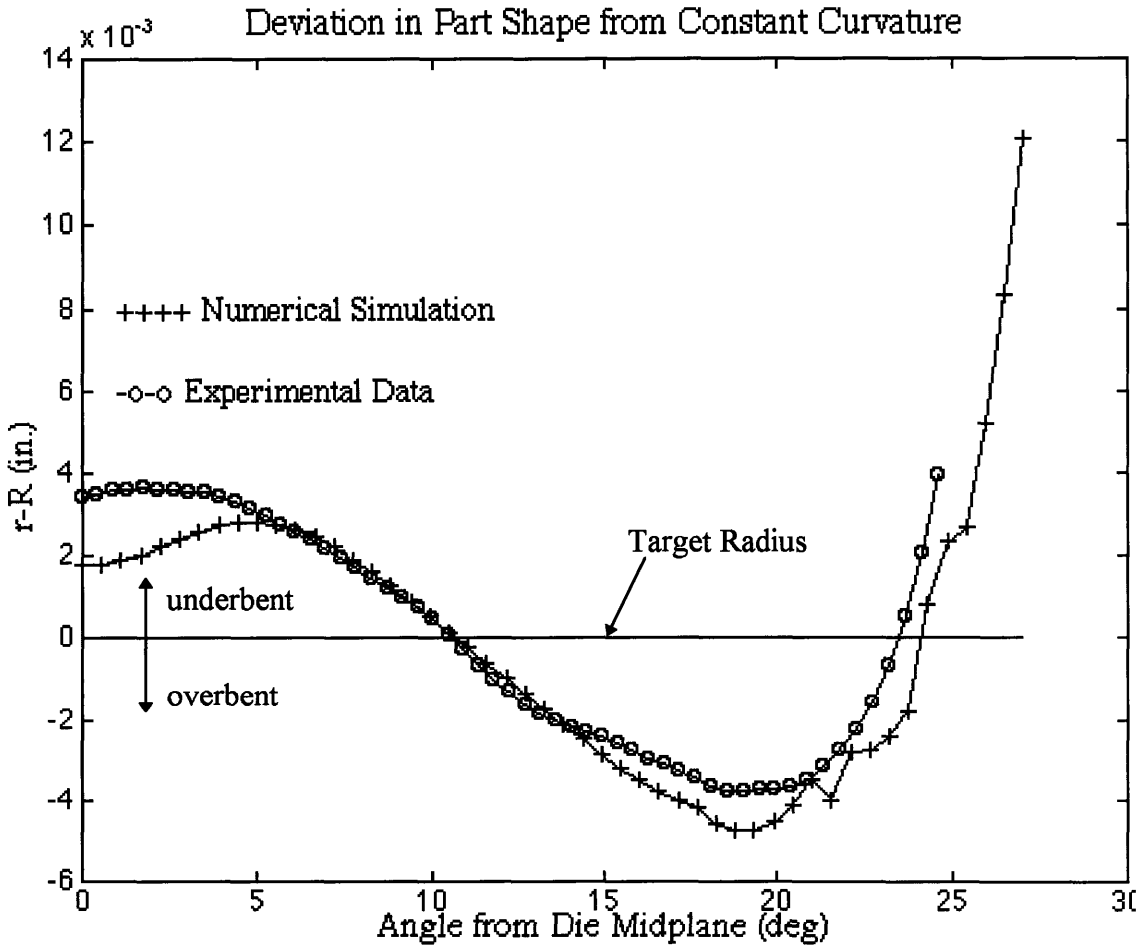

Figure 6.22: Deviation in Part Shape from Constant Curvature for Experimental and Numerical Data

The availability of an accurate model of the process allows us to pursue an alternative approach to predetermine the optimal die shape (Die_{opt}), to provide the desired part shape ($Part_{ref}$). This approach has been termed the "springforward algorithm" [Karafillis and Boyce, 1995]:

1. A simulation of a forming operation on a die (Die_{ref}) with the same shape as the part reference shape is carried out. This first step provides an estimate of the distribution of forces and moments acting on the sheet in the loaded configuration (upon removal of these loads the sheet will spring back to an unloaded configuration which will not coincide with the reference shape).

2. The second step is a simulation of the opposite of a springback event: we start with an unloaded sheet in the desired (reference) shape, and apply to it the forces and moments calculated in the first step, in order to bring it into its loaded configuration.

3. The last step is an extrapolation procedure to obtain the die shape (Die_{fw}), which corresponds to the loaded part shape obtained in the second step. A new surface is created by offsetting the surface defined by the loaded part shape by an amount corresponding to the interpolator thickness and radius of the spherical tip of the pins. This new surface defines the positions of the centers of the spherical tips in the new discrete die.

The die shape resulting from this procedure may differ from Die_{opt}, so that the parts formed over it will not perfectly match the reference shape, for two main reasons:

- The model of the process may not be sufficiently accurate. This problem can be resolved by properly adjusting the model parameters in order to obtain a better agreement of numerical predictions and experimental data.

- In order to obtain Die_{opt}, the reference shape should be 'sprung forward' using the loads which corresponds to a part loaded over Die_{opt} (this data is clearly not available as Die_{opt} is not known). Rather, in step 2 we apply the loads obtained for a part formed over Die_{ref}, an approximation which will tend to underestimate the actual loads and

give less springforward. This problem can be reduced by iterating steps 1 through 3 (using Die_{fw} in step 1 instead of Die_{ref})

One cycle of the springforward algorithm has been executed to obtain a new configuration for the die, Die_{fw}, and Figure 6.23 compares measures of part shapes formed over Die_{ref}, and over Die_{fw}, with the actual reference shape. Clearly, a single iteration of the algorithm provide substantial compensation of the springback effect. Figure 6.24 compares the die shapes obtained with one iteration of the springforward algorithm (Die_{fw}), with the die shape obtained with four iterations of the closed-loop shape-control algorithm. Additional iterations of the springforward algorithm should result in an improved agreement between the two methods. Notice that both methods try to compensate for the variation in curvature for the part shape formed over constant curvature dies, by creating a die with variable curvature. Figure 6.25 shows the deviation of the local radius of curvature from an average radius for both dies, and it is apparent that the two die shapes show striking similarities.

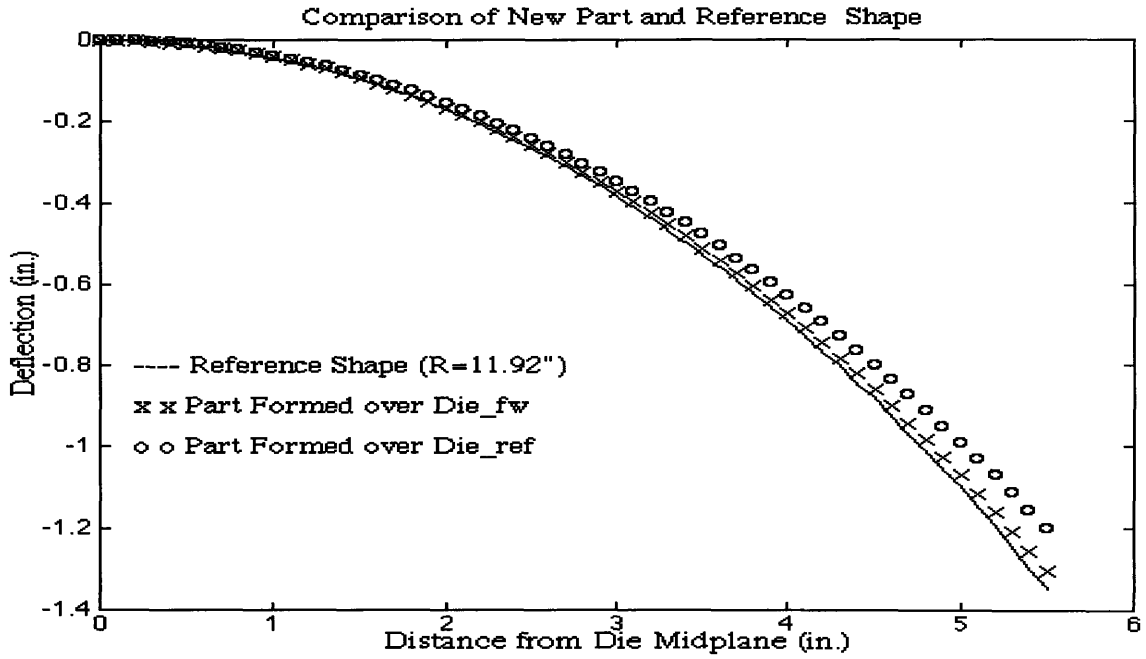

Figure 6.23: Comparison of Parts Formed Over the Sprung Forward Die Shape (Die_fw) and a Die With Reference Part Shape (Die_ref)

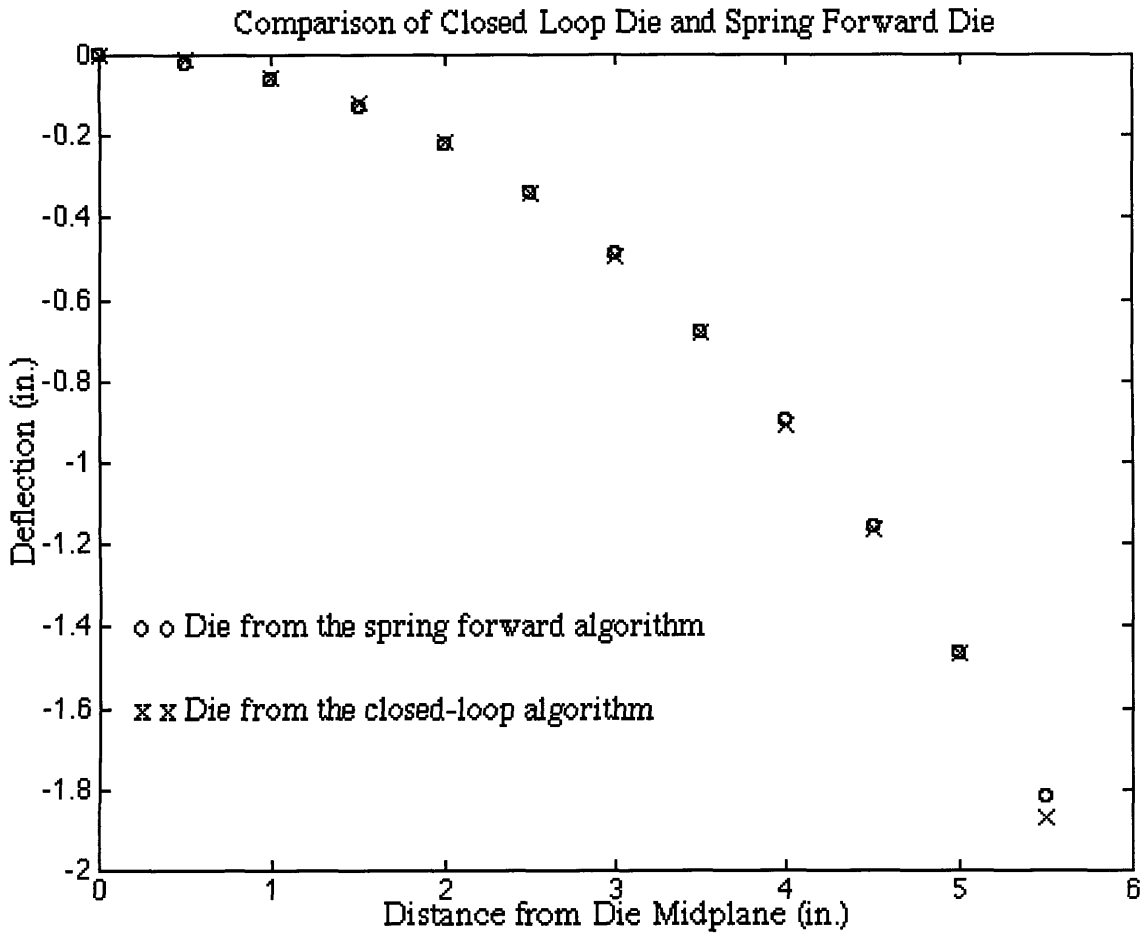

Figure 6.24: Comparison Between Closed Loop Converged Die and Spring Forward Die

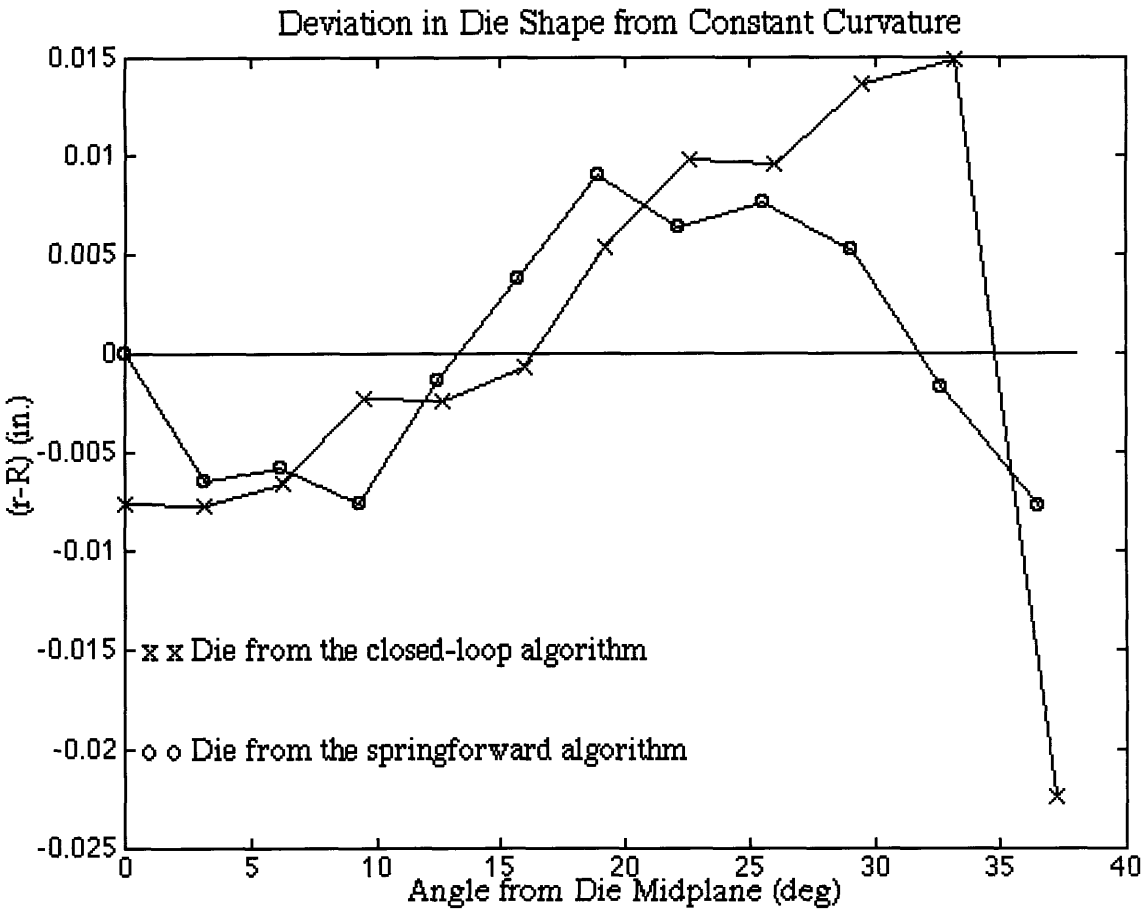

Figure 6.25: Deviation in Part Shape from Constant Curvature for Closed Loop Converged and Spring Forward Data

CHAPTER 7: CONCLUSION

7.1 Summary

The present day forming processes for sheet metal forming are slow, costly and outdated. The tooling is also very costly and unresponsive to even the slightest of part design changes. This inability for the tool to conform to different shapes has cost the sheet metal forming business millions of dollars in long lead times and high inventory costs. A flexible tool could offer much shorter lead times, eliminate all inventory costs for solid dies, and make rapid prototyping a possibility in the sheet metal forming industry.

The task of creating a flexible tooling system is currently being attacked from two sides; hardware and software. The discrete die stretch forming press iterates through die shapes using the closed loop shape control algorithm to cause a part to converge on a specified reference shape. Concurrently, there is considerable finite element modeling being done to simulate the stretch forming process. The modeling iterates using a "spring forward" algorithm to predict the next die shape. Once the simulation techniques have been perfected, the simulated data will be used to replace the inital open loop trials for the shape control algorithm.

There has been much previous work done on the discrete die press and closed loop shape control algorithm. By the end of the theses by Eigen [Eigen, 1992] and Ousterhout [Ousterhout, 1991], the system was complete for the matched die forming process. Many people contributed to the retrofit of the machine to give it stretch forming capabilities. Once constructed, the stretch forming machine was characterized for repeatability and tested using the shape control algorithm. The repeatability study demonstrated that despite loading the sheet metal into the machine, and trimming the part on the sheet metal shear differently, the machine still had a maximum error of only 0.020 inches at the end of

the part. When all operations concerned with forming a part were done consistently, the error dropped below 0.010 inches.

Once the machine was characterized, convergence tests were performed to confirm that the closed loop shape control algorithm worked for the stretch forming process. The stopping criteria for the convergence test used the machine capability for forming, of 0.020 inches, as the limit for the error between the part and reference shapes. After only two iterations of the algorithm, the part converged to the reference shape. If the first two open loop shapes were closer to the shape desired, the algorithm would have the correct die shape after only one iteration.

7.2 Future Work

The most immediate problem that must be addressed is the one dealing with three dimensional forming. The machine is able to form parts with secondary curvature, yet there are many hidden problems that accompany the added dimension. The ability to form these parts is actually the least of the problems, but procedures that were trivial in the two-dimensional case, such as trimming and measurement, become very difficult issues when secondary curvature is introduced. No longer can the sheet metal shear be used to trim the parts, nor can the CMM fixturing device be used to hold the part during measurement. Research will have to be done to investigate the possibility of using a water jet or laser cutting tool in order to trim these complex shapes. A new fixturing device will have to be constructed for the purpose of holding the part during the trimming operation. The actual measurement procedure using the CMM will not get more complex, though more points will have to be taken and thus measurement times will increase dramatically. But, as with the trimming operation, there must be investigation into the fixturing problem to assure good referencing and consistent clamping from part to part.

Once the hardware issues have been addressed, the problems associated with adding the extra dimension to the shape control algorithm must be. Ousterhout did a considerable amount of work making the closed loop shape control algorithm work for three-dimensional matched die formed parts. This work can be used as a stepping stone, off which the problems with stretch forming three-dimensional forming may be attacked.

The biggest forseeable problem which will be encountered trying to run a convergence test in three-dimensions will be referencing and data manipulation. As discussed in Chapter 6, the problem with finding the actual center of the part necessary for accurately describing a part for the algorithm was a formidable. When an extra dimension is added, another method for accurately describing the part shape must be divised. There are no longer only two degrees of motion for the part, rotation around the y-axis and translation, to worry about, but now there are two rotations and translations that must be compensated.

As demonstrated in Chapter 6, the simulation techniques are accurately modeling the stretch forming process given specific forming parameters. The "spring forward" algorithm has also proven to change the die shape in the right direction to compensate for springback on a single iteration. Additional iterations of the spring forward algorithm should result in improved results in the formed part.

In conclusion, the MIT discrete die stretch forming machine is capable of forming accurate and repeatable parts. The closed loop shape control algorithm was able to compensate for the error in die shape, to create a part that converged to the reference shape. The finite element simulations proved to accurately model the stretch forming process and the "spring forward" algorithm was able to create a die that caused the part shape to converge to the reference shape.

REFERENCES

Hamm III, J. E.., Manager Technical Support for Tool Manufacturing and Test Operations, Northrup Grumman Comercial Aircraft Division, P.E., Personal communication.

Hardt, D. E., Boyce, M. C., Ousterhout, K. B., and Karafillis, A. P., "A Flexible Forming System for Sheet Metal", Proc. NSF Conference on Design and Manufacturing Research, 1992.

Eigen, G. F., "Smoothing Methods for Discrete Die Forming", S.M. Thesis, MIT, 1992.

Walczyk, D. F., "Rapid Fabrication Methods for Sheet Metal Forming Dies", Ph.D. Thesis, MIT, 1996.

Webb, R. D., "Spatial Frequency Based Closed LoopControl in Sheet Metal Forming", Ph.D. Thesis, MIT, 1987.

Ousterhout, K. B., "Design and Control of a Flexible Process for Three-Dimensional Sheet Metal Forming", Ph.D. Thesis, MIT, 1991.

Webb, R.D., "Adaptive Control of a Flexible Die System for Forming Sheet Metal Parts", S.M. Thesis, MIT, 1981.

Webb, R. D. and Hardt, D. E. , "A Transfer Function Description of Sheet Metal Forming for Process Control", Journal of Engineering and Industry, 1991.

Parris, A. N., "Precision Improvements in Stretch Forming for Precision Assembly of Aircraft" (Preliminary Title), Ph.D. Thesis, MIT, 1996.

Dr. Socrate, S., MIT, personal communication with a very nice person.

Boyce, M. C. and Karafillis, A. P., "Tooling and Design for Sheet Metal Forming Processes Compensating for Springback Error", International Journal of Machine Tools and Manufacture, 1995.

Galil Motion Control Inc., DMC-1000 Manual Rev. 1.5, 1995.

Math Works Inc., MATLAB User's Guide, 1993

APPENDIX A - Galil Programs

The following programs were written using the Galil DMC-1000 software

HOME.DMC adjusts hydraulic cylinders to their home positions

```
#HOME
MG""
MG"HOMING CYLINDERS..."
MG""
XQ#HOMEZ,1
XQ#HOMEW,2
MG""
EN

#HOMEZ
JG ,,-2000,
ZOLD = _TPZ
BG Z
WT 200
#ZHOME
ZPOS = _TPZ
ZDIF = ZPOS - ZOLD
ZOLD = ZPOS
JP#ZHOME, @ABS[ZDIF] > 3
STZ
AMZ
PRZ = 9000
BGZ
AMZ
MG"Z AXIS AT HOME POSITION."
EN

#HOMEW
JG ,,,-2000
WOLD = _TPW
BG W
```

```
WT 200
#WHOME
WPOS = _TPW
DIF2 = WPOS - WOLD
WOLD = WPOS
JP#WHOME, @ABS[DIF2] > 3
STW
AMW
PRW = 9000
BGW
AMW
MG"W AXIS AT HOME POSITION."
EN
```

SET30D.DMC Sets the discrete die to 30 degree die shape

```
#SETUP

DM X[24]
X[0] = 0
X[1] = 0.25
X[2] = 0.5217
X[3] = 0.7612
X[4] = 0.9707
X[5] = 1.1520
X[6] = 1.3067
X[7] = 1.4359
X[8] = 1.5404
X[9] = 1.6210
X[10] = 1.6782
X[11] = 1.7124
X[12] = 1.7237
X[13] = 1.7124
X[14] = 1.6782
X[15] = 1.6210
X[16] = 1.5404
X[17] = 1.4359
X[18] = 1.3067
X[19] = 1.1520
X[20] = 0.9707
X[21] = 0.7612
```

```
X[22] = 0.5217
X[23] = 0.2500

N = 1
MG""

PRH = 9431
SPH = 3000
BGH
AMH

#LOOP
DIST = X[N]*10060 + 10500
MG"COLUMN",N {F2.0}," LENGTH IS", X[N] {F1.4}
PRX = DIST
BGX
AMX
PRX = -DIST
BGX
AMX
PRH = 5085
SPH = 2000
BGH
AMH
N = N + 1
JP#LOOP , N < 24

MG""
MG"PIN SETUP COMPLETE."
EN
```

WRAP.DMC program for forming a part in force control

```
#WRAP

A=0
KVW=.15
KVZ=.15

IN"ENTER PRELOAD FORCE",PRE
```

```
IN"ENTER TRAVEL (INCHES)",INCHES

TRAVEL = INCHES*10060
YSPEED = 2*10060/60

MG""
MG"PRELOAD IN PROGRESS ..."

XQ#PREZ,1
XQ#FORCEW,2
#LOOP
JP#LOOP,A=0
MG""
MG"PRELOADING IS COMPLETE"
MG"Z CYLINDER IS AT",@AN[1]*4640
MG"W CYLINDER IS AT",@AN[2]*4620

JGY = 2*YSPEED
BGY
#LIMIT
JP#LIMIT,@AN[5]<1
STY
MG""
MG"PART AGAINST DIE"
MG"Z CYLINDER IS AT",@AN[1]*4640
MG"W CYLINDER IS AT",@AN[2]*4620

JGY = YSPEED
YPOS = _TPY
YOLD = _TPY
S=YPOS+TRAVEL
BG Y
WT 7000
XQ#FORCEZ,3
MG""
MG"Z CYLINDER ENABLED"
MG"Z CYLINDER IS AT",@AN[1]*4640
MG"W CYLINDER IS AT",@AN[2]*4620
#WRAPA
YNEW = _TPY
ADJ = .25 * ( YNEW - YOLD ) / TRAVEL
KVW=.15 + ADJ
KVZ=.15 + ADJ
```

```
JP#WRAPA, _TPY<S
MG""
MG"Z CYLINDER IS AT",@AN[1]*4640
MG"W CYLINDER IS AT",@AN[2]*4620
MG""
MG"THE Z GAIN IS ",KVZ
MG"THE W GAIN IS ",KVW
ST YWZ
HX 2
HX 3
MG""
MG"TEST COMPLETE."
EN

#PREZ
JG ,,-150
BG Z
#CYCLE
FZ=@AN[1]*4640
VZ=KVZ*(FZ-PRE)
JG ,,VZ
JP#CYCLE,FZ <0.95*PRE
ST Z
MG""
MG"Z CYLINDER AT 95% OF PRELOAD ",FZ
EN

#FORCEW
JG ,,,-150
BGW
#CYCLEW
FW=@AN[2]*4620
VW = KVW*(FW-PRE)
JG ,,,VW
JS#END,(FW-PRE)>-20
JP#CYCLEW
#END
A=1
EN
ST W
EN

#FORCEZ
```

```
JG ,,-150
BG Z
#CYCLEZ
FZ=@AN[1]*4640
VZ=KVZ*(FZ-PRE)
JG ,,VZ
JP#CYCLEZ
ST Z
EN
```

APPENDIX B - MATLAB Files

COMPARE (meas1, meas2)

```
%compares two part shapes and finds the error between the
%two parts at every x coordinate

function error=compare(meas1, meas2)

global xmeas1 zmeas1 xmeas2 zmeas2 X Z1 Z2 Error Err1 XPert ZPert1;
global ShiftX m c d e Err1 MSE;

xmeas1 = meas1(:,1); %%x-coordinate of first measurement file
zmeas1 = meas1(:,2); %%z-coordinate of first measurement file

xmeas2 = meas2(:,1); %%x-coordinate of second measurement file
zmeas2 = meas2(:,2); %%z-coordinate of second measurement file

MSE = 0;
X = 0:.05:11.99; %%set up a common X to spline to

Z1 = interp1(xmeas1, zmeas1, X,'spline'); %%create Z points using X for first part
Z2 = interp1(xmeas2, zmeas2, X,'spline'); %%create Z points using X for second part

offset  = max(Z2) - max(Z1)
Z2 = Z2 - offset;

error = Z2 - Z1; %%difference between Z points for two parts

ShiftX = -.2:.005:.2; %%change in X,to move one part over the other to find min error

c=size(ShiftX);
d=size(X);
e=size(error);

for m = 1:1:c(:,2)
        Err=0;
        XPert = X + ShiftX(m); %%change X
```

```
        ZPert1 = interp1(X, Z1, XPert, 'spline'); %%change Z

        for x = 1:1:d(:,2);
                Err = Err + (Z2(x) - ZPert1(x)) * (Z2(x) - ZPert1(x)); %%find MSE for
changed variables
                Err1(m,x) = (Z2(x) - ZPert1(x)); %%keeps track of error for every point
        end
        Error(m) = Err; %%MSE for each different X
end

for i=1:e(:,1)

        MSE = MSE + error(i)*error(i); %%MSE without changing X

end

plot(Error);
title('MSE for Change in X');
xlabel('Shift in X: (Number -1) * 0.005 inches - 0.2 inches');
ylabel('MSE of Z Dimension Due to Shift in X');

figure(2)

plot(Err1(find(Error==min(Error)), :));
title('Exact Error for Least MSE Shift');
xlabel('Number of Points Taken Along X Axis');
ylabel('Error Z2 - Z1 After Parts Set to Same Z Coord at the Center');
```

REFSHAPE (angle)

```
%%solves for die shape given angle made from
%%center line and Rd

function [Z, R, y] = refshape(angle)

global X Z y;

D = 18.25;  %%
t = 0.063; %%thickness of sheet

X = 0:.5:11;
```

```
Theta = angle * pi / 180;

R = 5.5/sin(Theta);
RR = R + sqrt(2)/4 + 0.5 + t/2;

deltaZ = R*cos(Theta);

Z = sqrt ((R*R) - ((X - 5.5).*(X - 5.5))) - deltaZ + 0.25;%%.25 arbitrary offset

y = RR * (1 - cos(Theta)) + (D - RR * sin(Theta)) * tan(Theta);
```

REFSHAPE2 (R)

```
%%creates a die shape given the radius of curvature

function [Z, Theta, y] = refshape(R)

global X Z y;

D = 18.25;  %%distance from center of die to center of trunion
t = 0.063; %%thickness of sheet

X = 0:.5:11;

Theta = asin(5.5/R)*180/pi;
theta=Theta*pi/180;

RR = R + sqrt(2)/4 + 0.5 + t/2;

deltaZ = R*cos(theta);

Z = sqrt ((R*R) - ((X - 5.5).*(X - 5.5))) - deltaZ + 0.25;%%.25 arbitrary offset

y = RR * (1 - cos(theta)) + (D - RR * sin(theta)) * tan(theta);
```

SIMONA2

```
%%manipulates raw data fromthe CMM and puts it in proper format
%%center points are found using excel file: err_anal (error analysis)

load trans2.dat;
load thirtythreedeg2.dat;
load thirtythreedeg3.dat;

xlot = 0:0.05:12;

x1 = trans2(:,1);
x2 = thirtythreedeg2(:,1);
x3 = thirtythreedeg3(:,1);

z1 = trans2(:,2);
z2 = thirtythreedeg2(:,2);
z3 = thirtythreedeg3(:,2);

z1 = interp1(x1, z1, xlot,'spline');
z2 = interp1(x2, z2, xlot,'spline');
z3 = interp1(x3, z3, xlot,'spline');


x1max = 5.864738;
x2max = 5.796727;
x3max = 5.847516;

xx1 = xlot - x1max;
xx2 = xlot - x2max;
xx3 = xlot - x3max;

xdata = -5.5:0.1:5.5;

zz1 = interp1(xx1, z1, xdata,'spline');
zz2 = interp1(xx2, z2, xdata,'spline');
zz3 = interp1(xx3, z3, xdata,'spline');

zz2 = zz2 - (max(zz2) - max(zz1));
zz3 = zz3 - (max(zz3) - max(zz1));

plot(xdata,zz1);
hold on;
```

```
%plot(xdata,zz1,'o');
%plot(xdata,zz2,'g+');
plot(xdata,zz2,'g');
%plot(xdata,zz3,'rx');
plot(xdata,zz3,'r');

xxx1 = -5.5:0.5:5.5;

zzz1 = interp1(xdata, zz1, xxx1,'spline');
zzz2 = interp1(xdata, zz2, xxx1,'spline');
zzz3 = interp1(xdata, zz3, xxx1,'spline');

xxx1 =xxx1+5.5;
%%use yellow data for 33.749 degree part

zdata2 =[zzz1  zzz2  zzz3];
```

DIENEXT2 (die1, die2, part1, aprt2, R)

```
%%dienext creates the next die shape given the previous two die
%%and part shapes, and radius of desired part
%%part1 and part2 are vectors with x and z components.
%%die1 and die2 are vectors with only z components
%%R is radius of desired part = radius of pin centers + .9166
%%for 1/2 inch of elvax

function dnext = dienext(die1, die2, part1, part2, R)

global xd ref x2 z2 ZD2 Ref Z2 ZD1 Z1;

t = 11; %%length from center of first pin to center of last pin

x1=part1(:,1); %%x-coords of first part data
x2=part2(:,1); %%x-coords of second  part data
z1=part1(:,2); %%z-coords of first  part data
z2=part2(:,2); %%z-coords of second  part data

zz1 = z1 + (max(z2) - max(z1)); %% centering the two curves

xd = (0:0.5:11)'; %%x-coordinates for the dies
```

```
zd1 = die1';
zd2 = die2';

zd1 = zd1 + (max(zd2) - max(zd1)); %%centering curves

ref = refshape2(R)'; %%Creates z coords of reference shape
ref = ref - (max(ref) - max(z2));

%% Fourier Transform Stuff

Z1 = fft(zz1,23); %%transform of 30d part
Z2 = fft(z2,23); %%transform of 33...d part

ZD1 = fft(zd1,23); %%transform of 30d die
ZD2 = fft(zd2,23); %%transform of 33d die

Ref = fft(ref,23); %%transform of refernce shape

Dnext = ZD2 + (Ref - Z2) .* ((ZD2 - ZD1) ./ (Z2 - Z1));

dnext = real(ifft(Dnext,23));
dnext = dnext - (max(dnext) - max(zd2));

plot(x1,zz1);
hold on;
plot(x1,zz1,'o');
plot(x2,z2,'g');
plot(x2,z2,'g+');
grid;
xlabel('Distance From Center of First Pin to Center of Last Pin (in.)');
ylabel('Height of Pins (in.)');
title('Parts Formed Over Die3 and Die4');
text(3,0.9,'o  Part Formed Over Die3 -> R ~ 11.11');
text(3,0.7,'+  Part Formed Over Die4 -> R ~ 11.06');

figure(2);

plot(xd,zd1);
hold on;
plot(xd,zd1,'o');
plot(xd,zd2,'g');
plot(xd,zd2,'g+');
grid;
```

```
xlabel('Distance From Center of First Pin to Center of Last Pin (in.)');
ylabel('Height of Pins (in.)');
title('Die 3 and Die 4');
text(2,0.9,'o  Die3 -> R = First Closed Loop + 0.9166');
text(2,0.7,'+  Die4 -> R = Second Closed Loop + 0.9166');

figure(3);

plot(xd,zd1);
hold on;
plot(xd,zd1,'o');
plot(xd,zd2,'g');
plot(xd,zd2,'g+');
plot(xd,dnext,'r');
plot(xd,dnext,'rx');
grid;
xlabel('Distance From Center of First Pin to Center of Last Pin (in.)');
ylabel('Height of Pins (in.)');
title('Die3, Die4 and Next Die Shape');
text(3,0.9,'o  Die2 -> R = 9.9 + 0.9166');
text(3,0.7,'+  Die3 -> R = First Closed Loop + 0.9166');
text(3,0.5,'x Second Closed Loop Die Shape');

figure(4)

plot(x2,z2);
hold on
plot(x2,z2,'o');
plot(xd, ref,'g');
plot(xd,ref,'gx');
grid;
xlabel('Distance From Center of First Pin to Center of Last Pin (in.)');
ylabel('Height of Pins (in.)');
title('Part 4 and Reference Shape');
text(3,0.9,'o  Part 4 -> R ~ 11.06');
text(3,0.7,'+  Reference -> Ra = 11');

figure(5)

plot(xd,(z2-ref));
hold on;
plot(xd,(z2-ref),'o');
grid;
```

```
xlabel('Distance From Center of First Pin to Center of Last Pin (in.)');
ylabel('Error Between 4th Part Shape and Reference Shape (in.)');
title('Error Between Part 4 and Reference Shape Along the Die');
```